Cardiorespiratory Monitoring by Microphone via Tracheal Sounds in the Context of Implanted Phrenic Nerve Stimulation

Xinyue Lu

THESIS TO OBTAIN THE GRADE OF DOCTOR OF THE UNIVERSITY OF MONTPELLIER

In Automatic and Microelectronic Systems

Doctoral School: I2S (Information Systems Structures)

Research unit: NeuroResp, LIRMM, INRIA-CAMIN, UMRS1158, Sorbonne University

Cardiorespiratory Monitoring by Microphone via Tracheal Sounds in the Context of Implanted Phrenic Nerve Stimulation

Prensented by LU Xinyue on March 23, 2020

Under the direction of [Christine AZEVEDO COSTE] and [Thomas SIMILOWSKI]

Before the jury composed of

Thomas PENZEL	Professor	University of Charite	Reporter
Norbert NOURY	Professor	University of Lyon1	Reporter
Julie FONTECAVE-JALLON	Lecturer	University of Grenoble-Alpes	Examiner
Phillipe FRAISSE	Professor	University of Montpellier	President of jury
Christine AZEVEDO	Research director	INRIA-CAMIN	Thesis director
David GUIRAUD	Research director	INRIA-CAMIN	Invited
Serge RENAUX	Company director	NeuroResp	Invited

致谢 我爱 以及 爱我的人们

Contents

List of Figures

List of Tables

List of acronyms

AASM American Academy of Sleep Medicine

AHI Apnoea-Hypopnoea Index

AM amplitude modulation

CO_2 carbon dioxide

CPAM primary Health Insurance Fund: Caisse primaire d'assurance maladie

CSA central sleep apnoea

DP diaphragm pacing

ECG electrocardiogram

EDR ECG-derived respiration

EEG electroencephalography

EMG electromyography

EOG electro-oculography

HAS Haute Autorité de Santé

HF-SCS high frequency spinal cord stimulation

HRV heart rate variation

ICSD-2 international Classification of Sleep Disorders

ID-PNS intra-diaphragmatic phrenic nerve stimulation

IRP induction respiratory plethysmography

IT-PNS intra-thoracic phrenic nerve stimulation

O_2 oxygen

OSA Obstructive sleep apnoea

$PaCO_2$ partial pressure of carbon dioxide

PaO_2 partial pressure of oxygen

PCG phonocardiography

PDR Phonocardiogarm-derived determination of respiratory rhythm

PSG polysomnography

PTT pulse transit time

SaO_2 oxygen saturation

SCI spinal cord injury

SSA specificity sensitivity and accuracy

SSP suprasternal pressure

TS tracheal sounds

TV-PNS trans-venous phrenic nerve stimulation

Introduction

Individuals with a respiratory paralysis are essentially supplied by mechanical ventilation. However, severe drawbacks of mechanical ventilation were reported: low autonomy, high health costs, infection risk due to tracheotomy, etc. When patients' phrenic nerves and diaphragms are still functional, implanted diaphragm pacing (DP) can provide them a more natural respiration. Compared to classic mechanical ventilation, implanted DP can cancel some of the disadvantages mentioned above, and can also help to significantly improve speech and recover some olfactory sensation because air passe through the nose and/or the mouth.

But existing implanted DP systems can not monitor patient's induced respiration and they stimulate at constant intensity and frequency - they work in open-loop. It means that stimulation intensity, pulse width and frequency are fixed at the installation of the implant, updated at each control visit, but do not adapt to patient's continuous situation evolution because of the absence of respiratory monitoring. To close the loop, an ambulatory respiratory monitoring solution needs to be developed. Adding adaptive abilities to existing systems would improve the efficiency of the delivered stimulation.

The gold standard for apnea/hypoventilation evaluation is the polygraph, which includes a pulse oximeter and at least one respiratory flow sensor . In a clinical use, flow sensors could be nasal cannula, pneumotachograph, thermistor or plethysmograph. But these sensors need to be placed over the face or are sensitive to patient's movements. They are therefore not compatible with an implanted DP system which is portable and for a daily living use. With this in mind, this thesis investigated an acoustic method. The proposed tracheal sounds recording requires only one tiny support of microphones fixed on the neck with a support, which is the only physical contact with the patient.

Many previous studies have shown some positive results on apnoea detection from tracheal sounds in sleep apnea, especially for obstructive sleep apnea. Their detection algorithms are either based on the envelope of sound signals (in time domain) . Some groups also used statistical methods for respiratory phase detection and classification, and even for air flow estimation associated with sounds entropy or the log of the sounds

variance. But only few methods were developed for real-time applications (processing delay within seconds) with robustness requirements, indeed, all these studies have been carried out in quiet and controlled acoustic environments with stable sources of noises, and with limited movements of the subjects (during sleep).

The present thesis aims at a real-time and continuous breath and heart beats detection (day and night), even during wakefulness in noisy environments. The recorded tracheal sounds contain not only respiratory sounds, but also heart beats sounds (PCG) so that some basic cardiac information, as cardiac rhythm, could be calculated. Furthermore, inspired by ECG-derived respiration, the similar method could also be applied on PCG to get respiratory information. We proposed a new algorithm to detect respiration phases, by combining the signal processing both in the temporal (envelope and PCG-derived respiration) and the frequency domains. We assessed the performances of the algorithm in emulated noisy environments.

Chapter 1

General introduction

1.1 Physiology introduction

This section is based on [5] and [6].

1.1.1 Electrophysiology

The nervous system is a complex system on which all of the body's functions depend. This system consists of 2 parts (Fig. 1.1):

- Central nervous system: the brain and the spinal cord;
- Peripheral nervous system: the autonomic nervous system, the enteric nervous system and the peripheral nerves.

The enteric nervous system controls the activity of the digestive tract but won't be discussed in this thesis. The central nervous system is responsible for receiving, integrating and transmitting information; The autonomic nervous system regulates the action of internal organs in the context of the integrated functioning of the organism; The peripheral nerves are pathways responsible for driving information (nerve impulses). Sensory information are sent from sensory receptors into spinal cord by afferent nerves, and motor information are sent from spinal cord to effector (e.g. muscles) by afferent nerves.

The neuron is the functional unit of the nervous system, and they are very differentiated. One neuron cell body gives rise to two types of extensions: an axon and dendrites (Fig. 1.2). The dendrites are very branched and receive information from many other nerve

cells and the axon transmits information to other neurons or to non-neuronal cells such as muscles.

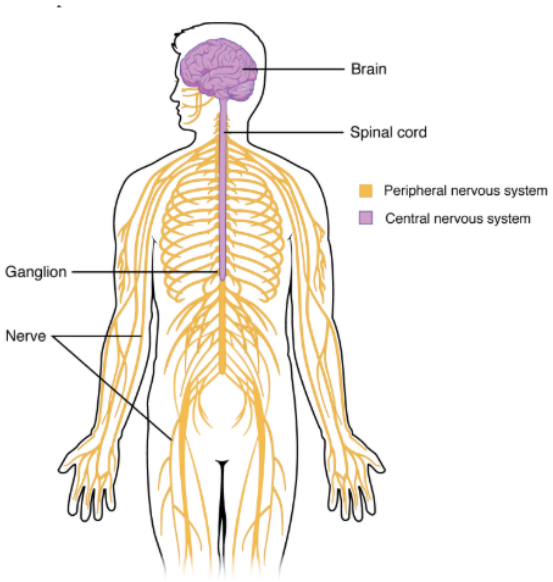

Figure 1.1: Nervous system.

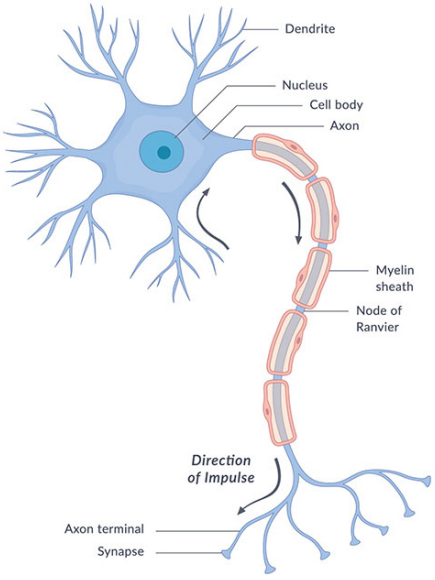

Figure 1.2: Neuron structure.

The neurons innervate to muscles are called motoneurons. Their bodies locate the spinal cord (central nervous system), their axons group together in fascicles and travel in nervous thrones (the efferent nerve) to reach their target organs . Otherwise, the neuron carries sensitive information is called sensory neuron, its cell body is right next to the spinal cord and its axon has two sides: the carried information are transmitted from the side connected to receptor to another side going into spinal cord (afferent nerve).

Taking the example of respiration (Fig. 1.3), the respiratory command is sent from respiratory center and transmit through spinal cord to the body of respiratory motoneuron, then this command travels on efferent pathway of phrenic nerve to respiratory muscles (red lines on Fig. 1.3). Meanwhile, some sensory information (e.g. pain) can be transmit to spinal cord by afferent pathway and may be sent to brain to be treated (green lines on Fig. 1.3). More respiratory details will be described in §1.1.2.

Information generated and transmitted by nervous system (nerve impulse) are in fact electrical impulses, called action potential, initiated in neuron bodies and then transmit on axons to target cells or organs. Because of ionic molecules with different electrical charges at two sides of neuron cell membrane, it exists a differential potential between inside and outside of the neuron cell. In resting state, this neuronal membrane potential is -70 mV (Fig. 1.4). But when there are some stimulus, some ionic molecules may cross through the membrane, these exchanges make the potential increase (depolarisation). If the stimulus reaches a minimum intensity (the threshold, depending on type of neuron), the action potential occurs in form of all-or-nothing: it won't be generated if a stimulus intensity

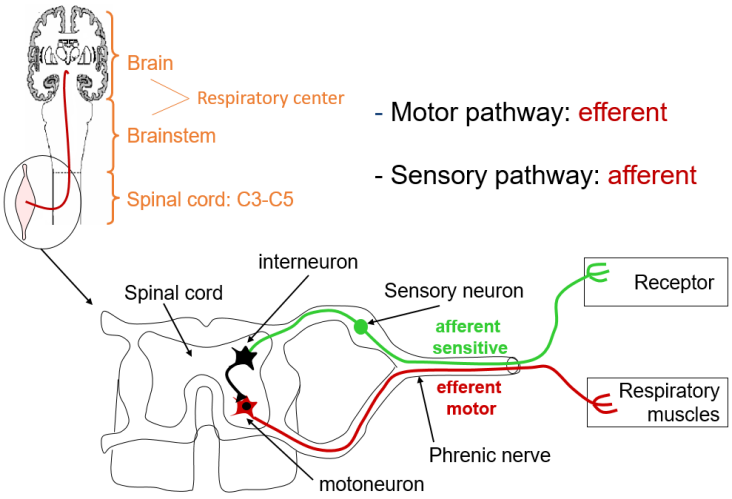

Figure 1.3: The spinal pathway during respiration.

not high enough, and it will stay at the same amplitude and duration even if the stimulus intensity is much higher than the threshold. Once an action potential occurs, it will stimulate another action potential in neighbor zone so the electrical impulse propagates. These nerve impulses can lead to muscle contractions when they reach targeted muscles.

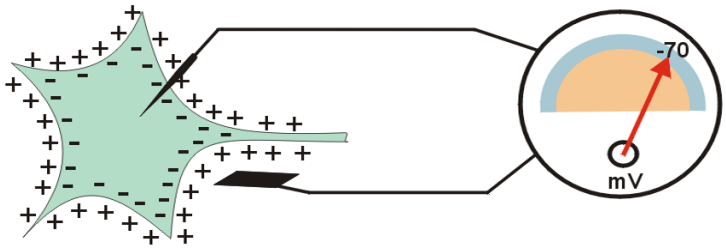

Figure 1.4: The resting potential.

1.1.2 Respiratory system

Respiratory mechanism

Internal or cellular respiration produces the energy required by animals to maintain a normal level of activity. During this process, oxygen (O_2) is used by the mitochondria and carbon dioxide (CO_2) is produced. The necessary O_2 is taken from the atmosphere, while the CO_2 produced is removed from the body during external respiration, which is the subject of this study. The key point of external respiration is the process of gas exchanges that take place between air and blood in deep areas of the lungs. The structure of the respiratory system is illustrated in Fig. 1.5.

The lungs are the main organs of the respiratory system located in the rib cage, they offer the respiratory surface (the alveoli) where the gas exchange happens. Before reaching

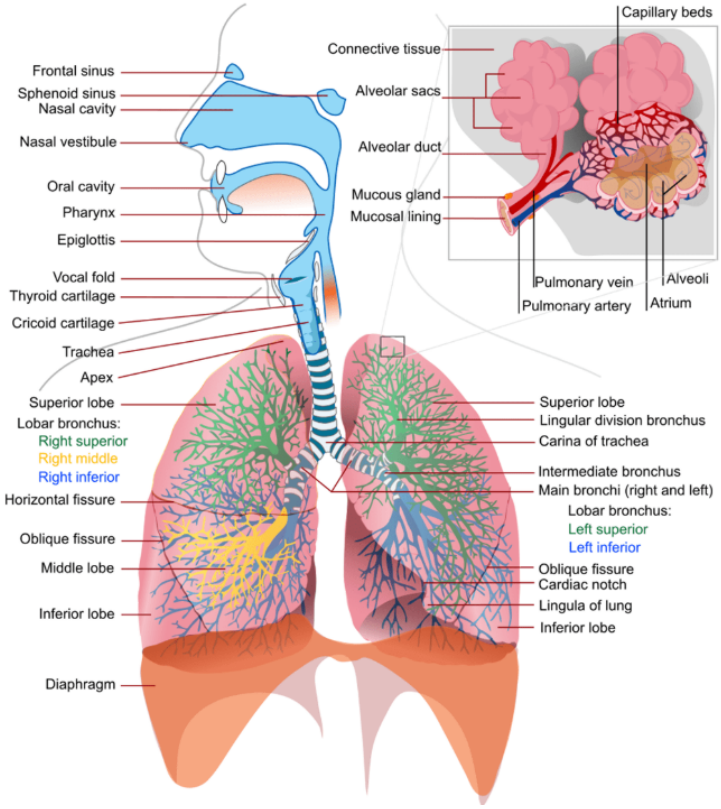

Figure 1.5: The structure of respiratory system.

the level of the lungs, the air must pass through the upper airway (the nasal cavities, the pharynx, the larynx and trachea) and then enter the bronchi and bronchioles. The lungs are not able to inflate themselves; they inflate with air through the intervention of respiratory muscles that induce variations in the size of the thoracic cage. (Fig. 1.6).

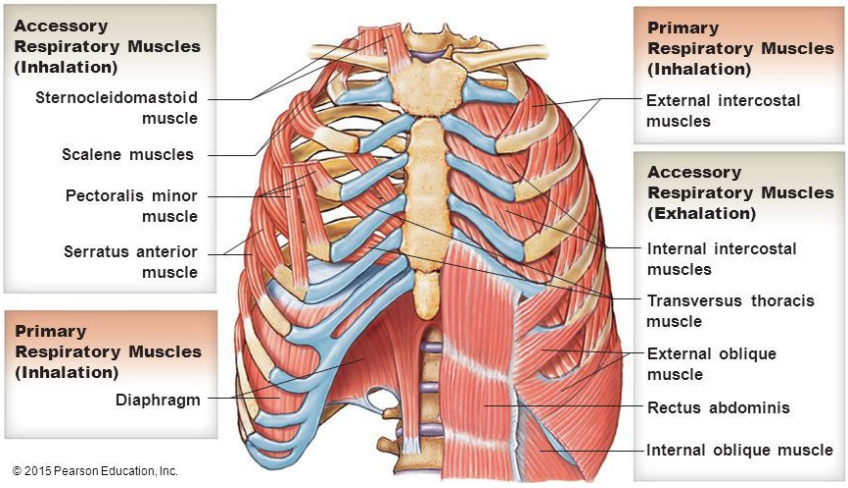

Figure 1.6: Respiratory muscle organization.

The main respiratory muscle is the diaphragm, it forms a continuous layer that separates the thorax from the abdomen. At rest it forms a sort of dome, but when it contracts during inspiration, it flattens to increase the thoracic volume. Like liquids and gases, air

will always move from a zone of high pressure to a zone of low pressure. When thoracic volume increases, the pressure inside the lungs (alveolar pressure) falls down to be lower than the atmospheric pressure so that air enters into the lungs. This is the process of inspiration. At this moment, some abductor and dilator muscles of the upper airway are also activated to stabilize the airway and to prevent its collapse (obstruction) from negative intra-airway pressure due to diaphragm contraction [7]. During expiration, the diaphragm slowly relaxes and the elastic recoil force reduces thoracic volume so that the alveolar pressure exceeds inducing passive exhalation. These processes are illustrated in Fig. 1.7.

If the demand of O_2 increases, other respiratory muscles could be recruited. The activity of external intercostal muscles can stretch the thoracic cage upwardly and outwardly to increase supplementary thoracic volume, so increase inspiratory volume. On the other hand, the internal intercostal muscles and abdominal muscles can be required during exercise to assist decreasing thoracic volume and so the passive expiration becomes active.

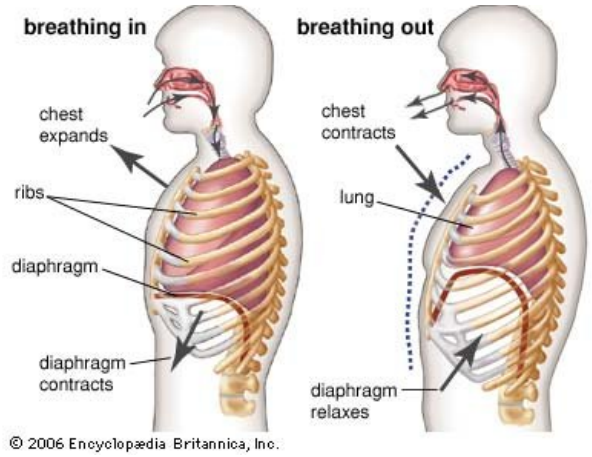

Figure 1.7: Inspiration and expiration.

Respiratory regulation

The respiratory muscles do not contract spontaneously but in response to efferent activity of the phrenic and intercostal nerves. The diaphragms are the main respiratory muscles, they are innervated by phrenic nerves originating in the cervical spine from the C3, C4 and C5 roots. As the example shown in §1.1.1, the respiratory command (nerve impulses) are sent from the respiratory center which is located in the brain and the brainstem, the commands pass through the cervical spine and phrenic nerve to provoke diaphragm contraction. This respiratory center can be divided into two parts (Fig. 1.8): the higher center (cerebral cortex, hypothalamus) controlling conscious respiration, and the respiratory rhythmicity center (medulla oblongata) controlling the unconscious respiration. The former can override the latter with conscious decisions such as breathing

exercises. In medulla oblongata, we distinguish two groups of neurons that discharge potential actions with an intrinsic rhythm corresponding to the respiratory cycle: the dorsal respiratory neurons (inspiratory neurons) and the ventral respiratory neurons (inspiratory and expiratory neurons). These two groups of neurons work together in the way of reciprocal inhibition: one adds its activity when another initiates it.

The unconscious controls are determined by chemical and mechanical receptors. In general, ventilation is stimulated by gas exchanges: a lack of oxygen (hypoxia) and a rise in CO_2 (hypercapnia). The partial pressures of the blood gases are detected by peripheral and central chemoreceptors. They respond to variations in partial pressure of oxygen (PaO_2), partial pressure of carbon dioxide ($PaCO_2$), and arterial pH and are the only receptors that respond to hypoxia. Central chemoreceptors are located in the brainstem and respond to most of the chemical stimuli of ventilation. Fig. 1.9 illustrates the principle of respiratory regulation.

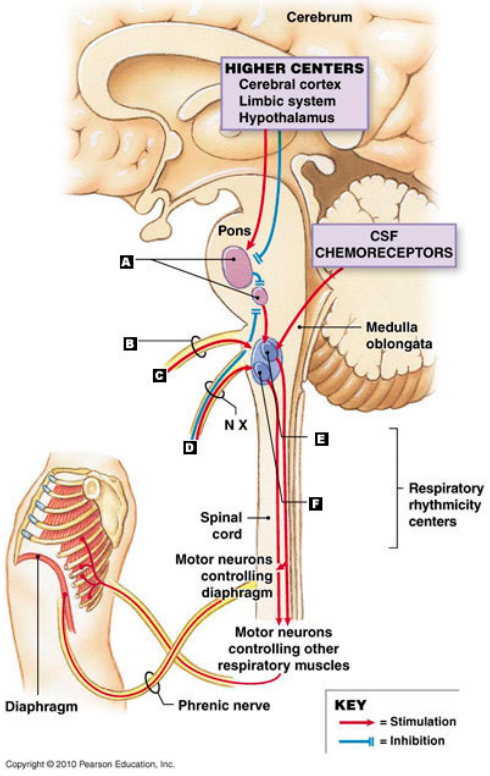

Figure 1.8: Breathing rate control.

1.1.3 Cardiac system

As the O_2 brought by inspiration needs to be transported over the body and the produced CO_2 needs to be brought to the lungs to be removed outside the body by expiration, our body has a circulatory system that allows the body's cells to exchange

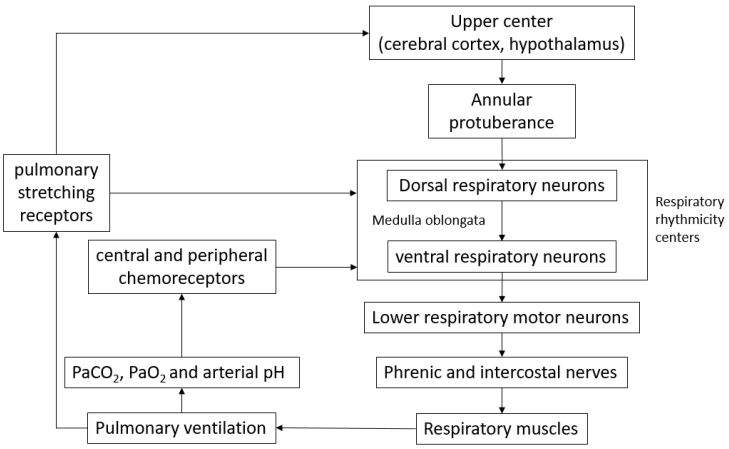

Figure 1.9: Diagram of respiratory regulation.

oxygen metabolism products and nutrients with the blood systems. In this process, our heart works as a pump to circulate the blood over the body.

Cardiac anatomy

The heart is located in the thoracic cage, on left side, in a fibrous bag called the pericardium which prevents an excessive dilation of the heart when it fills with too much blood. The pericardium is attached to the diaphragm, which allows the apex of the heart to be relatively fixed.

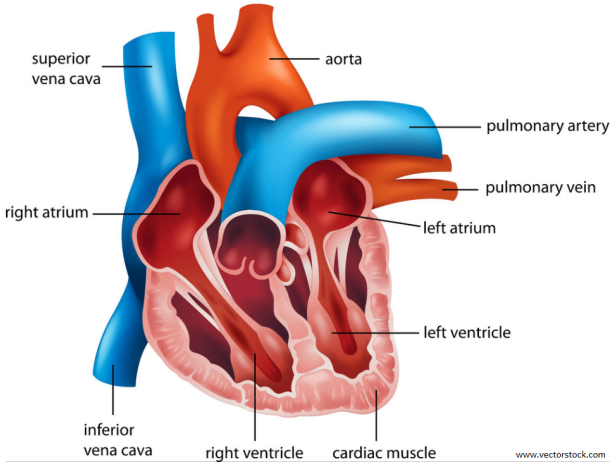

Figure 1.10: Heart anatomy.

The heart is about the size of a closed fist and is made up of four muscular cavities: two atria and two ventricles, which lie side by side, separated by a muscular sheet called the septum (Fig. 1.10). The circulation is organized in such a way that the right part of the heart ejects the blood through the lungs (pulmonary circulation) and the left part of the heart pumps the blood into the rest of the body (systemic circulation). The two circulations are therefore placed in series (Fig. 1.11). Atria are thin-walled cavities that

receive blood from large veins and distribute it into the ventricles that provide the force needed to propel the blood through the pulmonary and systemic circulation. The atria are separated from the ventricles by a fibrous septum that contains the four heart valves: the atrioventricular valves and the aortic and pulmonary valves, theses valves can prevent back-flow of blood. And the cardiac muscle is called myocardium.

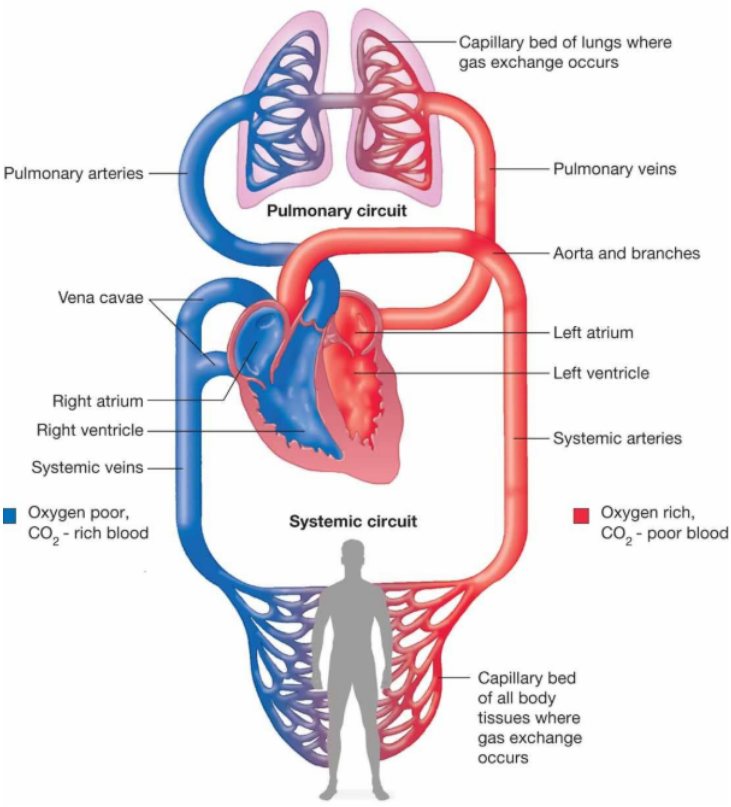

Figure 1.11: Blood circulation between heart, lungs and other body tissues.

Cardiac cycle

Not like respiratory muscles, the heart beats spontaneously. It shows a proper rhythmicity that is independent of any extrinsic nervous system. The excitation (action potentials) is initiated by a group of specialized cells, located in the sinus node, near the point of entry of the large veins in the right atria. The spontaneous depolarization wave (nerve impulses, 60-100 times per minute) begins from the sinus node, it spreads first through the two atria, then it goes into the ventricles with a delay about 0.1 seconds allowing contraction of the atria before the ventricular muscle is excited. After that, the electrical pulse (nerve impulses) is conducted throughout the rest of the heart.

As the mechanism of air going in and out our body, the blood flows form higher pressure areas towards lower pressure areas. When a cardiac muscular cavity contracts (atria or ventricles), the pressure within this cavity increases, and the blood is pushed out. As a

result, venous blood from the body and from the lungs enters the empty atria and flows into the empty ventricles (atrial and ventricular diastole), and the last blood volume is forced into ventricles by atrial contraction (atrial systole); then ventricular contraction (ventricular systole) ejects blood out through arteries; finally, the ventricles relaxes and the myocardium waits for the end of its refractory period to begin another cycle.

1.2 Respiratory paralysis

As presented in §1.1.2, the respiratory muscles contractions (the breathing) are controlled by spontaneous command from the respiratory center. If this respiratory command is absent or interrupted, spontaneous breathing is no longer possible. This is called respiratory paralysis, and depending on the original reason of paralysis, it can be divided into two groups: central respiratory paralysis and acquired respiratory paralysis. Patients with respiratory paralysis are dependent on artificial ventilation.

1.2.1 High spinal cord injury

A damage to the spinal cord (nervous pathway is damaged) can cause temporary or permanent changes in its function, like loss of muscle function, sensation, etc. If the damage happens at cervical level (above C5), the transmission of respiratory commands may be interrupted. This case is an acquired respiratory analysis. In France, the incidence of patients with cervical spinal cord injury depending on artificial ventilation support is estimated around 12.7 per one million inhabitants, among which 6.5% requires long-term mechanical ventilation [8].

1.2.2 The Ondine syndrome

In the case of the central respiratory paralysis, the ventilatory impulses generated by the brain stem are lacking. It can be caused by brain stem lesions or drugs and substances, etc [9]. When this lack of ventilatory impulses happens during sleep, it induces Central Sleep Apnoea (CSA). Congenital cases are very rare, such as congenital central alveolar hypoventilation. This kind of CSA is often referred to Ondine's curse, so it is also called Ondine syndrome. In 2008, only 1000 total cases were known in the world [10], about 60 patients were in France, and 10%-15% whithin them have a artificial ventilatory dependence [11].

Most of the time, we breath automatically without thinking about it. The respiratory center will send respiratory commands in response of different levels of gases in the blood (1.1.2). But for patients with Ondine syndrome, their respiratory center are not sensible to changes of gases in blood due to a mutation in gene (PHOX2B: it codes for a protein involved in the development of the autonomic nervous system during the embryonic stage). Fortunately, on awakening, the extra motor area (an area of the cortex that is not normally involved in automatic breathing) comes to the rescue. It commands a regular breathing,

regardless of the need for oxygen. As soon as sleep occurs, this area becomes inactive and the patient may stop breathing spontaneously [12].

1.2.3 Treatments

For patients with respiratory paralysis, artificial ventilation can replace or help to restore patient's ventilatory function. The most common treatment is mechanical ventilation which pushes air into patient's lungs through tracheotomy (an incision on the front of the neck and opening a direct airway through this incision in the trachea with a tube). However, severe drawbacks of mechanical ventilation are reported: (1) the induced positive pressure disturbs the venous return [13], (2) ventilators are noisy and limit mobility which reduces the quality of life, (3) tracheotomy may cause respiratory infections, reduction of olfaction, taste and speech [14].

As presented in §1.1.1, action potential (nerve impulse) is generated by a stimulus on neuron. In fact, this stimulus can be artificial. It means, the respiratory command sent from respiratory center is missing or interrupted, but it can be reproduced by an artificial electrical stimulation after the damaged region on the respiratory pathway. In the case where phrenic nerves and diaphragm remain functional (the motoneurons innervated to diaphragm are still complete, the nervous pathway from phrenic nerve to diaphragm has no damage), the mechanical ventilation can be replaced by another artificial ventilation: Diaphragm Pacing (DP), which could cancel some of the disadvantages mentioned above. Furthermore, DP induces a more natural respiration and reduces health care costs [13][14].

1.3 The diaphragm pacing

1.3.1 History

The first DP (stimulation on the phrenic nerve) goes back to the discovery of electricity. In 1819, diaphragmatic contraction induced by phrenic nerve stimulation is described for the first time. Leroy d'Etiolles put the concept of DP into practice in 1829. Next, Duchenne De Boulogne described in detail the technique of DP by stimulation of the phrenic nerve on the neck [15]. It was in the 1970s that W. Glenn and his team proposed the first clinical applications of implanted DP (by phrenic nerve stimulation), and this technique has been used to date [13].

The implanted DP was introduced in France around 1985, by a team led by Dr.Jean-François Brûlé at Helio-Marin Hospital in Berck, but stopped after the latter's death. From

the mid of 1990s, this activity was put in place again by the pulmonology team of Pitié-Salpêtrière Hospital Group. Until 2015, this activity resulted in a total of 47 implantations in patients with tetraplegia and patients with central hypoventilation. The accumulated knowledge and results contributed to the positive opinion that was expressed by the Haute Autorité de Santé (HAS) regarding the technique in 2009, then to the registration of two stimulators (Atrostim® and NeurRxDP4®). The cost of using the registered devices can benefice from the reimbursement of social security, which is important for promoting the wide use of implanted DP systems.

1.3.2 Diaphragm pacing technique

Depending on the targeted tissue activated by electrical stimulation, the DP techniques can be divided into four categories:

Intra-thoracic phrenic nerve stimulation (IT-PNS)

This technique corresponds to an implantation of electrodes in direct contact with the phrenic nerves, at the level of the thorax. Two commercial systems rely on this technique: Atrostim® (AtroTech, Tampere, Finland) and Mark IV Breathing Pacemaker® (Avery Biomedical Devices, USA 1.13). The two systems have a similar structure (Fig. 1.12): An inner part includes the electrodes; Another external part includes the electric pulse generator (controller). The connection between these two parts is done by radio-frequency with a subcutaneous receptor and an external antenna (wireless connexion). The electrodes are implanted by mini-thoracotomy, on each phrenic nerve with VATS or under video-surgery.

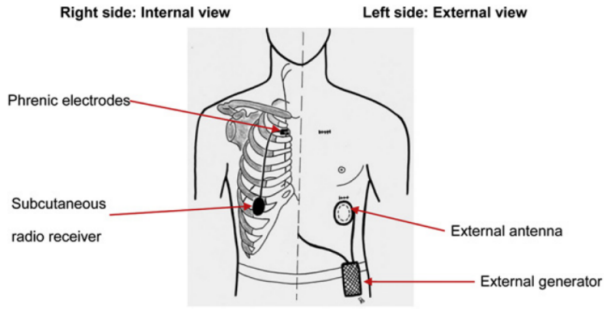

Figure 1.12: General structure of implanted DP system.

Figure 1.13: The IT-PNS stimulator – Mark IV Breathing Pacemaker®.

Until 1996, based on 64 following patients who have been implanted with Atrostim® device for an average of 2 years, about 50% were able to maintain full-time IT-PNS, while about 80% of them were able to maintain the stimulation on the day only [16]. In

France, the IT-PNS is the most used technique with the Atrostim® system. Between 1997 and 2007, for an implantation duration of more than 3 years, ventilatory weaning was obtained in 18 out of 20 patients [14]. According to the report activity 2011-2015 ("post-reimbursement") of intrathoracic phrenic nerve stimulation within the "Multidisciplinary Group of Respiratory Neurostimulation" coordinated by the Department of Pneumology and Medical Resuscitation of Pitié-Salpêtrière, during the period of 2011-2015, 24 months after implantation, 9 out of 12 patients had achieved autonomy with the stimulation system for at least 12 hours per day, corresponding to a total weaning capacity of the artificial ventilation (including 3 patients who died before 24 months). For two patients, ventilatory autonomy was 4 hours and 2 hours, respectively.

Intra-diaphragmatic phrenic nerve stimulation (ID-PNS)

The ID-PNS is based on the implantation of intramuscular electrodes near the terminations of the phrenic nerves in the diaphragm, by laparoscopic way. To do this, a mapping is performed perioperatively to identify the phrenic motor point in each diaphragm, and two stimulation electrodes are at this level. Only one system is available on the market with this technique, NeurRxDP4® (Synapse, Oberlin, Ohio, USA). This system also has an inner part (electrodes) and an outer part (generator), but both parts are connected by a transcutaneous cable (shown in Fig. 1.14).

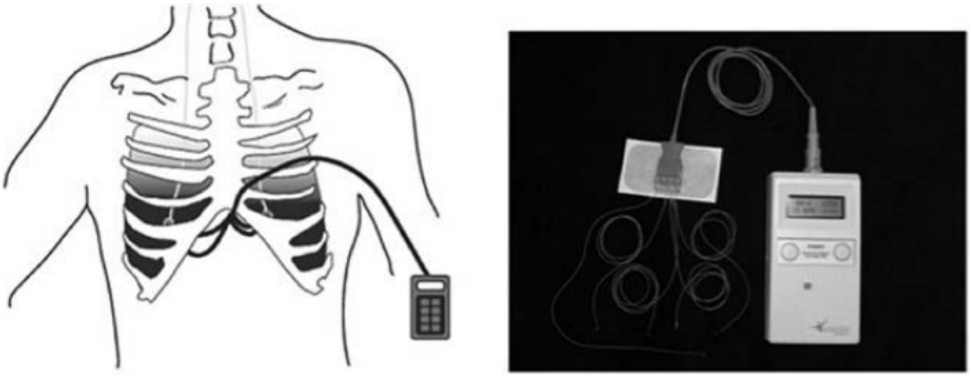

Figure 1.14: The ID-PNS stimulator – NeurRxDP4® [15].

With the NeurRxDP4® device, a study of 51 patients shows that approximately 50% of the patients were able to maintain full-time stimulation. For patients not using the device for full-time, the duration of application could range from 4 hours to 5 hours. A total of 49 high spinal cord injury (SCI) implanted patients (96%) were with a complete weaning (>12 hours stimulation per day) from mechanical ventilation [16]. In France, NeurRxDP4® is also registered in the HAS, and can therefore be reimbursed by social security. For tetraplegic patients, ID-PNS is effective and has been reported to be easier to implement and less expensive than its intrathoracic counterpart [17]. In contrast, shoulder

pain and infection problems have been described in the literature, and this pain might be caused by the high stimulation intensity [17].

Transvenous phrenic nerve stimulation (TV-PNS)

The TV-PNS is based on the implantation of electrodes in the subclavian vein at a point near the phrenic nerve. It is a temporary unilateral stimulation. This technique is specifically used to treat CSA, especially in the case of cardiac stroke. The device is implanted by an electrophysiologist in the cardiac suite, in general, under conscious sedation. The remedē® system (Respicardia Inc., Minnetonka, MN, USA) is the only TV-PNS system on the market (shown in Fig. 1.15). This system is fully implantable, it has a stimulation probe and a detection probe to provide stimulation in case of CSA. Since 2015, the first pilot studies on different stimulation durations have all shown a significant reduction in Apnoea-Hypopnoea Index (AHI) (the number of sleep apnoea or hypopnoea events per hour) and an improvement in sleep quality [18][19][20][21].

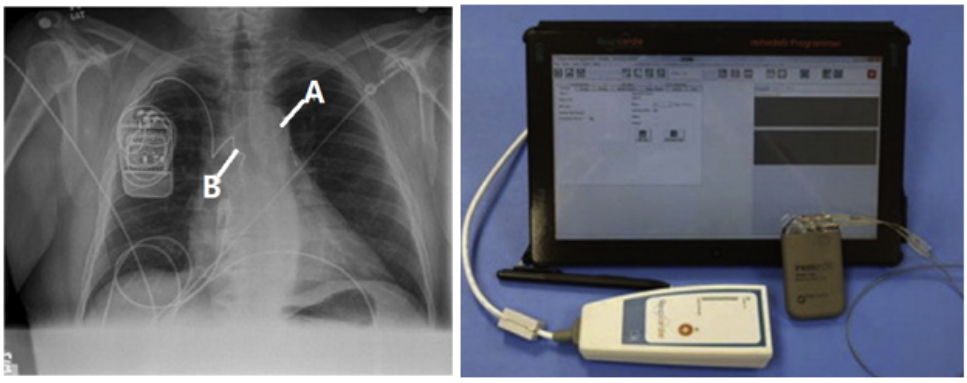

Figure 1.15: The TV-PNS stimulator – remedē® [15].

There is also another transvenous phrenic stimulation (SP-TV) on the same principle but it is non-invasive. The goal is to stimulate the diaphragm during mechanical ventilation to avoid or strengthen the atrophied diaphragms, and to alleviate the disadvantages of mechanical ventilation (exp, improvement of venous return). In the First-in-Human protocol of TV-PNS on 23 patients, significant reductions in pressure-time-product of the ventilator were obtained [22].

High frequency spinal cord stimulation (high frequency spinal cord stimulation (HF-SCS))

The HF-SCS is a high frequency stimulation ($>$ 300Hz) applied directly on the spinal cord at the thoracic level. This technique can activate not only the phrenic nerves, but

also the intercostal muscles (ventral T2) and the exhalation muscles (dorsal T9-T11). On the other hand, certain movements (legs, arms, ...) and sensations (pains, tingling, ...) are also activated [16][23]. For the moment, there is still no device available on the market. Stimulation of the intercostal muscles is an effective method for providing long-term ventilatory support by combining it with phrenic stimulation [16]. In addition, 3 patients with high tetraplegia who had been implanted with the HF-SCS system had improved ability to eliminate secretions by HF-SCS-stimulated cough [24]. The latest research on 11 dogs has shown that, unlike the dorsal HF-SCS at the level T9 which causes positive pressure in the thorax (active exhalation), the ventral HF-SCS at same level of the spine causes a strong negative pressure (inspiration) from weak stimulation currents. This method could therefore be an alternative method to restore ventilation in patients with SCI with ventilatory dependence [23].

1.3.3 AtroStim

In this study, the implanted DP system used is the AtroStim® (AtroTech, Tampere, Finland). It is an IT-PNS system. For the implanted part, it has symmetrical structure for the left and right sides, furthermore these two sides can work independently. The AtroStim® is also the only IT-PNS system which has multiple stimulation contacts: 4 contacts on each side, and these 4 contacts stimulate the phrenic nerve alternatively (Fig. 1.16). Compared to the unipolar stimulation, the design of alternative stimulation with multiple contacts activates only one part of the phrenic nerve at time, so that the intensity and the frequency of stimulation can be reduced to prevent the fatigue of diaphragm. More over, all these 4 contacts can also work independently.

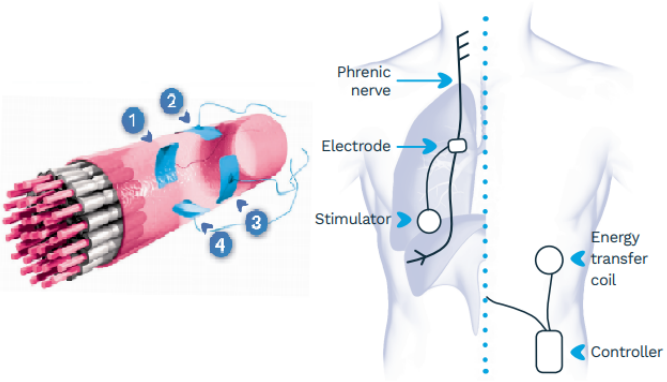

Figure 1.16: Structure of the AtroStim®.

At the installation of the device, stimulation parameters are set into the external controller. During stimulation, the controller sends power and stimulation commands to implanted radiofrequency receivers. This radiofrequency communication is based on amplitude modulation (AM). As shown in Fig. 1.17, the message signal is a rectangular

waveform, and the carrier signal is a sinusoid waveform which frequency is 25 MHz. The period of message signal corresponds to the stimulation period, and the duty cycle of this rectangular waveform (the ratio between the pulse width and the period) controls the stimulation intensity.

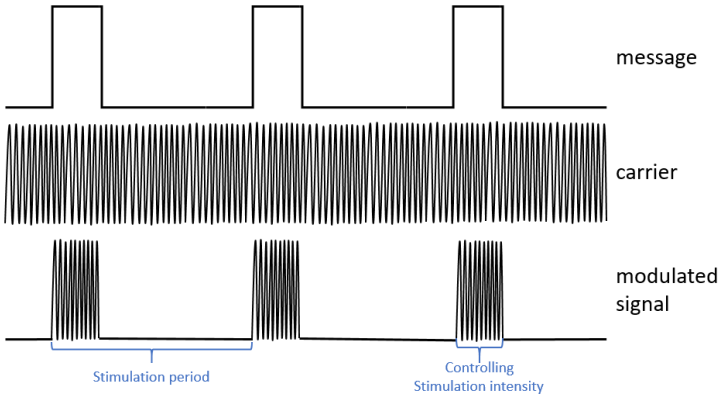

Figure 1.17: Sending stimulation information by radiofrequency communication – AtroStim®.

According to the received commands, electrical pulses (stimulus) are sent through the quadripolar electrodes alternatively to provoke diaphragmatic contractions, so to have an inspiration (Fig. 1.18). During the respiratory cycle, inspiration is an active movement whereas expiration is passive. Therefore, IT-PNS is by nature limited to inspiration. Two cycles of stimulation signals of the AtroStim® system are illustrated in Fig. 1.19. One breathing cycle lasts T_1, including inspiration phase T_2 (it is also the stimulation duration) and the expiration phase ($T_1 \rightarrow T_2$). Each red vertical line in this figure represents one stimulation pulse which pulse-width is 200 μs. The minimum stimulation intensity (threshold) is I_{TH}. And I_{TV} is the intensity corresponding to the tidal volume, it is also the maximum stimulation intensity. During T2, the stimulation begins at the intensity of I_{TH}, and increases at each pulse until the I_{TV}, then remains at the I_{TV} until the end of T_2. Except stimulation pulse-width, all other stimulation parameters mentioned above are manually adjustable depending on patient's situation during and after implantation operation.

A ramp stimulates muscle fibers progressively to avoid a fast contraction of the diaphragm. This mimics the natural recruitment of motor units during spontaneous inspiration. In general, the inspiration would begin when stimulation intensity reaches the I_{TV}.

1.3.4 Aim of thesis: DP in close loop

Even though DP has several advantages over the classical mechanical ventilation, it is not safe enough to maintain a full-time ventilatory assistance because of the absence

Figure 1.18: Stimulation procedure.

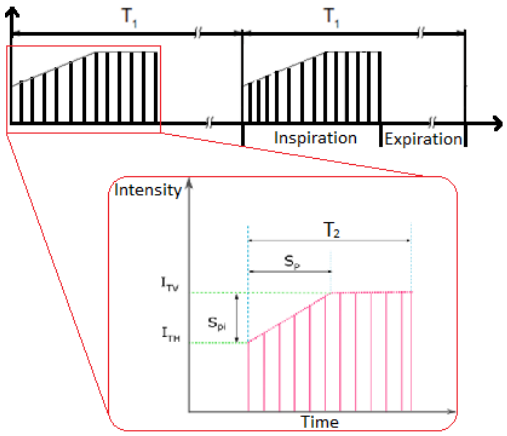

Figure 1.19: Stimulation signal of AtroStim®.

of any "efficacy alarm" [16]. For example, DP systems alarms warn users of electronic failure, but, contrary in the case of mechanical ventilators, do not warn about ventilatory inefficiency. Indeed, DP systems do not embark any ventilatory monitoring. As described in §1.1.2, upper airways muscles can help to stabilize airways. Diaphragms contract to create negative inter-pressure during inspiration. If at this process that upper airways muscles are relax or contract much later than diaphragm, upper airways are not stable and may collapse because of this inter-pressure. This may happen to high tetraplegic patients with DP system [7], because they can't feel the diaphragm contraction (efferent pathway is also damaged due to spinal cord injury) to synchronize their upper airways muscles' activities. Especially in sleeping (lying) because the largest upper airways muscle (tongue) relaxes and slips towards pharynx that inducing more possibility of upper airway collapse (Fig. 1.20). As a result, patients cannot be left alone during the day and usually return to mechanical ventilation during the night for safety reasons, e.g. obstructive sleep apnoea.

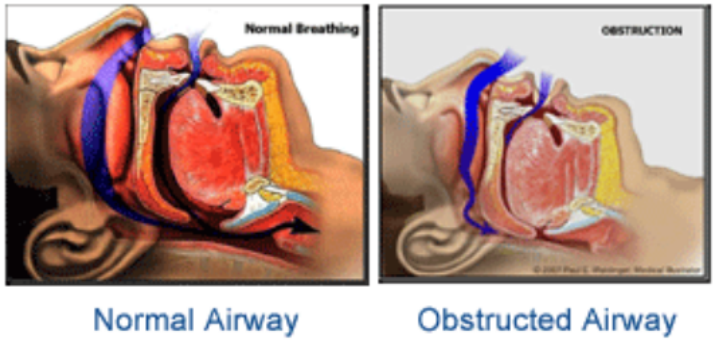

Figure 1.20: Obstructive apnea because of airway collapse in sleeping.

In addition, all existing DP systems work in open-loop; indeed, stimulation is delivered with constant predefined parameters. It means that stimulation intensity, pulse width and frequency are fixed at the installation of the implant, updated at each control visit, but do not adapt to patient's continuous situation evolution because of the absence of respiratory

monitoring. To close the loop, an ambulatory respiratory monitoring solution needs to be developed.

In this thesis, the first aim is to detect if patient is breathing or not; and secondly is to offer detailed respiratory information: inspiration/expiration, pauses, respiratory rhythm, volume, etc. Finally, for patients implanted DP system or patients with sleep apnoea problems, it's also important to evaluate their cardiac activities.

1.4 Clinic cardiorespiratory monitoring

The American Academy of Sleep Medicine (AASM) from 1999 and the international Classification of Sleep Disorders (ICSD-2) have defined some abnormal respiratory events as [25]:

- Hypopnoea: A decrease from *baseline** in the amplitude of a valid measurement of breathing during sleep that either reaches 50% with an oxygen desaturation of 3% or an arousal, or alternatively a 30% reduction with 4% oxygen desaturation.

  **Baseline:*

  - *For subjects with stable respiration: average amplitude of stable respiration within 2 minutes before the event.*
  - *For subjects without stable respiration: average amplitude of the 3 most extensive cycles within 2 minutes before the start of the event.*

- Apnoea: The cessation of breathing (respiratory flow) lasting for more than 10 seconds.

- Obstructive Sleep Apnoea (OSA): An apnoea or hypopnoea for more than 10 seconds with presence of ventilatory effort.

- Central Sleep Apnoea (CSA): An apnoea without presence of ventilatory effort.

- Mix apnoea: Apnoea begins as a CSA but ends up with presence ventilatory efforts.

To evaluate the degree of severity of sleep apnoea, the Apnoea-Hypopnoea Index (AHI) is introduced on the number of apnoeas and hypopnoeas occurring during 1h of sleep. This severity is classed as: mild ($5 \leq AHI \leq 15$ $events.h^{-1}$), moderate ($15 < AHI < 30$ $events.h^{-1}$) and severe($AHI \geq 30$ $events.h^{-1}$) [26].

According to these definitions, two essential parameters are important to measure, evaluate and identify abnormal respiratory events: the respiratory ventilation (air flow) and the respiratory effort. Furthermore, for classifying hypopnoea, the oxygen saturation and snoring are also needed to be measured.

In this section, some clinic methods to detect/quantify respiratory air flow, to evaluate respiratory effort and to monitoring cardiac activity are presented.

1.4.1 Ventilation measurement

Pneumotachograph

The traditional pneumotachograph (Lilly type) is a device which measures the differential pressure between before and after a membrane in the tube to calculate the volume of air passed. This is the only available solution to quantitatively measure respiratory flow, and is considered as the reference method. However, there are other innovative pneumotachographs that are in the form of a mask rather than a spirometer (Fig. 1.21). The principles of this type of pneumotachograph depends on the sensors used in spirometers. These sensors can be ultrasonic, mechanical (Turbine), thermal, etc. [27] It is necessary to wear a mask to avoid the leak of gas which is uncomfortable. The traditional pneumotachograph must be heated up to 37 degrees to avoid condensation, it is also not very pleasant for the user. Snoring is an event that is thought to indicate an obstruction, it is favored by the opening of the mouth. As the mask covers the mouth it reduces snoring noises and disrupts the quality of sleep.

Nasal cannula

The nasal telescope is a small device placed at the end of the nose (Fig. 1.22). It measures nasal pressure changing during respiration, and the volume can be estimated as approximately the root square of the measured pressure:

$$P \approx \dot{V}^2$$

The results obtained can vary a lot if the patient expires using the mouth or if he has a nasal obstruction. Moreover, a displacement of the sensor can cause a loss of signal.

Figure 1.21: The pneumotachograph.

Figure 1.22: The nasal cannula.

Figure 1.23: The inductance plethysmography.

Plethysmography

Plethysmography contains a chest and an abdominal band. It evaluates the tidal volume by the summation of the thoracic and abdominal movements after calibration. But, on the other hand, it is difficult to stabilize the calibration during the night when patients change position. The types of sensors used for plethysmography can vary:

- The induction respiratory plethysmography (IRP) is based on an electromagnetic measurement of a section's surface variations;
- Bio-impedance sensors measure changes in chest impedance related to breathing. There are also piezoelectric straps and cushions ultra-sensitive to movement.

Thermistors

Like the nasal telescope, the thermistor is placed at the end of the nose (Fig. 1.24). It is based on the difference of temperature between the exhaled air and the inspired air. More precisely, it detects the expiration when the exhaled air heats the sensor. Sensitivity of the sensor is lower if the ambient temperature is high. In addition, the sensor no longer works if it is in contact with the skin. The thermistor does not perform fairly accurate measurements (the flow variation is not linear with the temperature variation), so it is recommended not to use the thermistors alone for the detection of respiratory events.

1.4.2 Respiratory effort evaluation

Esophageal pressure

This is the reference method for measuring respiratory efforts, and the recommended method for highlighting high-resistance episodes. The pressure sensor permanently touches the posterior wall of the pharynx (Fig. 1.25), which is uncomfortable for patients and disrupts the quality of sleep. The dynamics of the airway is also changed.

Thoraco-abdominal movements

The principle is to look for a phase shift between thoracic and abdominal movements. The measurements can be performed similarly to the plethysmography mentioned above. On the other hand, the variations are influenced by the displacement of the sensors, the change of position, the stage of sleep and the degree of obesity. Moreover, the visual

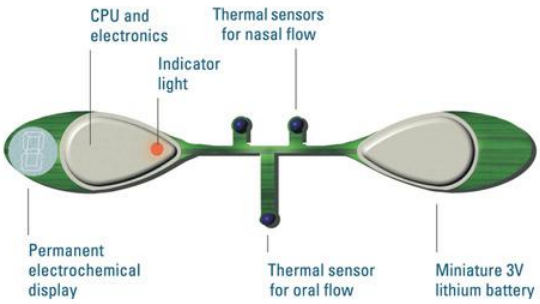

Figure 1.24: The thermistor SleepStrip®.

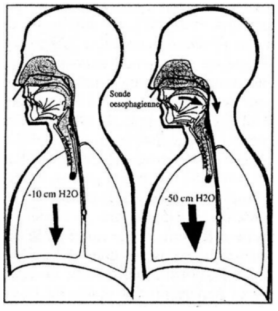

Figure 1.25: The esophageal pressure [28].

analysis of the phase shift is not always easy, and it is possible to have obstructive events without thoraco-abdominal phase shift. A comparative study showed that 37% of screened apnoeas as central on the straps (inductance) are reclassified as obstructive or mixed on the esophageal pressure data [29]. This method gives important errors on apnoea classifications.

The pulse transit time (PTT)

The pulse transit time is the time required for the wave corresponding to the pulse to travel the distance between the aortic valve and the last phalanx, which is about 250 ms. This method is based on the fact that velocity is proportional to the rigidity of the arterial wall. The increase in PTT reflects the increase in respiratory efforts, and the micro-arousals are associated with a decrease in PTT. This method can give accurate results, but it has only been validated on a small population and few events. In addition, the measurements are sensitive to artifacts.

1.4.3 Cardiac diagnostic: ECG and PCG

As explained in §1.1.3, the heartbeat is due to an activity initiated by an electrical impulse that is conducted throughout the myocardium. This electrical impulse is in fact in the orm of action potentials (specific potential difference), and these action potentials can be recorded by correctly placing electrodes on the chest as with Electrocardiogram (ECG). As said in 1.1.3, the atria contracts before ventricles, and the action potentials present different characteristics in those different regions (Fig. 1.26), the registered ECG is the sum of these different action potentials, and it gives insight into both normal and abnormal heart function.

The first detectable wave (P wave), appears when the impulse spreads to the atrial myocardium, depolarizing the atria. Then three waves appear together: Q, R and S and

so-called QRS complex corresponding to the depolarisation of 2 ventricles. At the end, the T wave occurs and indicates the ventricular repolarization.

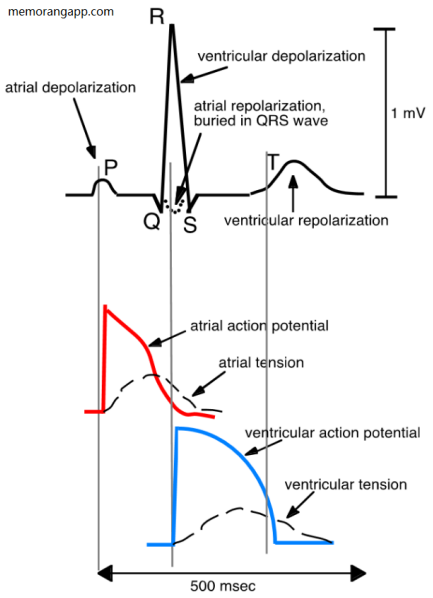

Figure 1.26: Relationship between the onset and duration of action potentials of cardiac cells during an isolated cardiac cycle and corresponding ECG pattern

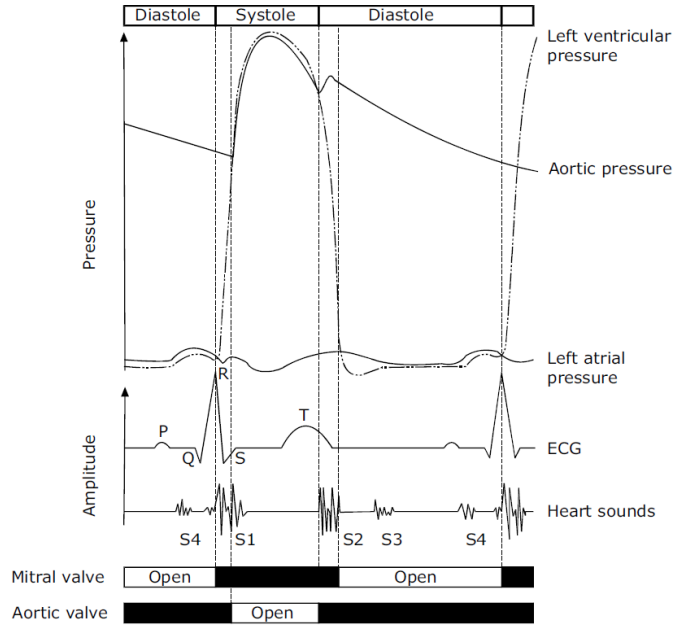

Figure 1.27: The four heart sounds in relation to various hemodynamic events and the ECG. [6].

Another method to evaluate cardiac function is through heart sounds: Phonocardiogram (PCG). Normally, there are 2 to 4 heart sounds, called S1-S4, shown in Fig. 1.27. The first sound (S1) occurs during the closing of the atrioventricular valves, corresponding to QRS complex in ECG but with a slight delay. The second sound (S2) occurs at the time of the closing of the aortic and pulmonary valves, corresponding to the end of T wave or just after it in ECG. The interval between S1 and S2 corresponds to the systole period, and similarly, the interval between S2 and S1 corresponds to the diastole period. S3 and S4 are both related to the diastolic filling period [6]. S3 and S4 cannot always be recorded (depending on subjects and recording system) and give less information, so they are less discussed than S1 and S2.

The interval from one heart beat to another is not fixed, this variation is called heart rate variation (HRV). This explains why cardiac rhythm is always calculated as an average over a period of time (e.g. 30 seconds). But the HRV is an important reflex to both sympathetic and parasympathetic activity during sleep. Thanks to this reflex, some researchers use the HRV to illustrate sleep stages, but it's influenced by age [30]. The HRV is processed by calculating the interval R-R in ECG.

1.4.4 Other measurements

Snoring measurement

Snoring measurements are usually carried out either by one or two microphones positioned in the room, or by microphones glued on the patient.

Measurements of oxygen saturation

The oxygen desaturation of hemoglobin falls within the definition of certain hypopnoeas. The measurement is performed by means of an oximeter (an infrared type sensor). It emits two different lights that will be absorbed by hemoglobins and oxymoglobins with different rates. A receiver then receives the unabsorbed light to calculate the oxygen saturation (SaO_2). The oximeter can also give the heart rate because the oxygen saturation / desaturation cycle corresponds to the contraction of the heart muscle.

The time window used for averaging heart rate is important for choosing an oximeter. A long time window can over-smooth the signal, making difficult to see the influence of desaturation on the calculation of the index of hypnoea. So, to obtain a good classification result, it is advisable to choose oximeters that have a high sampling frequency (> 1 Hz) adapted to an averaging window of a maximum duration of 3 s to 5 s. But the respiratory detection result with oximeter only is still not accurate, especially for prolonged/long-time apnoea, because the sensors are often placed at the fingers extremities, but blood flows towards the vitals organism when lack of oxygen.

gaseous exchange measurements

Capnography is a graphical representation of the changes in CO2 concentration in respiratory gases. It is useful for monitoring CO2 production, pulmonary perfusion and alveolar ventilation of the patient. The measurements are made by an arterial catheter or an infrared sensor that measures CO2 concentration in the expired air. In some cases, the O2 pressure and the transcutaneous CO pressure are also measured.

1.4.5 Polysomnography and polygraphy

The PSG is a measurement applied on sleep, respiration, cardiovascular signals and movements. In general, it requires the acquisition of 3 main signals: the electroencephalography (EEG), electro-oculography (EOG) and the electromyography (EMG).

In France, the primary Health Insurance Fund: Caisse primaire d'assurance maladie (CPAM), gives the definition of PSG as: The polysomnography includes simultaneous EEG on one or two leads, EOG on one lead, and one of the following recordings:

- EEG on at least eight leads (10-20 international electrod placement);
- EMG on at least two leads for the tone of mentails and submentails muscles;
- Cardiorespiratory physiological parameters: noises, flow and respiratory effort, oxygen saturation (SaO_2) and heart rate.

The PSG is considered as the "gold standard" for the scoring of sleep and associated events[26], but the operation of PSG is complicated. In this case, respiratory polygraphy is introduced as a role of a simplified version of polysomnography, it does not perform neurophysiological measurements. Its definition given by the CPAM is as follows: "The nocturnal respiratory polygraphy includes the simultaneous realization of the following examinations: measurement of the SaO_2 by oximetry and nasobuccal air flow, and/or quantification of the snoring with recording of the tracheal noises, and/or evaluation of respiratory efforts, and/or analysis of the body position, over a nocturnal period of at least 6 hours. "

1.4.6 Examples of characterizations of abnormal respiratory events

Two examples of sleep apnoea adopted from [26] are presented. Figures shown below correspond to recorded signals from PSG. The signals correspond to: THOR RES – thoracic respiratory band; ABDO RES – abdominal respiratory band; F – front; B – back; L – left side; R – right side.

CSA

Fig. 1.28 presents 10-min recordings from PSG. It shows the presences of CSA because when there was no nasal pressure (marked in rectangles), the THOR RES and the ABDO RES are also absents (no respiratory effort).

OSA

Fig. 1.29 presents 5-min recording from PSG. Not like in 1.4.6, when nasal airflow is absent, there were still thoracic and abdominal movements (marked in rectangles). It indicates some OSA.

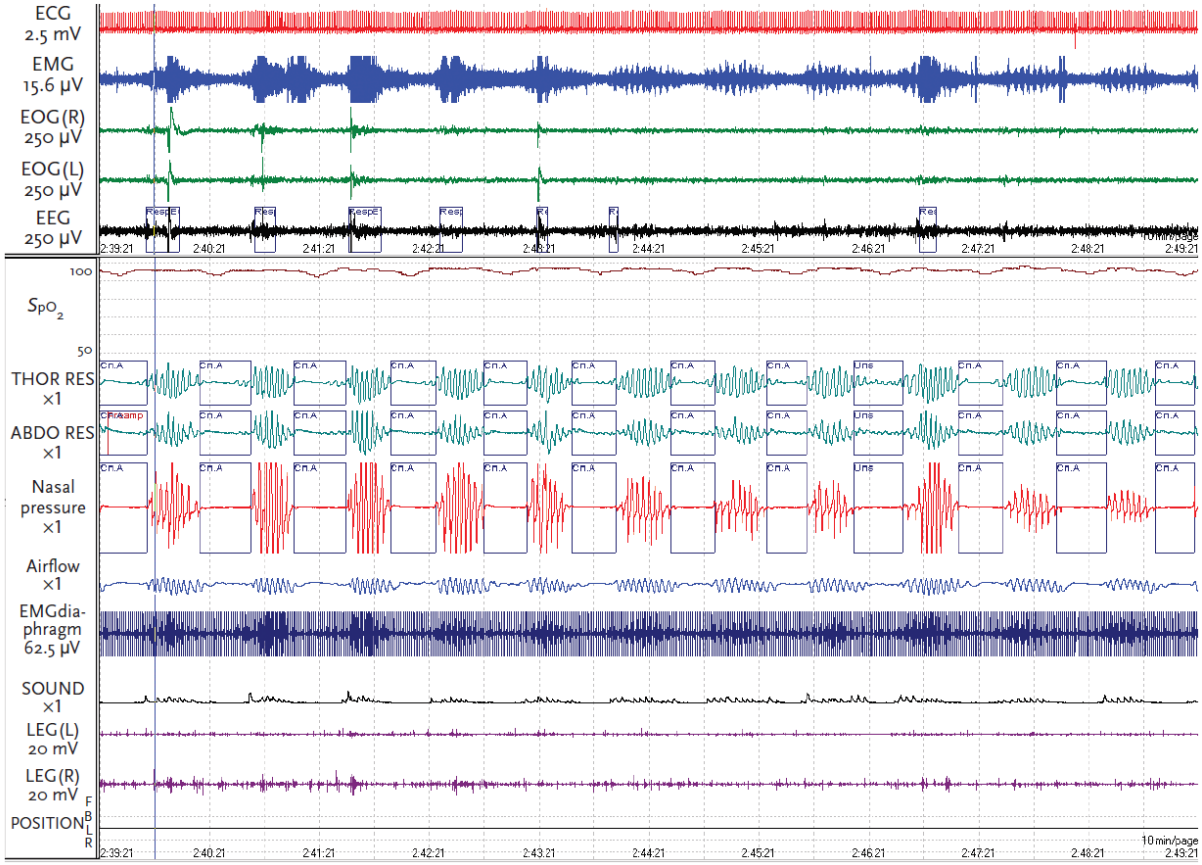

Figure 1.28: Example of PSG signals showing some CSA.

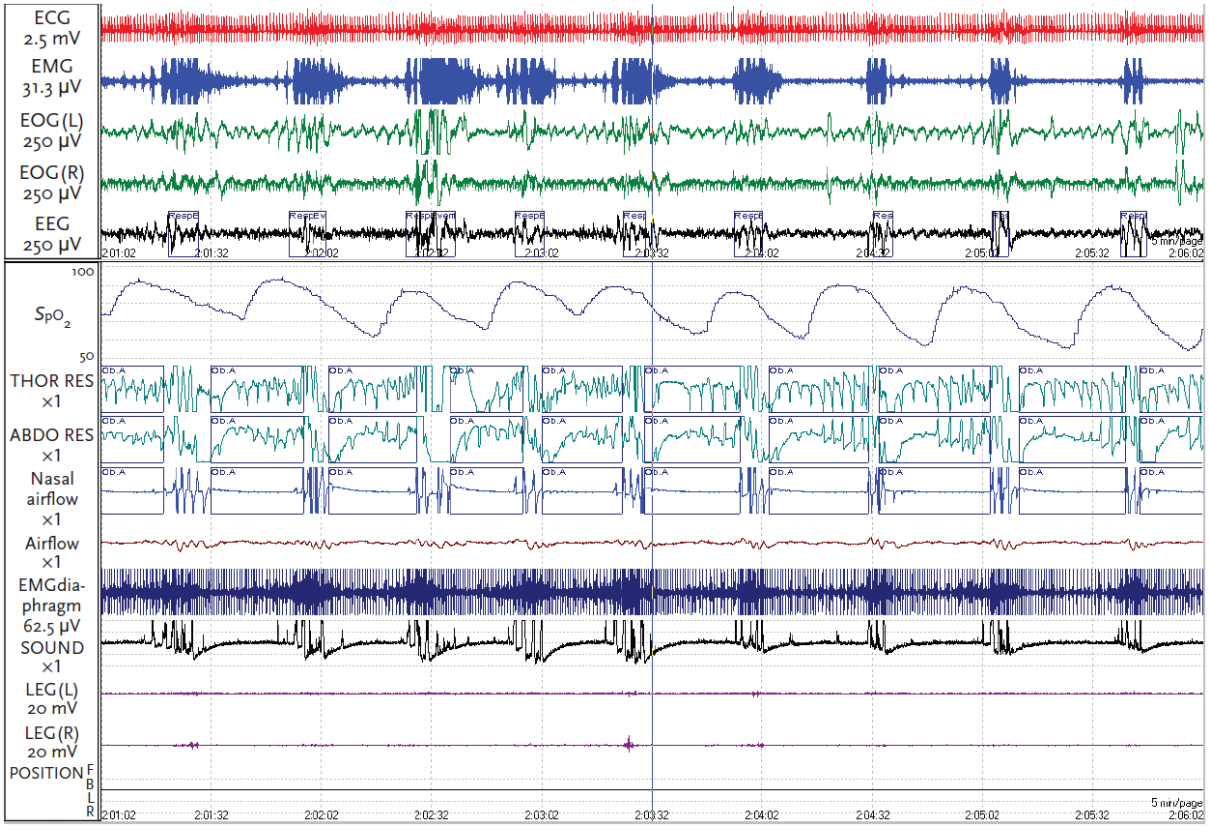

Figure 1.29: Example of PSG signals showing some OSA.

1.5 Respiratory detection from TS

1.5.1 Method selection

In the future, NEURORESP company intends to develop a portable respiratory polygraphy device which would play an important role in diagnostic assistance and home respiratory recording. As mentioned before (§1.3.1), for a customer to be reimbursed, a device has to be registered at HAS. This is a key point for patients to buy a medical device. The first condition to register in HAS is that the design of the device corresponds to the definition given by CPAM (definitions presented in §1.4.5).

In this thesis, the primary aim is to detect apnoea either to provide an alarm in case of apnoea while phrenic nerve stimulation is supposed to pace the diaphragm or to register automatically apnoea events during sleep apnoea. The secondary aim is to get a quantitative evaluation of the quality of the inspiration or to further investigate the type of apnoea (central of obstructive). As described in §1.4.5, the designed system is not intended to perform any neurophysiological measurement, but needs to be able to evaluate respiratory effort in order to identify central and obstructive apnoea, it is about a polygraph. According to the CPAM definition of polygraph (see §1.4.5), several sensor combinations could be acceptable. One ideal composition for diagnostic aid would be the use of an oximeter plus an airflow sensor and a respiratory effort sensor. However, the system should be usable without an extra surgery or with existing devices so that the monitoring device needs to be non-invasive and as invisible as possible. The existing measurement methods presented above (§1.4) are either too sensible to movements (e.g. plethysmography, ECG), or cumbersome with equipment placed on the patient face (e.g. nasal cannula, thermistor), or not portable (e.g. pneumotachograph, esophageal pressure).

In order to counteract the drawback of existing solutions, we propose a respiratory monitoring method using tracheal sounds (TS). We believe that this could be a good choice as this method is easy to apply and could be non-invasive. The use of TS has been recommended in ambulatory sleep apnoea diagnostic devices in 2004 [31]. Furthermore, TS contains respiratory sounds (to detect the presence of airflow) and cardiac sounds (like PCG). One interesting aspect is that the amplitude of cardiac sounds (S1/S2 peaks) varies regularly following the thoracic volume changes, which means the respiratory effort could be derived from this variation.

In summary, in following the definition given by CPAM, an ideal respiratory detection device should be ambulatory and non-invasive, should be suitable for long term and real-time recordings, and has to give a robust results. We also believe it would be interesting

to monitor other vital signals like cardiac rhythm, which could be possible to evaluate respiratory effort. So the chosen design of device would be microphones (TS) plus an oximeter (SaO_2).

1.5.2 Respiratory sounds

A sound is generated by a vibrating object and propagates under the form of waves. In the case of TS, the vibrating object is the air passing through airways - the turbulent airflow, and causing pressure vibrations that are transmitted to the body surface (e.g. the neck) throughout the tracheal wall and the surrounding tissues. Indeed, the recorded sounds directly from body surface are tracheal wall vibrations, not regular acoustic sounds. Thanks to this characteristic, the suprasternal pressure (SSP) can be extracted to evaluate the respiratory effort by some surface sensor [32], e.g. an accelerometer.

The tracheal wall vibrations (body surface tissue vibrations) also induce atmosphere pressure changes in the surrounding area as the sounds propagate in the air, so that we can "hear" the TS. This means that TS can be recorded indirectly by a microphone placed in the air close to the neck. As proposed in [33], some specific designs of the microphone support can be used to improve the quality of TS taking advantage of the resonance inside the concave support. We have used a similar approach as presented in §2.1.1.

Compared to lungs' sounds, tracheal sounds are more sensitive to airflow changes and are often considered to be purer and less filtered breath sounds [34]. With different airways structure (dimension), the characteristics of TS could vary because resonance of the airflow changes. One example is that children had significantly louder and higher frequency components TS than adults [35]. This phenomenon is also useful in studying abnormalities of the upper airway, as OSA screening tool in wakefulness [36].

1.5.3 The historical context of TS processing

The respiratory detection using tracheal sounds had been widely studied in the past.

- In 1980, Krumpe et al. first showed that an apnoea could be identified by the interruption of laryngeal sounds recorded at the neck [37][34].
- In 1982, Cummiskey et al. [38] demonstrated that using TS sensor to detect apnoea and hypopnea could have similar results compared to reference sensors such as the nasal pressure cannula.

- In 1988, Penzel et al. [39] developed a new product to differentiate obstructive apnoeas and hyperventilation occurrence in real time through the recording of snoring sounds from one laryngeal microphone.

- In 1989, Meslier et al. [40] were the firsts to show a good correlation in the detection of the number of apnoeas and their duration obtained from TS and synchronized pneumotachograph signals. This was performed on healthy participants.

- In 1990, also on healthy subjects, Soufflet et al. [41] showed a correlation between the TS and the respiratory flow and concluded that TS could be used to calculate the flow rate.

- In 2001, Chuah et al. [42] calculated the power spectrum in specific frequency bands for both the chest sounds and the tracheal sounds. Using peak picking technique, the former was used to detect respiratory phases and the latter was used to detect breathing onsets. On 17 sets of data (from 11 healthy subjects, aged 4-35), this method reached 93% of phase detection accuracy and 100% of breath onset detection accuracy.

- In 2004, Hult et al. [43] improved their detection method from 2000 [44]. They calculated the frequency content of tracheal sounds between 300 Hz and 1100 Hz in real-time, and applied a threshold detection approach to identify the presence of airflow. Finally, they could differentiate inspiration/expiration phases by verifying the pause duration, the respiratory events order and the frequency content in specific frequency bands. This improved method showed more than 90% of detection rate on two groups (heart decease and intensive care unit) of 10 patients.

- In 2008, Corbishley et al. [33] demonstrated that the suprasternal notch was the best place to record tracheal sounds. They also analysed the influence of inter-body noises and artifacts noises on respiratory sounds recordings. unfortunately, this influence (noises frequency band, amplitude, etc) may change according to different recording systems because recorded sounds characteristics highly depend on the used hardware [34]. This study finally proposed an algorithm that could be implemented into a miniature and low-powered sensing device. The algorithm was based on the temporal envelope detection with several user dependent threshold. This method was tested on 5 healthy participants in different situations (presence of surrounding noises, moving, falling, etc), the results reported in detected breathing time (91.3%), but apnoea events detection were specified.

- In 2009, Kulkas et al. [45] proposed to detect apnoea events based on the ratio of the power density between 0-50 Hz (heart beat) and between 0-600 Hz (heart beat and respiration). The processing was realized on a period of data, the longer

this period of data, the more accurate the detection results. When the data period was less than 5 seconds, the separability was less than 75%. In the same year, the same group developed another breathing detection method based on envelope extraction automatic patient-specific amplitude threshold determination [46]. On 6 patients with sleep apnoea, they obtained 100% of positive prediction values on 1434 respiratory cycles.

- In 2010, A.Yadollahi and Z.Moussavi [47] recorded both snoring sounds (a microphone hanging above patient's face) and tracheal sounds to detect apnoea. The recorded sounds were classified automatically based on their energy, zero crossing rate and formants. These 3 features (dimensions) were set to 1-dimensional space by using Fischer Linear Discriminant, then classified with Bayesian threshold. An overall accuracy of 90% was found. In the same year, A.Ydollahi et al. [48] had also proposed another detection method by combining tracheal sounds and SaO_2 signal recordings. They used the logarithm of the tracheal sounds variance in place of the energy of respiratory sounds [41][49] to estimate the respiratory relative respiratory flow. And some features (sounds energy, event duration, amplitude, etc.) were extracted based on this estimated flow signal. All these features were weighted and added together to determine apnoea with threshold detection. Finally, this method demonstrated a high correlation (0.96, $p<0.0001$) with PSG. Also in 2010, Mlynczak et al. [50] developed the first wireless TS sensor using a smartphone application. They studied the accuracy of a new method in differentiating between normal breathing sounds and snoring episodes.

- In 2014, Kalkbrenner et al. [51] developed a system to analyze sleep by tracheal sounds and movements recordings. A real-time method has been proposed to detect cardiac peaks. They compared detected cardiac peaks' amplitudes, intervals and frequency contents to estimate the next cardiac cycle. And respiratory phases were classified by using a threshold detection in the spectral power between 10-600 Hz.

- In 2016, Y.Nam et al. [52] proposed to use a smartphone to record nasal and tracheal sounds. They estimated breathing rate by using a Welch periodogram and an autoregressive spectrum. The result obtained from nasal sounds monitoring were excellent as the median errors were less than 1 %, but the use of tracheal sounds resulted in a poor estimation success.

- In 2017, Kalkbrenner et al. [53] improved their method by proposing an offline solution, which processed short-term and long-term envelopes of the tracheal sounds to evaluate the amplitude changes. They then combined these changes with movements (measured with IMUs) to detect sleep apnoea. They also introduced another algorithm to extract the hear beat with an amplitude threshold and a cardiac peak

interval threshold. This method was applied on 10 healthy subjects over a full-night recording, and compared with PSG and ECG. The sensitivity and specificity for apnoea detection reached up 92.8% and 99.7%, respectively. The estimated heart rate was also highly correlated with ECG.

- In 2018, Martin et al. [54] modified a workers' hearing protection device to record vital sounds from inner-ear. They estimated the cardiac rate and breathing rate by detecting temporal envelopes' peaks. This study showed an accurate cardiac detection but not for the breathing detection. Because compared to heart sounds, breathing sounds were too weak at inner-ear.

Actually, two products are available on the market using tracheal sounds for sleep studies. The first one is PneaVoX (CIDELEC, France, Fig. 1.30a) which could work with various PSG. Besides microphones, it equips an accelerometer to detect suprasternal pressure. This system filters recorded tracheal sounds to isolate the snoring part and the respiration part and then, using envelope detection combining suprasternal pressure signal (evaluating respiratory effort) to distinguish respiration, apnoea (central or obstructive) and snoring. The second product is Rainbow RRa (Masimo, USA, Fig. 1.30b). This product aims at monitoring the breathing rate from tracheal sounds. And it needs to be used with the Masimo Rainbow SET platform which could synchronize many other vital signals by using sensors from the same brand, as the oxygen saturation, heart rate, etc.

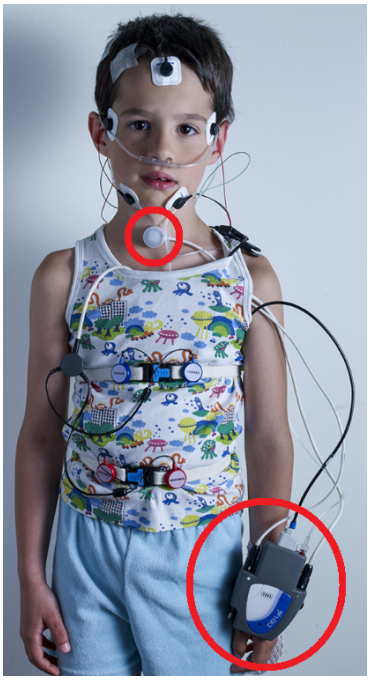

(a) PneaVox – Tracheal sounds and suprasternal pressure sensor.

(b) Protocol 3 – Recording example in lying position – Spectrogram.

Figure 1.30: Commercially available tracheal sounds sensors.

Among all the respiratory detection methods/products mentioned above, few could be used in real-time. And most of them aimed at sleep apnoea detection. This means that their application is possible only in the context of low noises and artifact (e.g. movements of patients) conditions. Moreover, only Corbishley et al. [33] studied the influence of internal body noises and environment noises on tracheal sounds recordings. But their study processed the recorded sounds only in temporal domain which makes it difficult to recognize some specific noises. Furthermore, their algorithm set 4 thresholds which are all user specific and were not adaptive. In conclusion all these methods are not suitable for a continuous daily life support use.

In this thesis, a real-time processing algorithm combining both temporal and frequency detection has been proposed. More importantly, in addition to heart rate, cardiac peaks were also extracted for analysing its variation in temporal amplitude. Because after observing certain recordings, cardiac sounds intensity varies depending on the respiration due to the thoracic volume changing. This method is called PDR, it was inspired by EDR, but the respiration is derived from PCG in place of ECG.

1.5.4 EDR and PDR

During respiration, chest movements change the distances between ECG electrodes, so affect the morphology of QRS-complexes (presented in §1.4.3). Based on these changes, the respiration could be measured indirectly from ECG signals – EDR. Depending on the chosen changing parameter, several EDR methods could be applied. The study of M.Schmidt et al. compared these different methods (changing parameters) [55] as follows:

- Central moment: the quantification of RS-slopes by 4^{th} order central moments.
- RS-slope: the maximum temporal derivative between R- and S-wave.
- RS-distance: the variation of the RS-interval length.
- QRS-Complex area: the integration of the ECG between Q-peak and S-peak.
- R-wave amplitude.
- Respiratory sinus arrhythmia: the differences of adjacent heart beats – RR-intervals (heart beat intervals). Because the central nervous system synchronized heart rate and respiration as the way that heart rate accelerates during inspiration and slows down during expiration.

In the case of PCG, there is no such QRS-complexes, but its position corresponds to S1 (§1.4.3). And the amplitude of cardiac peaks are also influenced by thoracic volume

changing due to the respiration. So among these methods above, the R-wave amplitude (S peaks amplitude in PCG) and the respiratory sinus arrhythmia (S1-S1 or S2-S2 in PCG) could also be applied to get PDR.

The first step is to detect cardiac peaks (S1 or S2) in extracted cardiac signal from tracheal sounds. Some presented studies in §1.5.3 processed also cardiac signals, but it looked only for FFT (frequency) of cardiac envelope to estimate heart rate. Martin et al. [54] detected cardiac peak by applying band-pass filter on cardiac signal's envelope and by threshold detection, but details was not described. The method of Kalkbrenner et al. [53] (predict next possible region then look for the local maxima inside this region) is possible to use in real-time, but the thresholds need to be adaptive because in some subjects the S peaks amplitude changing are too important due to respiration. More explication will be found in §2.2.3.

Moreover, the peak identification was realised directly on extracted cardiac sounds from tracheal sounds, this could be too noisy. In many studies, the envelogram of S1 and S2 would be first extracted for facilitating the cardiac peak detection. There were 2 wildly used methods to get S1 and S2 envelogram, the first is by shannon energy [56][57] and the second is by wavelet [58][59]. But in this thesis, the method by absolute value was chosen to get this envelogram (§3.2.5). The reason to pick this method will be discussed in §5.3.

Chapter 2

Experimental setup and data acquisition

2.1 Experimental setup

2.1.1 Microphone and support

Two uni-directional microphones (Pro-signal, ABM-708-RC) were used to record sounds: one for TS and one for environmental noise. The recorded environmental noise was intended to be applied to further reduce noise in the recorded TS, but it was not used in the present study (details in §5.4). The microphones were inserted into a bell-shaped support (Fig. 2.1a, whose design was inspired by [33]). The two microphones were located next to each other as illustrated in Fig. 2.1b. During manipulation, only the support was fixed on the neck at the suprasternal notch with two strips of adhesive tape (as shown in Fig. 2.2).

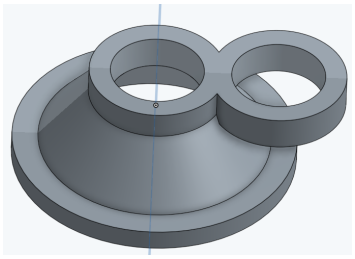

(a) Bell-shaped support

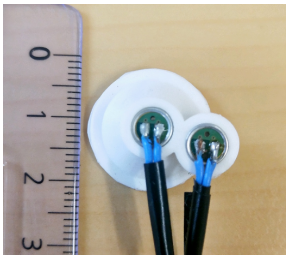

(b) Microphones and support

Figure 2.1: Illustration of the microphone setup.

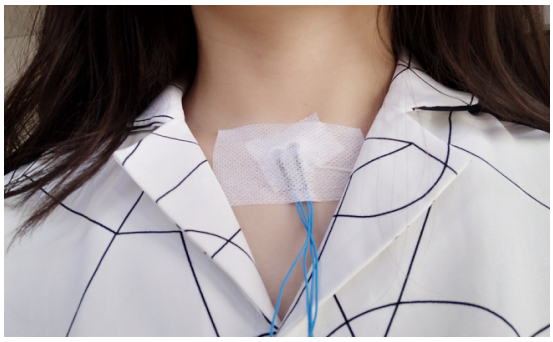

Figure 2.2: Position of the microphones: two microphones are inserted into the support that is fixed at suprasternal notch with two strips of adhesive tape.

2.1.2 Analog card

Tracheal sounds contain also environmental sounds (e.g. speech) which are much stronger than the respiratory sounds. To withdraw as much as possible these useless sounds, each microphone is connected to a customized analog card filters so that the useful band to that known to contain the respiratory and cardiac sounds is extracted and amplified before the acquisition.

Two 2^{nd} order Butterworth, Sallen & Key topology active filters were designed for filtering the sounds between 100 Hz to 1200 Hz. The filtered sounds are finally amplified 230 times. More details about the design of this analog card is presented in §Appendix A.

2.1.3 Signal acquisition

Two acquisition methods were applied depending on manipulation needs:

- High precision version: the PowerLab 16/35 (ADInstruments, Dunedin, New Zealand) acquisition device was used. This professional equipment can synchronize 16 inputs at once, and the sampling frequency can be adjusted up to 10 KHz between +5V and -5V per channel. Some other reference signals can also be synchronized with the PowerLab to evaluate the proposed detection method results: a low-resistance pneumotachograph (Hans Rudolf, 3700 series, linearity range 0–160l/min; Kansas City, MO, USA), an abdominal strap (AD Instrument/Pneumotrace II, UFI, Morro Bay, CA, USA) and 3 Ag/AgCl electrodes ECG (amplified with a Bio Amp : FE132, AD Instruments, Castle Hill, Australia). The power supply of PowerLab is connected to the electrical outlet, so this version of acquisition is not ambulatory.

- Portable version: the acquisition is done by NUCLEO-F429ZI electronic development card. The sampling frequency can be up to 8 KHz for one channel, and only 4 KHz

for two channels. Two batteries were used for power supply, this acquisition version has more portability but with a less acquisition precision.

All materials were shown in Fig. 2.3. The green circle is separated into 2 parts, each part presents one recording channel (one microphone). The portable acquisition card is put into an box showed in purple rectangular. The red rectangular represents the PowerLab 16/35.

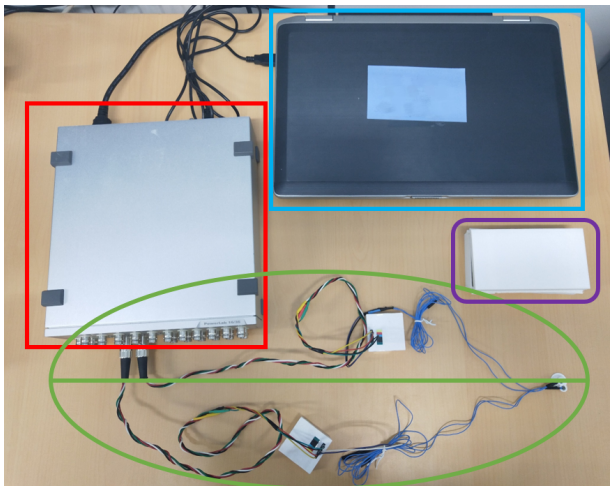

Figure 2.3: Materials of recording system.

All acquired signals are sent and processed using Matlab^{TM} (MathWorks, USA) with a computer (in blue circle).

2.1.4 Protocols

In this thesis, four protocols were designed. All protocols follow the same principle as illustrated below (Fig. 2.4). Only the microphone and the analog card were same for all protocols, other parts were changed according to different needs or for improvements.

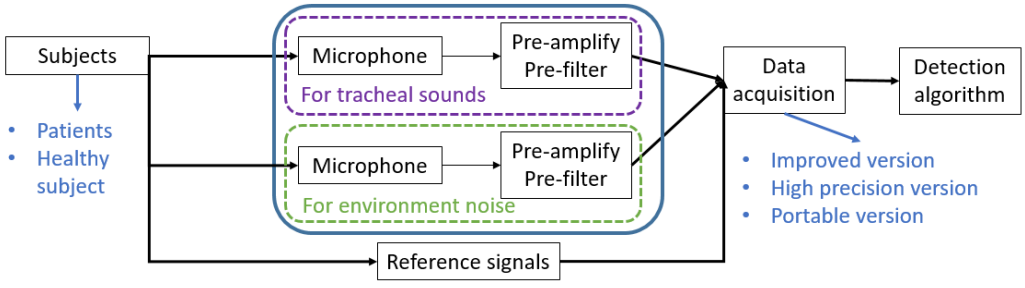

Figure 2.4: Principle of protocol design.

1. **Pilot protocol on healthy subjects** consisted in using the portable acquisition version with 18 healthy participants (4 women and 14 men aged from 20 to 60 years old). Signals were recorded in sitting position. All recordings were performed in the same room with the similar quiet environment. This protocol used on healthy volunteers to qualify the system setup (amplification and bandpass filter) without any other equipment, for protocol 3.

   Each recording lasted 30 seconds. The procedure consisted in 3 succeeding phases were the participants were asked to: (1) breath normally during the first 10s, (2) expire and then hold respiration for next 10s, (3) breath normally again for the last 10s.

2. **Pilot protocol on patient under IT-PNS** was also using the portable acquisition version, but with one participant who was implanted AtroStim IT-PNS device because of a high cervical cord tetraplegia following a ballistic lesion at the C2-C3 level. This patient gave his informed consent. This single trial was performed without any other equipment and was used to qualify the setup (amplification, bandpass filter) for the protocol 4.

   Two recordings of 30 s were performed during a visit routine at the hospital under medical doctor supervision. One recording was during phrenic nerve stimulation, another was during mechanical ventilation. Patient's usual stimulation configuration and parameters were unchanged.

3. **Clinic protocol on healthy subjects** was using the high precision acquisition version with 13 healthy participants, including 5 women and 8 men (Tab.2.1 age: 36 ± 10.37 years, weight: 66 ± 12.27 kg, height: 172 ± 7.84 cm). The study was conducted according to the principles of the Declaration of Helsinki and approved by the French Comité de Protection des Personnes Sud-Ouest & Outremer II, decision #2-18-12-MS1, 5 October 2018. The participants received detailed information about the study objective and methods and provided written informed consent. One example photo is shown in Fig. 2.5. The participant equipped a mask of pneumotachograph, an abdominal strap and 3 electrodes of ECG to compare the result with tracheal sounds.

   Each underwent two recordings of 2 minutes each: one in sitting position and the other in lying position. The 2-min sessions consisted of four parts: (1) normal respiration for 60 s, (2) apnea (spontaneous breath holding) for the next 10 s, (3) normal respiration while speaking for the next 20 s, and (4) normal respiration with strong environmental noise (a video with city traffic noise played right next to the microphones [60]) to the end.

4. **Clinic protocol on patients** aims at validating the new algorithm proposed in

Figure 2.5: One participant was being taken recordings for protocol 3.

this thesis on patients with sleep apnea or high tetraplegia. The idea is to assess the apnea detection on a representative sample on participants with sleep apnea and to assess the breathing events detection robustness on electrically assisted breathing on individual with tetraplegia equipped with an electrical stimulator implant. The study will be conducted according to the principles of the Declaration of Helsinki and approved by the French Comité de Protection des Personnes Sud-Ouest & Outremer II, decision #19-07-26-51403, 4 December 2019, an abstract (in french) could be found in §Appendix B. Two groups of patients will be included in short future:

- Population with sleep apnea: about 30 patients will be included, their TS recording will be synchronized with a full-night PSG at hospital. Recording processing for this group is to evaluate the performance of apnea detection of the new algorithm (because it is not possible to ask patients under IT-PNS to do apnea). The recordings will be processed with same algorithm in protocol 3 then compared with results of PSG.
- Population with high tetraplegia: 10 patients implanted with AtroStim IT-PNS system will be recorded when they realise their annual visit routine at hospital. The recording will be synchronized with a spirometer (respiratory volume measurement Fig. 2.6) and an oximeter to evaluate the new algorithm.

Subject number	Sex	Age	Height (cm)	Weight (kg)
1	F	35	165	66
2	F	51	168	57
3	M	35	170	64
4	F	28	160	53
5	M	25	183	75
6	F	31	158	52
7	M	27	180	65
8	M	50	175	79
9	M	51	180	56
10	F	36	173	74
11	M	50	170	65
12	M	25	173	70
13	M	30	180	95

Table 2.1: Information of the participants included in protocol 3: clinic protocol on healthy subjects.

The induced inspiration indicates the contraction of diaphragm, and sometimes 2 inspiration might appear for one respiratory cycle (details in in §2.2.2). So in this protocol, the EMG of diaphragms would also be measured to evaluate diaphragms contraction activities.

Figure 2.6: The spirometer for patients under IT-PNS.

An improved data acquisition version will be applied for this protocol. Instead of PowerLab or NUCLEO card, the acquisition instrument is changed to NI USB-6001 (National Instruments, USA), which is small like NUCLEO card but the acquisition performance could be precise enough as PowerLab. A kit of EMG measurements will also be added in recrording system, including: 3 channels of Biopac (USA) EMG amplifying/filtering instruments and an power supply card. The kit and two

channels microphones connect to NI acquisition card and will be synchronized with all recorded signals (Fig. 2.7). The validation of the detection method based on the specificity (at least 84.96%) and the accuracy (at least 90.48%). The calculation method will be presented in §4.

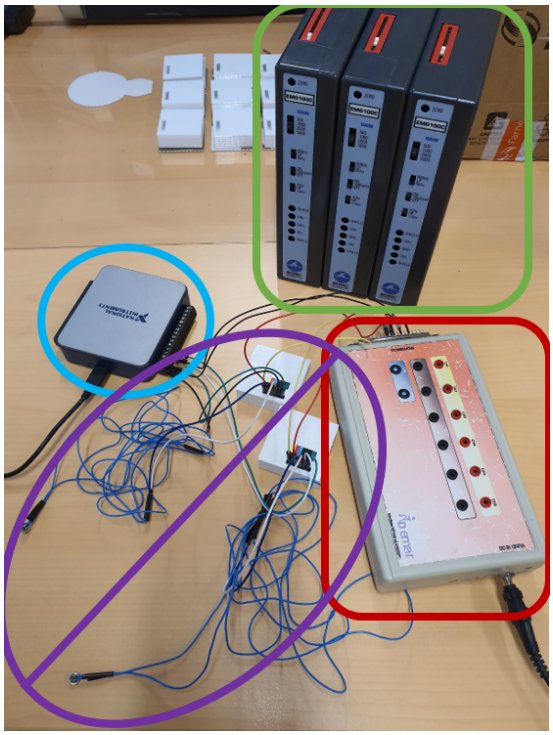

Figure 2.7: Improved experimental setup for protocol 4.

2.2 Preliminary data analysis for system specification

In this section, only some specific examples are shown to present signals' characteristics.

2.2.1 Recordings on healthy subjects with portable data acquisition card

In the context of spontaneous respiration, the respiratory frequency band from tracheal sounds varies depending on the recording system, but could normally be detected in 200 Hz-2000 Hz [34]. For the protocol 1, natural breathing has the most information between 100 Hz-900 Hz. Heart beat could be found between 0-300 Hz, but may differentiate according to the subject or the recording. To avoid frequency band overlap between respiration and heart beat, respiratory sounds need to be filtered between 300 and 900 Hz and heart sounds need to be filtered below 100 Hz. These frequency bands differ from those

related to induced inspiration (presented in §2.2.2). And as described in [52], for most recordings, there was no obvious frequency difference between inspiration and expiration.

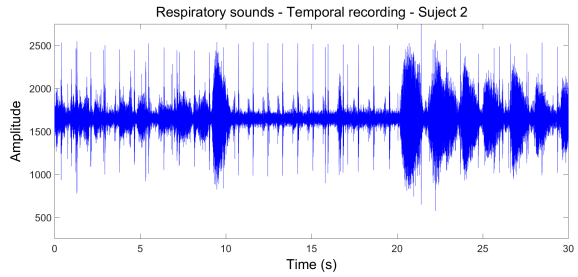

(a) Protocol 1 – First recording example.

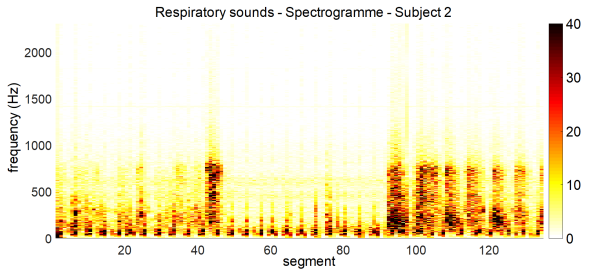

(b) Protocol 1 – First recording example – Spectrogram.

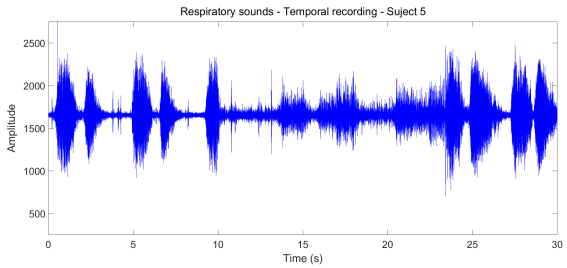

(c) Protocol 1 – Second recording example.

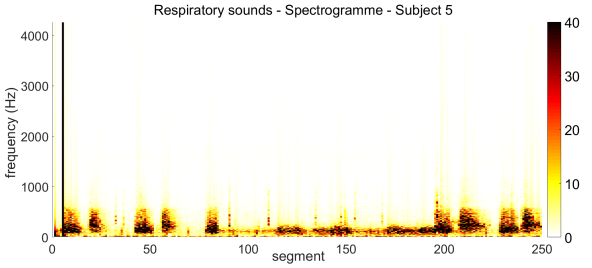

(d) Protocol 1 – Second recording example – Spectrogram.

Figure 2.8: Two recording examples from protocol 1 with their corresponding spectrogram.

Important changes in amplitude could be observed in the same recording, especially before and after apnoea. This is why some of the methods mentioned above (§1.5.3) with fixed temporal thresholds may not applicable in this case.

2.2.2 Recordings on high tetraplegia under IT-PNS

Data recorded under AtroStim IT-PNS is shown in Fig. 2.9a, and its spectrogram is shown in Fig. 2.9b. Examples of respiratory events are labeled in different colors, as well as some external noises. Frequency band for expiration is similar to the one of spontaneous normal expiration (both are passive actions), but there is one more band for inspiration: 2000-2500 Hz. This difference in higher frequency band could be a reference to identify the nature of inspiration, but it makes no difference for respiration detection. Some environment noises (in green circles) have obvious frequency and temporal "form" with respiratory phases so that could be easily recognized and eliminated. Even under stimulation, temporal amplitudes changes are still obvious between inspiration, expiration and pauses. But some groups of regular peaks occur about every 3.5 seconds in this recording, corresponding to the respiratory rhythm (17 times/min) determined by patient's

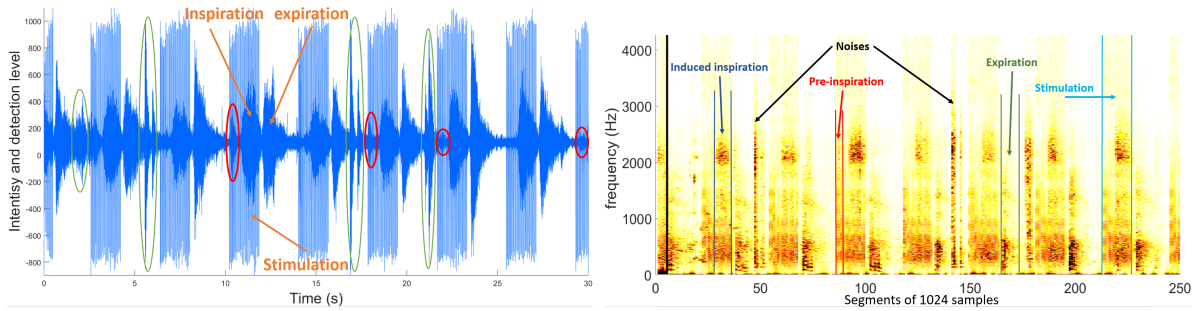

(a) Recording under stimulation in temporal domain.

(b) Recording under stimulation in frequency domain.

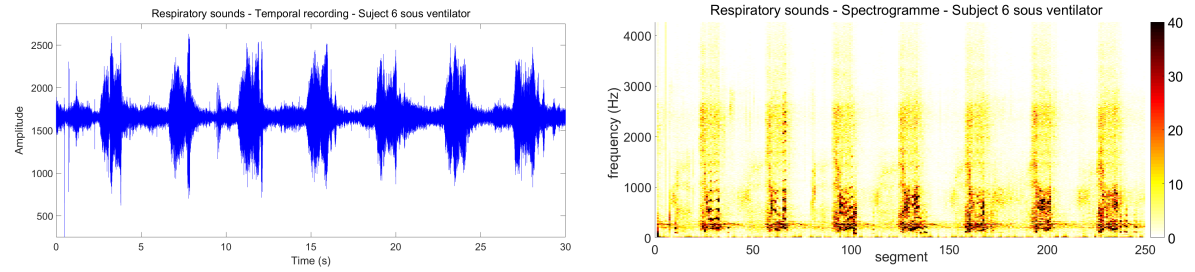

(c) Recording under ventilator in temporal domain.

(d) Recording under ventilator in frequency domain.

Figure 2.9: Two recordings of patients with IT-PNS and with mechanical ventilation.

stimulation system. Thinking of how the stimulation system works (in §1.3.3), these regular peaks were in fact electrical artifacts caused by radiofrequency communication, explained in Fig. 2.10. So these peaks could be considered as captured stimulation impulses.

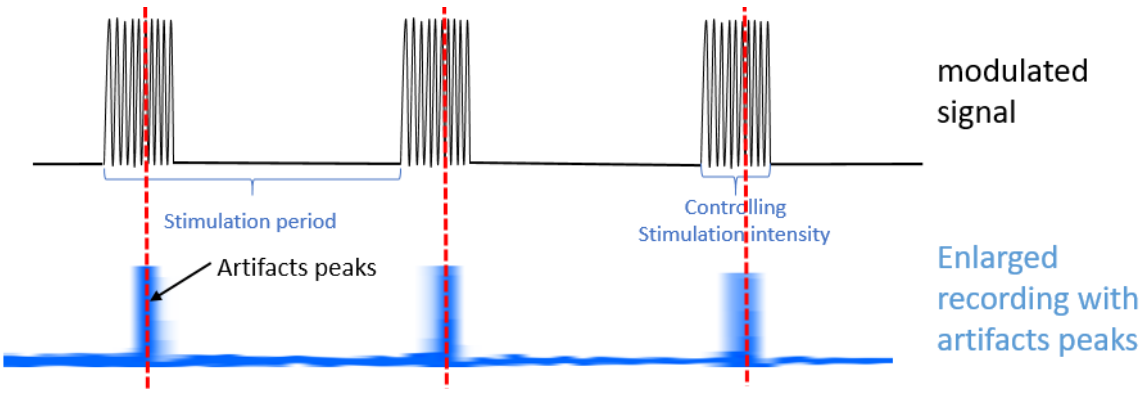

Figure 2.10: The artifacts peaks come from stat "ON" sent by radiofrequency – 25 MHz.

One zoomed zone of the breathing cycle is shown in Fig. 2.11. Each group of peaks lasts about 1.63 s within 40 peaks i.e. 25 Hz, corresponding to the stimulation frequency fixed in the stimulation system. As presented in §1.3.3, inspiration is induced when stimulation intensity reaches the intensity corresponding to tidal volume (I_{TV}). According to patient's stimulation parameters, his inspiration should begin 0.64 seconds later than the first peak of stimulation. But as shown in Fig. 2.11, in many cycles, another weak inspiration induced at the beginning of stimulation is present (identified by red cycles).

These pre-inspirations may be caused by some of the first contractions of the diaphragm muscle fibers. It could indicate a higher threshold stimulation intensity (I_{TH}) having been set.

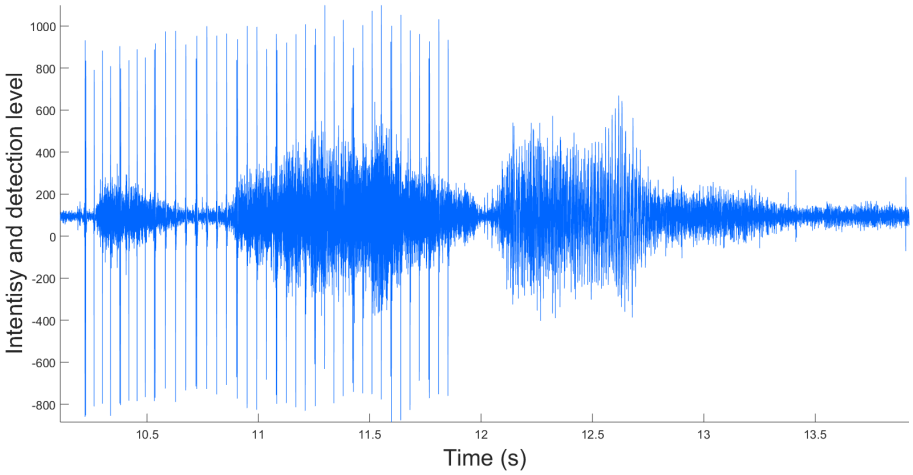

Figure 2.11: One enlarged respiratory cycle under IT-PNS.

The recording under the mechanical ventilation and its spectrogram are shown in Fig. 2.9c and Fig. 2.9d, respectively. Compared to stimulated inspiration, these inspirations performed by mechanical ventilation have much more important temporal amplitude because the ventilation machine made a lot of noise when it pressed air into the lungs. The same phenomena could be observed also in spectrogram. Contrarily, expirations were difficult to be observed in both domains. The main reason is the microphone was placed above the tracheotomy (Fig. 2.12) so that the air ventilated out through the tube connected to tracheotomy but not passed upper airways (no air passed under microphone to be recorded). The placement of microphone was too high also making the heart beat difficult to be recorded (too far from the heart). Finally, this recording wouldn't be taken account to test detection algorithm.

Figure 2.12: The placement of microphone for recordings under IT-PNS.

2.2.3 Recordings on healthy subjects with high precision acquisition instrument and reference signals

The Fig. 2.13 shows 2 recordings and its spectrogram from the same subjects but in position different. A reminder of the registration procedure is illustrated in the Fig. 2.13a. This protocol used same type of microphone and analog card circuit with protocol 1, so in recorded sounds, the respiratory and cardiac frequency band were similar with the ones in protocol 1 (100-900 Hz). And it's obvious that recorded tracheal sounds were more intensive in lying than in sitting.

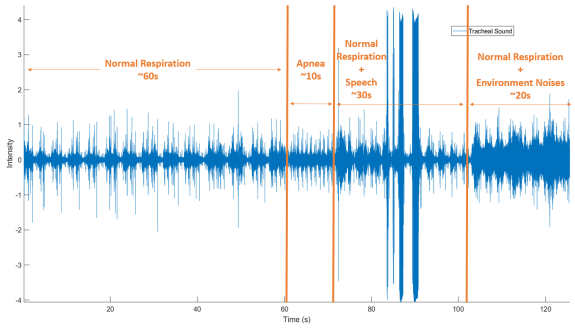

(a) Protocol 3 – Recording example in lying position.

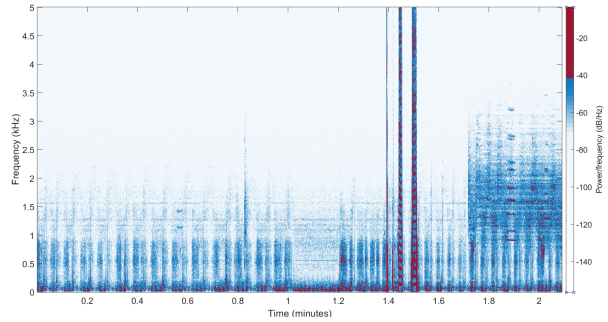

(b) Protocol 3 – Recording example in lying position – Spectrogram.

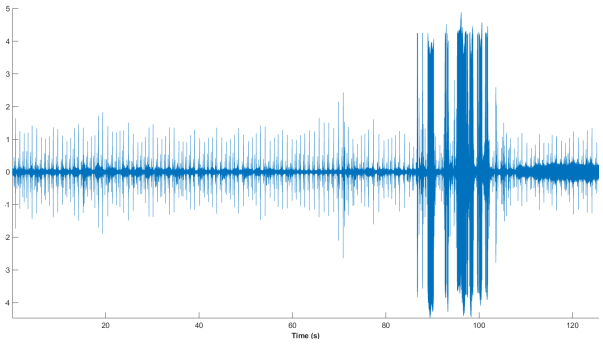

(c) Protocol 3 – Recording example in sitting position.

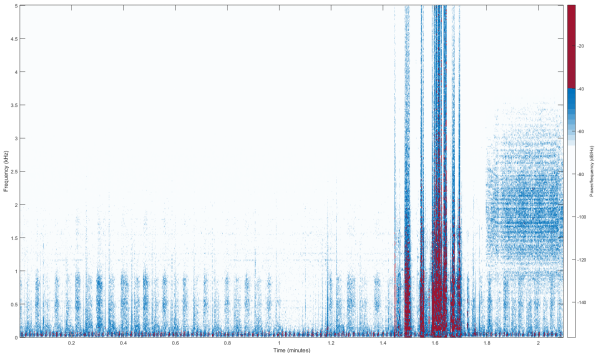

(d) Protocol 3 – Recording example in sitting position – Spectrogram.

Figure 2.13: Recording examples of one subject in different positions for protocol 3. Recording procedure: 0-60 s normal respiration (NR); 60-70 s apnea (holding breathing spontaneously, AP); 70-100 s normal respiration + speech (RS); 100-120 s normal respiration + environmental noise (RN).

For the last 20 seconds, same video was played in background (to ensure recording same frequency content of noises) with a smartphone. But the position of the smartphone was not fix to see if different intensity of noises would influence detection results. The cardiac peaks could be observed clearly, and their amplitude change a lot from the inspiration/expiration to pauses. This is why methods with fix threshold detection mentioned in §1.5.3 has not been used in this thesis.

Chapter 3

Algorithm for respiratory detection from tracheal sounds

3.1 Algorithm for pilot protocol

A preliminary respiratory detection algorithm was developed for the healthy subjects (protocol 1) and on one patient under implanted phrenic nerve stimulation (protocol 2). This algorithm was described in details in [1][2][3][4]. In simple terms, the recorded tracheal sounds were filtered with a high-pass filter at 300 Hz to eliminate cardiac influence. Then filtered sounds were processed both in temporal domain (envelope detection) and in frequency domain (PSD between 300-600 Hz) based on fixed patient-specific thresholds. An inspiration/expiration was considered as detected if it was detected in both two domains and their delay was less than one second.

3.2 Improved breathing detection algorithm for clinic protocol on healthy subjects

Based on the preliminary algorithm presented above, an improved algorithm was developed. In addition to the temporal envelope and the frequency detection, the PDR detection and cardiac information extraction would also be included. It is important to underline that the threshold applied in this method were non-patient-specific.

Recorded tracheal sounds ($ts(n)$) were processed in the temporal and frequency domains and also by the PDR method. The recordings were split into bins of $l\_seg = 16384$ sample (1.6384s) duration. This is convenient for the Fast Fourier Transform (FFT) algorithm

and enables the recording of at least one cardiac sound within each interval, assuming a heart-rat of minimum 38 bps. The global algorithm is shown on Fig. 3.1.

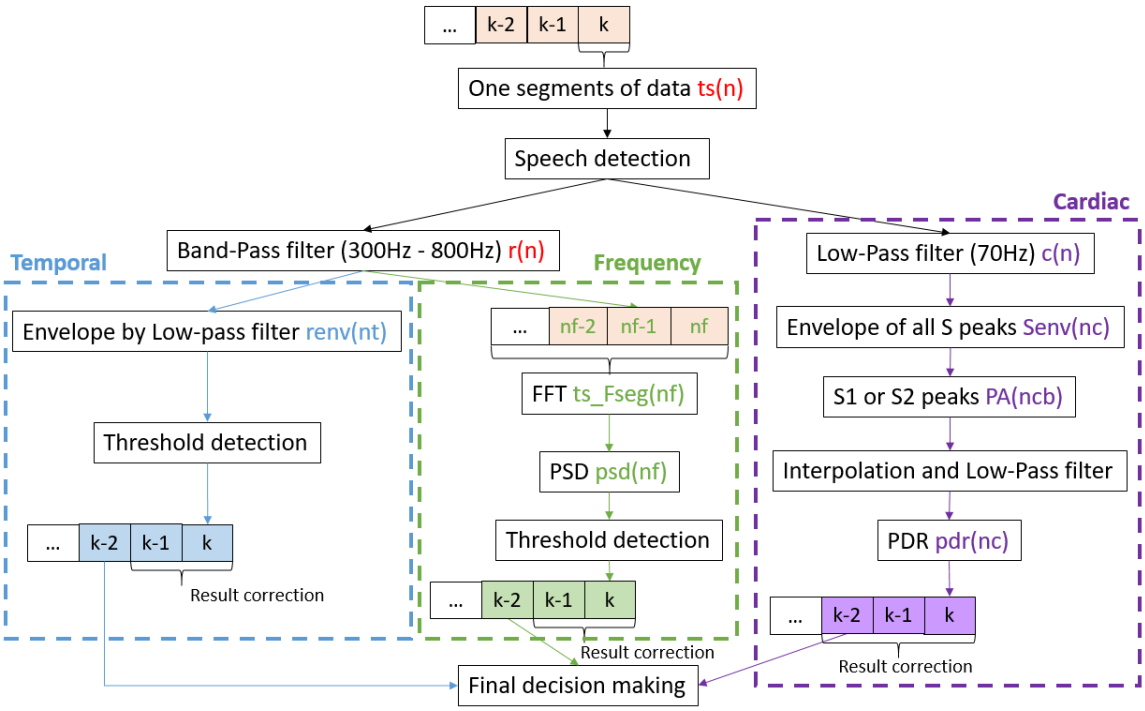

Figure 3.1: Diagram of the detection algorithm.

3.2.1 Speech detection

Speech or snoring can be considered as the expirations with the strongest intensity. These sounds have a much higher intensity and a simple detection based on a threshold on the Mean Absolute Value (MAV) was performed:

$$MAV(k) = \frac{\sum_{n=k\times l\_seg+1}^{(k+1)\times l\_seg} |s(n)|}{l\_seg},$$

where k is the index of the current bin. If this $MAV(k)$ exceeds 0.5, it indicates that speech/snoring has occurred during this bin.

3.2.2 Frequency band separation

Respiratory sounds are usually centered between 20 Hz and 2000 Hz, but this may differ depending on the acquisition system [34]. For our recording system, the respiratory frequency content was mostly centered between 100 Hz and 1500 Hz (Fig. 2.13b). Furthermore, assuming environmental noise at low and high frequencies just above 1200 Hz

State of $detect\_T(n)$	Explication	Conditions
0	Pause/apnea	$th\_T\_adapt(k) \leq th\_T\_min$
1	Inspiration/Expiration	$renv(n) > th\_T\_adapt(k)$
2	Speech/Snoring	$MAV(k) > 0.5$

Table 3.1: Temporal detection states

(Fig. Fig. 2.13d), we designed a steep band pass filter with an eighth-order Butterworth from 300 Hz to 800 Hz to extract the respiratory signal ($r(n)$). To extract the cardiac sound signal, we designed a steep low-pass filter that extracted its most significant part, an eighth-order Butterworth low-pass filter at 70Hz to get the phonocardiogram ($c(n)$).

3.2.3 Temporal envelope detection

The temporal envelope ($renv(n)$) of the respiratory signal was obtained by applying a second-order low-pass Butterworth filter at 0.8 Hz on the rectified signal $|r(n)|$. Then, two thresholds were applied on $renv(n)$:

1. The minimum threshold:

$$th\_T\_min = 110\% \times renv(3\_s\_apnea),$$

   where the $renv(3\_s\_apnea)$ is $renv(n)$ within any 3 seconds of apnea in the same recording;

2. The adaptive threshold:

$$th\_T\_adapt(k) = 90\% \times \frac{\sum_{n=k\times l\_seg+1}^{(k+1)\times l\_seg} renv(n)}{l\_seg}.$$

The result of the temporal envelope detection ($detect\_T(n)$) was fixed to three states, presented in Tab.3.1.

If $detec\_T = 1$ was obtained for bin k, an error correction method was applied on bins $k-1$ and k: a detected respiratory event was eliminated if it lasted less than 0.6 seconds because its duration was not in the normal range for an inspiration/expiration; $detec\_T(n)$ was forced to "0" if the interval from the previous detected event was less than 0.6 seconds. The middle-timing moment of a detected event was labeled ($detec\_T(n) = 1.5$) to indicate the position of this event to serve for the final decision-making. A temporal detection example is shown in Fig. 3.2a, where the pneumotachograph signal (in purple) is considered the reference, a positive signal indicates an inspiration, and a negative one indicates an

expiration. We also plotted the temporal envelope (in blue), the adaptive threshold (in pink), and the minimum threshold (in gray). The final temporal detection result is in red with the peak "middle-timing moment". The minimum interval and event duration are both 0.6 s.

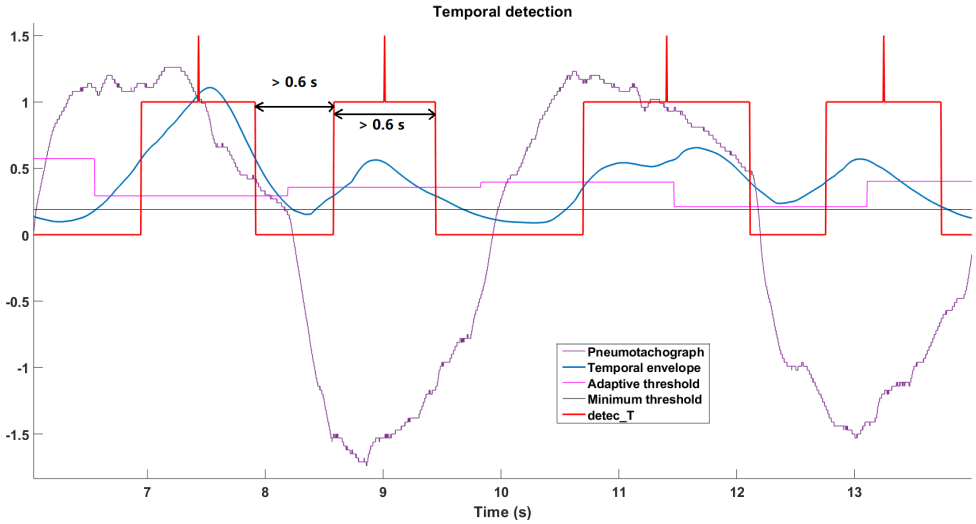

(a) Temporal envelope detection. The minimum interval and event duration are both 0.6 s.

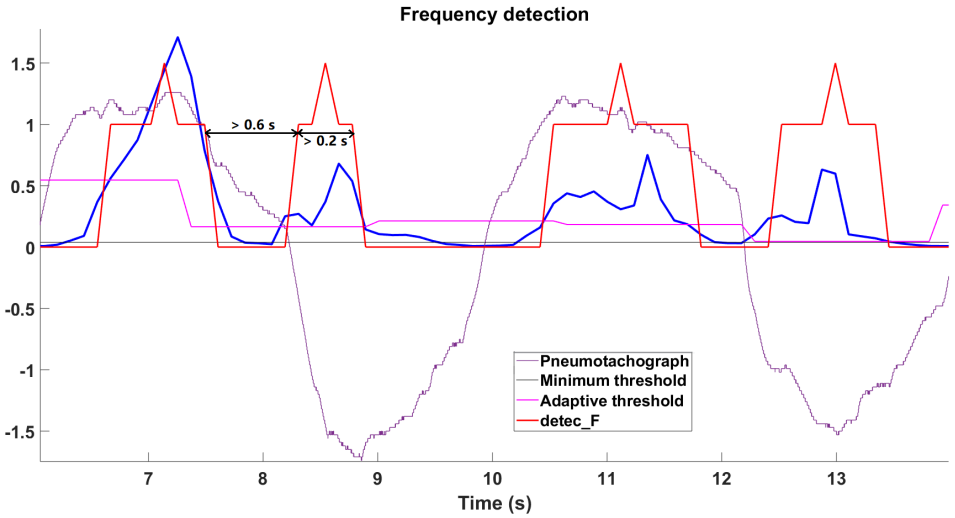

(b) Frequency detection. The minimum interval is 0.6 s and the minimum event duration is 0.2 s

Figure 3.2: Temporal and frequency detection result of the same period from the same recording. A positive (resp. negative) pneumotachograph reference signal (purple) indicates inspiration (resp. expiration). The adaptive (pink) and minimum thresholds (gray) are marked in the figure. The envelop signal (temporal or PSD) is in blue and the final detection result is in red with the peak "middle-timing moment".

State of $detect\_F(nf)$	Explication	Conditions
0	Pause/apnea	$th\_F\_adapt(k) \leq th\_F\_min$
1	Inspiration/Expiration	$psd(nf) > th\_F\_adapt(k)$
2	Speech/Snoring	$MAV(k) > 0.5$

Table 3.2: Frequency detection stats.

3.2.4 Frequency detection

In the frequency domain, one bin k of tracheal sounds $ts(n)$ was divided into segments of 2048 samples (15 segments per bin). An FFT was processed on these segments with a Hanning window and 50% overlap ($TS\_Fseg(nf)$). According to our recordings and frequency analysis, the useful frequency content was indeed between 400 Hz and 700 Hz: the PSD of this band was calculated ($psd(nf)$) as the frequency envelope. The detection part was similar to that described for the temporal envelope detection. Two thresholds were applied on $psd(nf)$:

1. The minimum threshold:

$$th\_F\_min = 110\% \times psd(3\_s\_apnea),$$

   where the $psd(3\_s\_apnea)$ is $psd(nf)$ within any 3 seconds of apnea;

2. The adaptive threshold:

$$th\_F\_adapt(k) = 90\% \times \frac{\sum_{nf=k\times nb\_seg+1}^{(k+1)\times nb\_seg} psd(nf)}{nb\_seg},$$

   where nb_seg is the number of segments per bin, which equals 15.

Like $detec\_T(n)$, the frequency detection signal $detec\_F(nf)$ also had three states, as presented in Tab.3.2, and the middle-timing moment of detected events was labeled as $detec\_F(nf) = 1.5$. For the error correction, the interval of each respiratory event should be longer than 0.6 second, and the minimum duration of each respiratory event is 0.2 seconds (illustrated in Fig. 3.2b).

3.2.5 PDR detection

In the cardiac domain, the MAV of the cardiac sound was computed every 0.06-second window (600 samples) with 0.03 seconds (50%) overlapping to obtain an envelope of S1

and S2 ($Senv(nc)$) [56]. The choice of this envelope method will be discussed in details in 5.3. As mentioned in 1.5.4, only S1 or S2 should be detected to represent the variation of amplitude due to respiration.

Inspired by the method of Kalkbrenner et al. [53], the detection of S1 or S2 was more robust in that the time intervals between these events could be bounded, as illustrated in Fig. 3.3. Time boundaries were defined as follows: where pa_tmin and pa_tmax are borders of this area in the time axis, based on the previous beat-to-beat interval marked with a black line (in Fig. 3.3) and defined with the following conditions:

$$pa\_tmin(ncb) = 80\% \times b\_b(ncb-1)$$
$$pa\_tmax(ncb) = 120\% \times b\_b(ncb-1)$$

$b\_b(ncb-1)$ is the previous beat-to-beat time interval. Moreover, the lower boundary is limited to 0.4 s (150 beats per minute (bpm)) and the higher to 1.2 s (50 bpm). The local maxima in the predicted area $PA(ncb)$ were considered the cardiac peak if its amplitude was higher than the adaptive threshold:

$$pa\_adap = 2 \times mean(Senv(nc));$$

At the same time, the pa_adap should be greater than the minimum intensity threshold presented with a black dotted line in Fig. 3.3) and defined as:

$$pa\_min = 30\% \times mean(Senv(first\_10\_seconds));$$

where $Senv(first\_10\_seconds)$ is the cardiac envelogram for the first 10-seconds of recording. If there was no matching peak in this area, $PA(ncb)$ was moved forward two samples to verify another local maxima.

A first-order interpolation between each detected peak (green dotted line in Fig. 3.3) was applied and the signal was upsampled at the same frequency of $Senv(nc)$. Then the signal was filtered at 0.25 Hz by a second-order low-pass Butterworth filter. The filtered signal represents the upper envelope of S1 (or S2). Our hypothesis was that its variation would be due to respiratory effort (changes in thoracic volume): an increase in the signal would indicate an inspiration while a decrease indicates an expiration. To reflect the correlation between the reference signals and the variation in the envelogram, we further assumed that its derivative was representative of the respiration phases as it was linked to the variation in the S1/S2 peak envelogram. We called this new curve PDR: phonocardiogram-derived determination of respiratory rhythm ($pdr(nc)$), indicating an inspiration when it is positive and an expiration when it is negative.

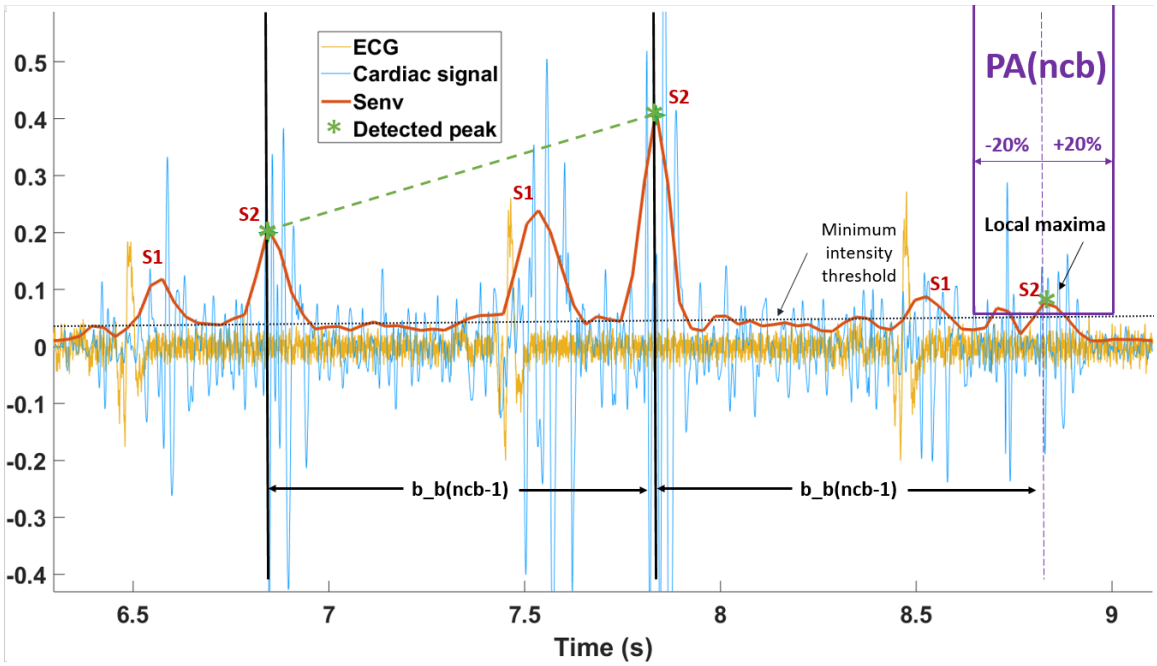

Figure 3.3: Cardiac S peak detection. There is a small delay between the ECG (yellow) and the extracted cardiac signal (blue). Predicting area PA(ncb) (purple) defined by ±20% of last heart beat-to-beat interval b_b(ncb − 1) and the adaptive threshold. The cardiac envelogram is in red and the detected cardiac peak (S1/S2) is marked by a green star.

State of $detect\_T(n)$	Explication	Conditions
-1	expiration	$pdr(nc) < 0$
1	Inspiration	$pdr(nc) > 0$
0	Pause/apnea	$event\ duration < 0.7s$ or $intervall < 0.1s$
2	Speech/Snoring	$MAV(k) > 0.5$

Table 3.3: Cardiac detection (PDR) stats.

Unlike the two previous detection domains, the PDR signal ($pdr(nc)$) was able to distinguish inspiration and expiration. Thus, the cardiac (PDR) detection signal $detec\_C(nc)$ had four states as presented in Tab.3.3, and the middle-timing moment of detected events were labeled as $detec\_C(nc) = 1.5$. If there were continuous inspirations/expirations, they were merged because usually inspiration and expiration alternate. The respiratory effort signal showed few respiratory pauses (about 0.2 s) or long duration respiratory events although some detected event durations could last more than 3 seconds. Thus, the error correction was applied on three bins: k, k-1 and k-2. This made a processing delay of about 3.2 s (2 bins), which is acceptable according to the definition of apnea (10 s of absence of air flow). An example of cardiac detection is shown in Fig. 3.4. The minimum respiratory event interval becomes 0.1 seconds, and minimum respiratory event duration fixes as 0.7 seconds.

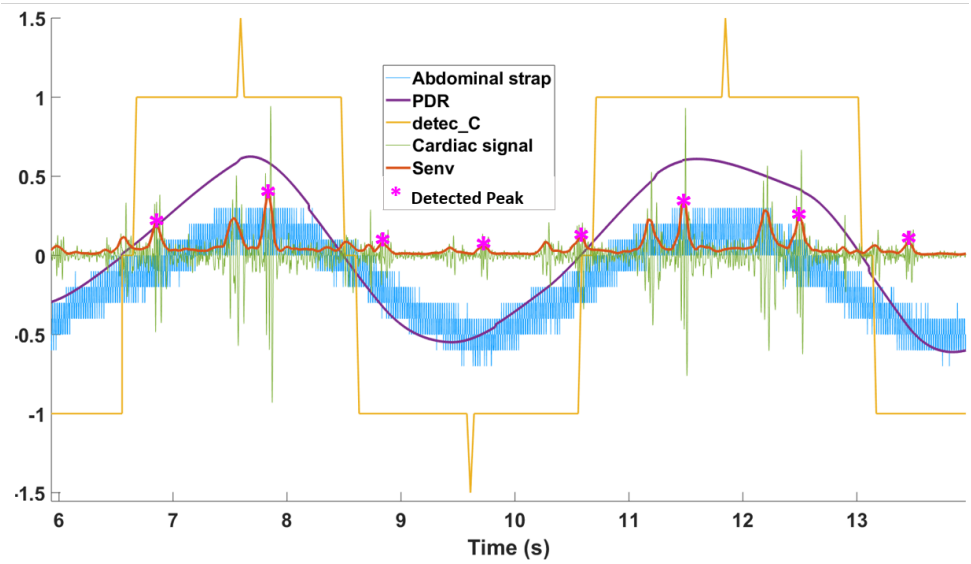

Figure 3.4: Phonocardiogram-derived determination of respiratory rhythm. The extracted cardiac signal is shown in green, and the processed envelogram is in red. Only one cardiac peak (S1/S2) detected (pink star) for each cardiac cycle. Positive (Negative) of the PDR detection result (yellow) indicates the inspiration (expiration) as reference signal.

3.2.6 Decision-making

The temporal and frequency envelope detected the presence of airflow (apnea or not), whereas PDR also assesses respiratory efforts to distinguish between central and obstructive apnea. The final detection was the fusion of the three detection domains. To detect apnea alone or the complete set of respiration phases, two decision-making methods are defined:

Apnea detection The parameter Q is used to evaluate the respiratory status and was calculated by the weighted average as follows:

$$Q = 1.5 \times \frac{\sum_{nt=1}^{NT} detec\_T(nt)}{NT} + 1.5 \times \frac{\sum_{nf=1}^{NF} detec\_F(nf)}{NF} + 0.5 \times \frac{\sum_{nc=1}^{NC} |detec\_C(nc)|}{NC}$$

For the bin $k-2$, the final decision ($detec(k-2)$) is made as:

$$detec(k-2) = \begin{cases} 1 \rightarrow respiration\ if\ Q \geq 1.5 \\ 0 \rightarrow pauses\ if\ Q < 1.5 \\ 2\ if\ speech/snoring \\ -1 \rightarrow apnea\ if\ pauses > 10s \end{cases}$$

An example is shown in Fig. 3.5. In theory, the PDR is used to evaluate respiratory effort. However, when the signal-to-noise ratio is low because of weak respiratory sounds, PDR detection may have a better result than those obtained in the temporal and frequency

domains. Nevertheless, most of the time, temporal and frequency domain detections were more sensitive, so the PDR detection results are less weighted.

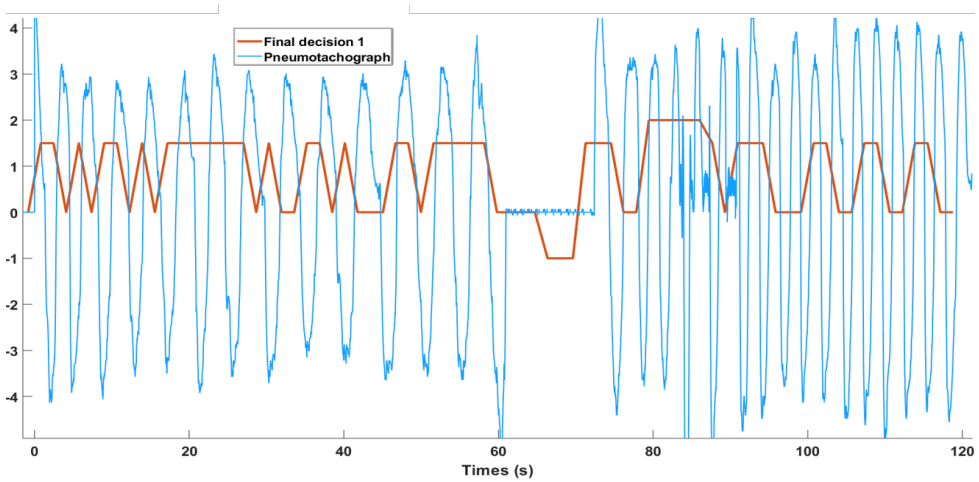

Figure 3.5: Final decision-making for apnea detection. The reference signal: pneumotachograph is in blue and the apnea detection signal is in red. Detection stat: 2 – Speech; 1.5 – Respiration; 0 – Pauses; -1 – apnea.

Respiratory event detection The second algorithm detects the presence of each respiratory event. A respiratory event was considered to be detected if it was detected in at least two of the three detection domains and the intervals between them were less than 1 second estimated with their middle-timing peak distances. An example is shown in Fig. 3.6.

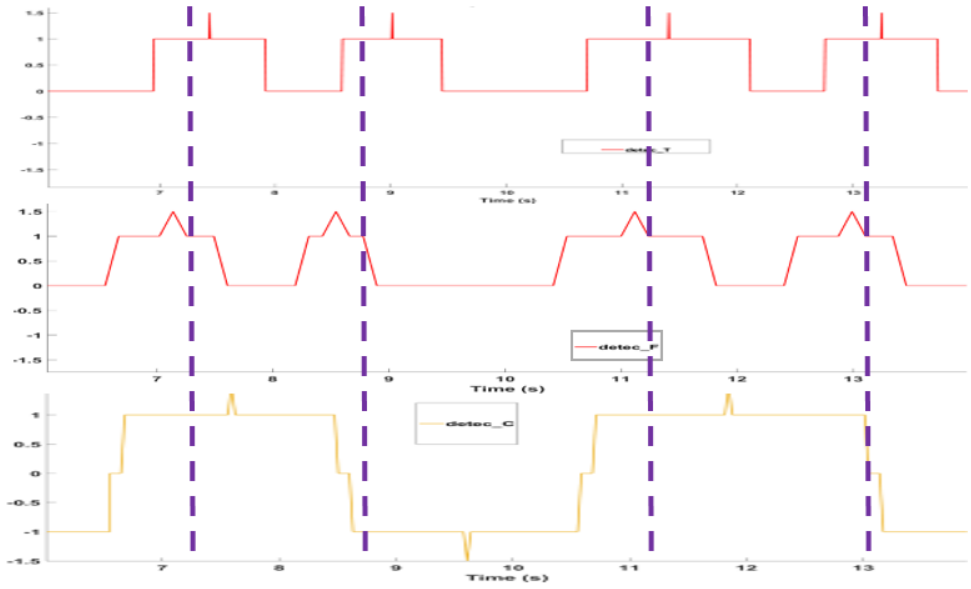

Figure 3.6: Final decision-making for respiratory event detection. Top: results from temporal detection; Middle: results from frequency detection; Bottom: results from cardiac (PDR) detection. The final detected events are marked in purple dashed lines.

3.2.7 Statistics

Several means comparing statistical tests were applied to show the influence of speech, noise and participant position. The compared data were: (1) SSA during NR+AP versus RS+RN (Fig. 2.13a), (2) SSA from sitting versus lying, (3) SSA of each detection domain versus the final combined results, (4) correlation between PDR and EDR, and (5) correlation between S-S and R-R intervals; all compared data were paired. Based on the Shapiro-Wilk test, if the data were normally distributed, the paired Student test was applied to compare means, otherwise the Wilcoxon test was applied to compare medians. If the p-value was $\geq$0.05, we concluded that the difference between the two paired samples was not significantly different.

Chapter 4

Results

4.1 Evaluation method

According to the two final decision-making methods (§3.2.6), the respiratory detection results were evaluated on: (1) the ratio of apnoea detection (only for protocol 3 – clinic protocol on healthy subjects), and (2) the performance of breathing phase detection with SSA, which are defined as follows:

$$Specificity = \frac{TN}{TN + FP}$$
$$Sensitivity = \frac{TP}{TP + FN}$$
$$Accuracy = \frac{TP + TN}{TP + TN + FP + FN}$$

where TN, FP, TP and FN are respectively the number of true negatives, false positives (Fig. 4.1a), true positives and false negatives (Fig. 4.1b).

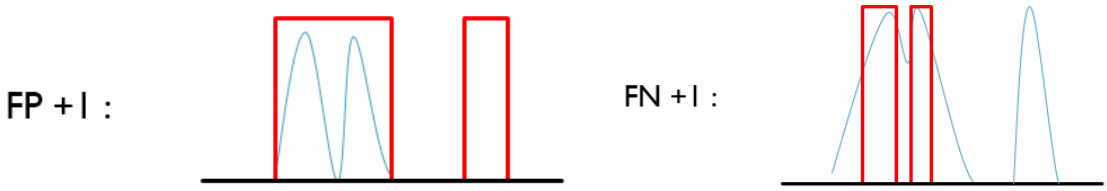

(a) Special false positive situation (b) Special false negative situation

Figure 4.1: Example of respiratory event counting. Respiratory envelope (in blue), detection signal (in red). (a) If two continuous respiratory events are recognized as a single event, or the pause/apnoea is detected as one respiratory event, a false positive detection will be reported; (b) If one respiratory event is recognized as two events, or one respiratory event is not detected, a false negative detection will be reported.

In our context, the detection system must not detect breaths that do not occur during apnoea, i.e., FP. Given the definition of apnoea which is an absence of respiratory flow for at least 10 s, and the observation that the respiratory rate is on average 15 cycles per minute, this leads to:

- the specificity of respiratory detection (breathing/apnoea) from TS must be >82.9%.
- the accuracy of respiratory detection (breathing/apnoea) from TS must be >90.5%.

The FN are less important for patient safety. Given that the sensitivity is inversely proportional to FN, we fixed a minimum of 80% corresponding to <25% of FN compared to TP.

4.2 Detection result for pilot protocol on healthy subjects (protocol 1)

An example of one breathing detection result is shown in Fig. 4.2. Three detection signals are illustrated in this figure: the temporal detection is in orange, the frequency detection is in green and the combined detection is in yellow. All detection signals have two states, indicating if there is a respiratory event (high) or not (low). In this example, all respiratory events are successfully detected.

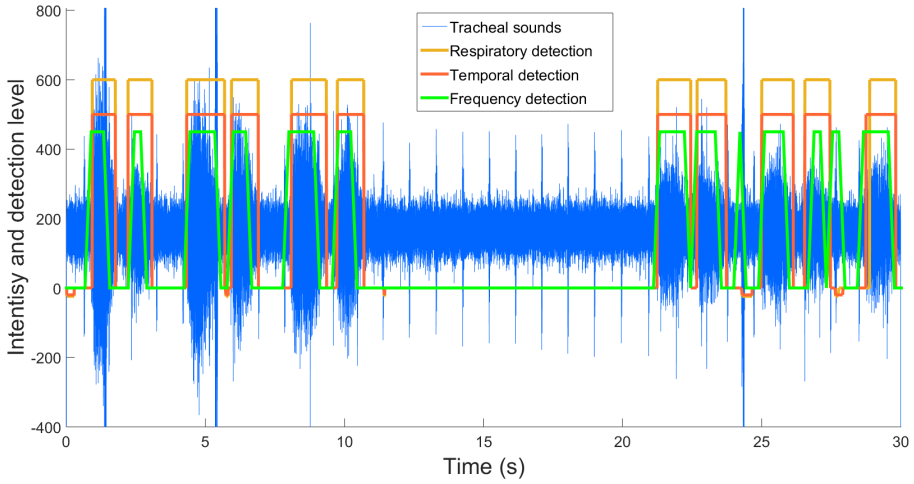

Figure 4.2: One example of detection result for a 30-seconds recording in protocol 1

For 18 recordings in protocol 1, all apnoea events were detected successfully. The Fig. 4.3 illustrated the specificity, sensitivity and the accuracy for each subject.

The mean values of detection result were 99.31%, 96.84% and 98.02% for specificity, sensitivity and accuracy, respectively. These results meet the minimum requirements for

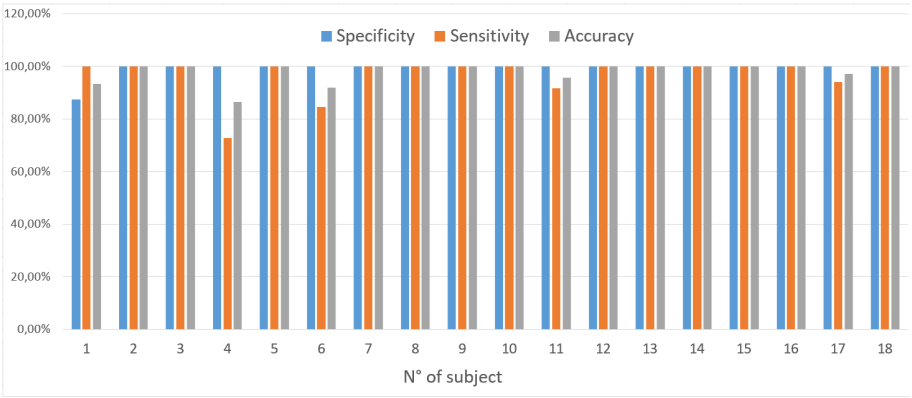

Figure 4.3: One example of detection result for a 30-seconds recording in protocol 1

the system. But there was no reference signal to compare, all the validations were done by hand. Furthermore, this method needs several patient-dependent fixing thresholds, which is not easy to apply in real-time.

4.3 Detection result for pilot protocol on patient under IT-PNS system (protocol 2)

An illustration of the detection result is presented in Fig. 4.4. The temporal detection result is shown in yellow, the frequency detection result is shown in purple and the final detection is shown in red.

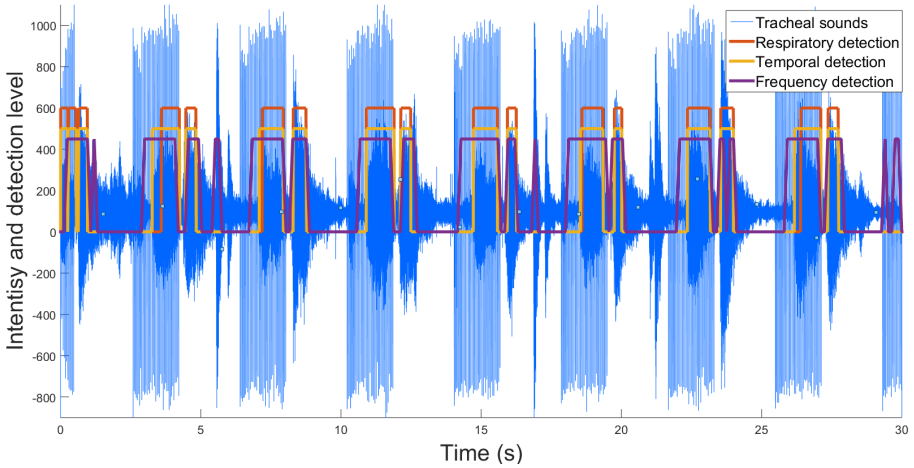

Figure 4.4: Detection result for the 30-seconds recording under IT-PNS

For this recording of 30 seconds, 9 induced inspirations and 8 expirations are all detected successfully. Some noises at 2 s, 6 s, 17 s and 21 s are eliminated. And all pre-inspirations (mentioned in 2.2.2) are not considerate as respiratory events.

Even-though only one recording data set was recorded in this protocol, the detection result demonstrated the feasibility of this respiratory detection method for users of implanted IT-PNS system. Furthermore, the captured stimulation signal could indicate a dysfunction of the pacing system (by verifying its stimulation cycle and its stimulation frequency) and recorded tracheal sounds could give a feedback of the electro-ventilation quality (duration, intensity and number of induced inspiration). The synchronization of these two information could indicate if the stimulation settings (intensity, frequency ...) are adapted. For example, in the present case, I_{TH} may be set too high (parameter details in §1.3.3) because some small pre-inspirations are induced at the beginning of the stimulation. Moreover, one possible application of this system during the implantation surgery would be to help verifying electrodes contacts and adjust stimulation settings instead of relying on the visual observation of diaphragm contractions as it is assessed usually.

4.4 Detection result for clinic protocol on healthy subject with reference signal (Protocol 3)

The proposed algorithm was applied on a total of 26 recordings of 2 minutes from 13 healthy participants, 13 in sitting and 13 in lying positions. All speech episodes were detected successfully in all the recordings.

4.4.1 Apnoea detection

The rate of successful apnoea detection was 92.3%. Among the 26 recordings that included a single apnoea phase, two were missed and detected as long pauses because of unexpected environmental noise. In seven recordings, one or two more apnoeas were reported because the recorded respiratory sounds were too weak.

4.4.2 Respiratory event detection

This method detects all breathing phases including apnoea. If only apnoea detection is looked at, the success rate was 88.5%, slightly less than the previous method (92.3%).

Looking at all respiratory events, for all 26 recordings, the average of these detection results (Fig. 4.5) is 99.4% for specificity (min 82.9%), 85.3% for sensitivity (min min 80%) and 91.5% for accuracy (min 90.5%), which meets the minimum performance required

for the system (described in 4.1). In more detail, all 26 recordings meet the required specificity, 19 out of 26 meet the required sensitivity, and 18 out of 26 meet the required accuracy.

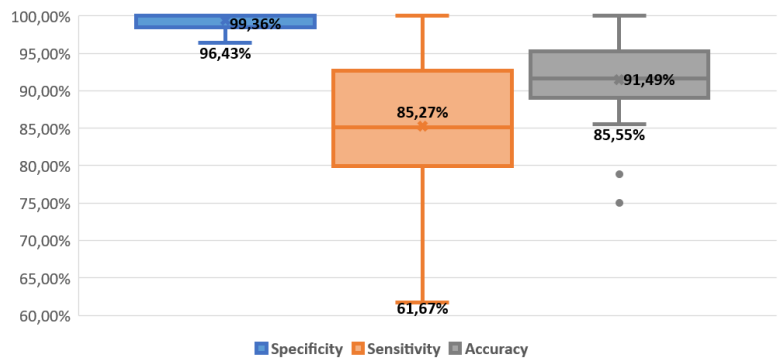

Figure 4.5: Box plot for final respiratory detection result – The line and the cross inside the box correspond to the median and the mean value, respectively. The box-limits represent the first and the third quartiles, the points highlight outliers, and the upper and lower bars represent the maximum and minimum values, respectively. Specificity: blue box; Sensitivity: orange box; Accuracy: gray box.

4.4.3 Influence of speech and noise

The influence of speech and noises on detection result is presented in Fig. 4.6.

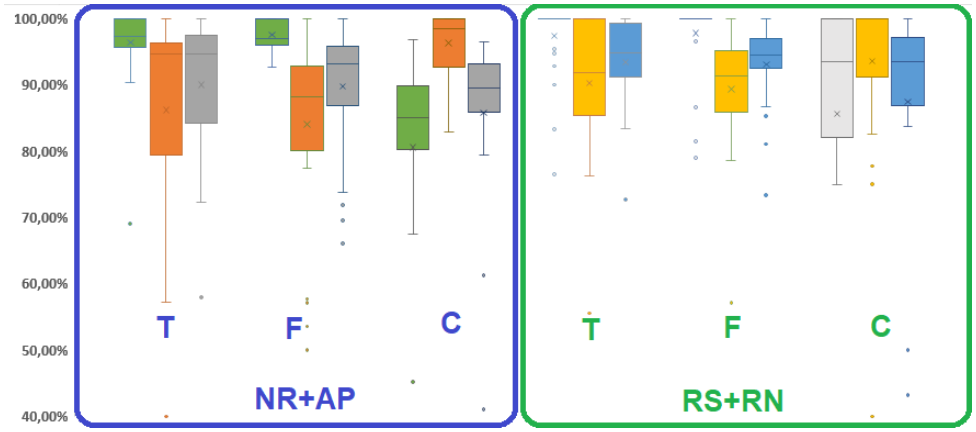

Figure 4.6: Influence of speech and noise on respiratory detection. Box plot (as box plot of Fig. 4.5) for specificity (green and light gray boxes), sensitivity (orange and yellow boxes) and accuracy (dark gray and blue boxes) of temporal (T), frequency (F) and cardiac (C) detection domains, separated in NR+AP phases (in blue rectangular) and RS+RN phases (in green rectangular).

Comparing the results of the NR+AP versus RS+RN phases, only the specificity in the frequency domain and cardiac detection domain were better during the RS+RN phase ($p < 0.05$, 4.1); no other parameters showed significant differences. This shows that noisy environments did not alter the detection results.

Detection domain	Median comparison	p-value
Temporal	Specificity	p= 0.0966
	sensitivity	p= 0.8829
	Accuracy	p= 0.3638
Frequency	Specificity	p=0.0088*
	sensitivity	p= 0.2032
	Accuracy	p= 0.1219
Cardiac (PDR)	Specificity	p=0.016*
	sensitivity	p= 0.7369
	Accuracy	p= 0.0851

Table 4.1: Median values comparing for specificity, sensitivity and accuracy of each detection domain – NR+AP vs. RS+RN.

Median comparison	p-value
Specificity	p=0.2079
sensitivity	p=0.7354
Accuracy	p=1

Table 4.2: Median values comparing for specificity, sensitivity and accuracy – sitting vs. lying.

4.4.4 Influence of position

Further examination of the detection results in the different participants positions were compared (Fig. 4.7) The specificity, sensitivity and accuracy showed no significant differences between sitting and lying positions (Tab.4.2).

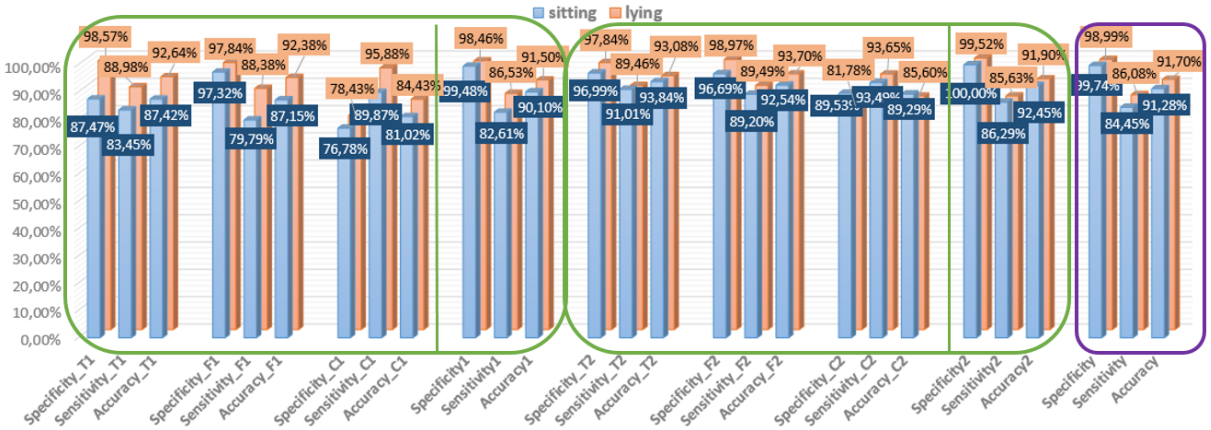

Figure 4.7: Box plot (like box plot of Fig. 4.5) for specificity (green rectangle), sensitivity (purple rectangle) and accuracy (red rectangle) in sitting (orange boxes) and lying (blue boxes) positions.

4.4.5 Advantage of combining several detection domains

The SSA of each detection domain and the global results (combined results from the 3 domains) are shown in Fig. 4.8. Specificity was significantly improved (reduced false

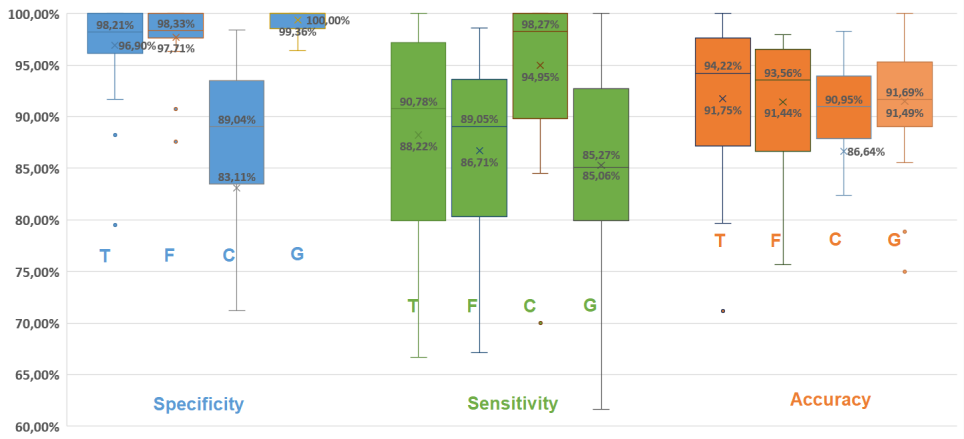

Figure 4.8: Box plot (as box plot of Fig. 4.5) for specificity (blue), sensitivity (green) and accuracy (orange) of temporal (T), frequency (F), cardiac (C) detection domains and global result (G).

Median comparison	Detection domain	p-value
Specificity	Temporal	p= 0.00889*
	Frequency	p= 0.01489*
	Cardiac	p= 9.896e-6*
Sensitivity	Temporal	p=0.09933
	Frequency	p= 0.6348
	Cardiac	p= 0.001801*
Accuracy	Temporal	p=0.8417
	Frequency	p= 0.8028
	Cardiac	p= 0.2079

Table 4.3: Median values comparing for SSA of each detection domain – single detection domain v.s. combining detection domain.

positives) with the combined detection approach compared to single domain detection (Tab.4.3). Sensitivity was significantly reduced (increased false negatives) with the combined detection approach compared to PDR detection. In all other comparisons, there was no significant difference.

4.4.6 Cardiac sound processing

As the PDR method is a new approach, we validated S1/S2 detection against classical R-peak detection from ECG recordings: R-peaks were detected through threshold detection and manually verified. In general, there should be one S1/S2 complex for each cardiac cycle corresponding to one R-peak. Both the reliability of the S-S interval (versus R-R interval) and PDR versus EDR (envelope of R-peak amplitude) were assessed.

The PDR and the EDR

The obtained PDR was compared with EDR because they both resulted from thoracic volume changes due to respiration.

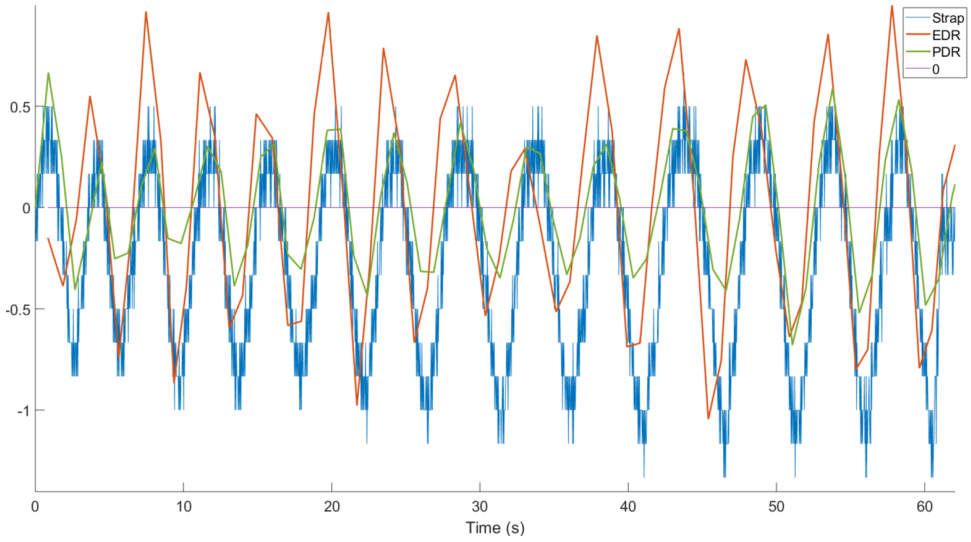

Figure 4.9: PDR (green) processed from tracheal sounds and EDR (red) processed from ECG and the thoracic strap signal (blue). Their positive (negative) slopes indicate inspiration (expiration).

For the example shown in Fig. 4.9, the amplitude variations of EDR vs. PDR were obviously not correlated and thus PDR cannot be used for assessing the quantitative volume of respiration. However, both signals seemed to oscillate in phase: we thus compared the respiration cycles in the PDR vs. EDR signals. To do so, local maxima of each curve $(iPDR(k), iEDR(k))$ were detected and their timing compared (Fig. 4.10).

A perfect match between the two should lead to a linear equation such as

$$iPDR(k) = a \times iEDR(k).$$

where a in theory is equal to 1. Indeed, when $iPDR(k)$ and $iEDR(k)$ are not matched (missed, shifted or additional peaks), it results in a variation ($a \neq 1$, (Fig. 4.11). Thus, the slope of the first-order linear regression fit line (a) could be a good indication to evaluate the correlation between EDR and PDR. Essentially, the closer slope (a) is to 1, the more PDR and EDR are correlated.

The result of all recordings is illustrated in Fig. 4.12, separated into the NR+AP phase, RS+RN phase (as described in Fig. 2.13a), and global results. The global mean slope was 0.77, which shows a good correlation between EDR and PDR. The Wilcoxon test (p=0.0067) showed that the results during NR+AP were better than the ones during RS+RN because the cardiac peaks were difficult to detect during speech.

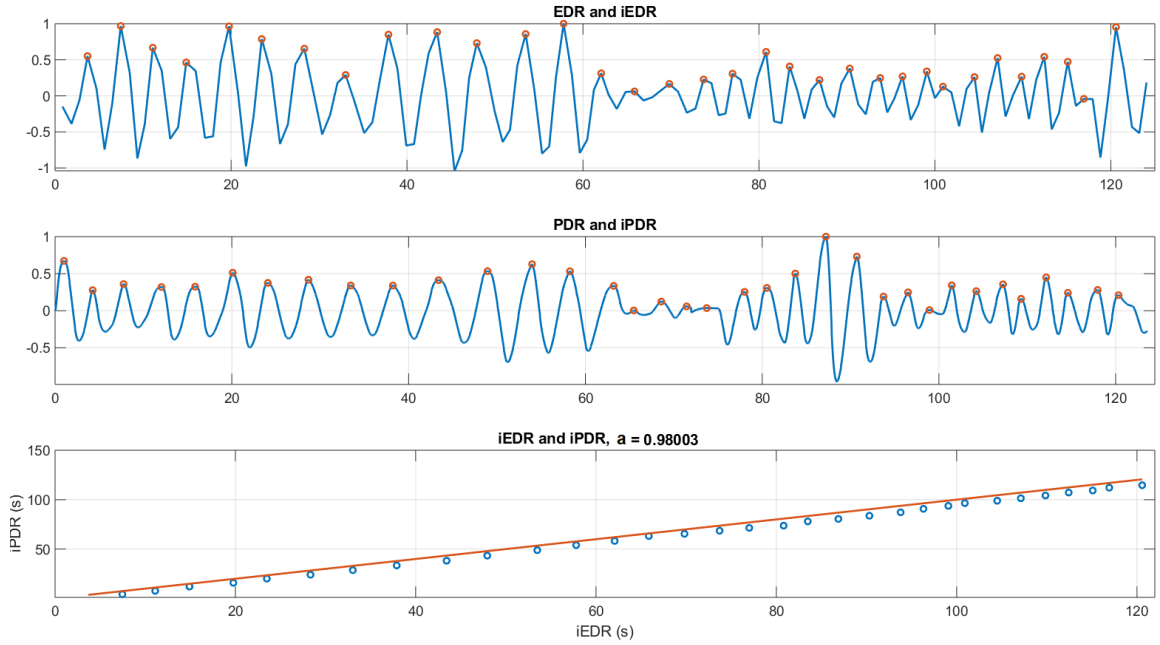

Figure 4.10: Top: the EDR signal and its local maxima (peaks) iEDR; Middle: the PDR signal and its local maxima iPDR; Bottom: the linear regression fit line between iEDR and iPDR ($a = 0.98$).

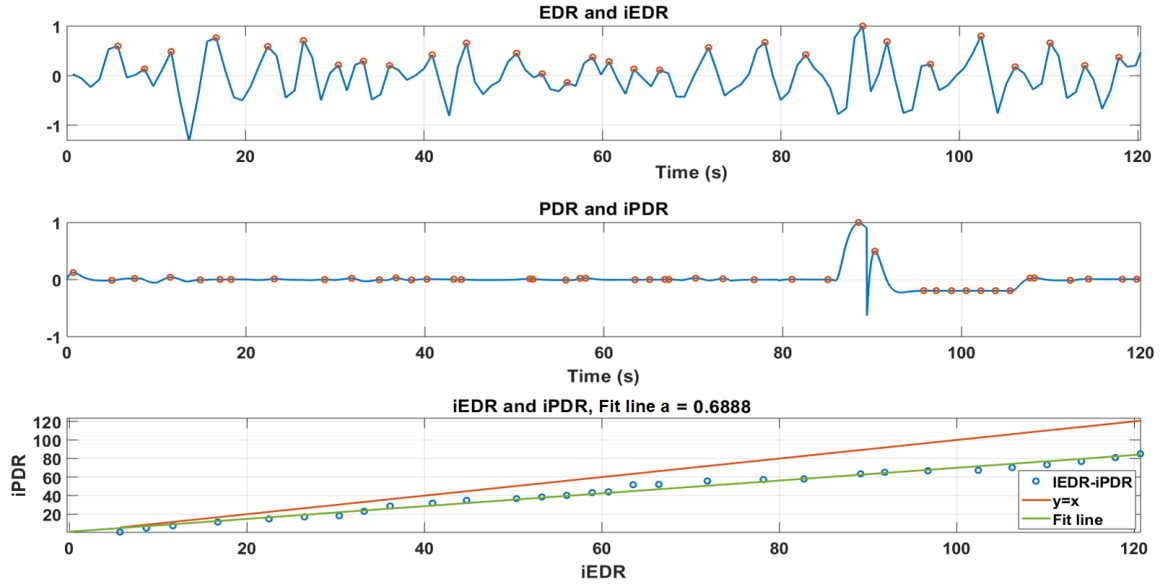

Figure 4.11: Top: the EDR signal and its local maxima (peaks) iEDR; Middle: the PDR signal and its local maxima iPDR; Bottom: the theory fit line(y=x) in red and the linear regression fit line between iEDR and iPDR ($a = 0.68$).

The PDR results were also evaluated in sitting and lying positions (Fig. 4.13) and the Student test showed no significant difference in the means (p=0.5359).

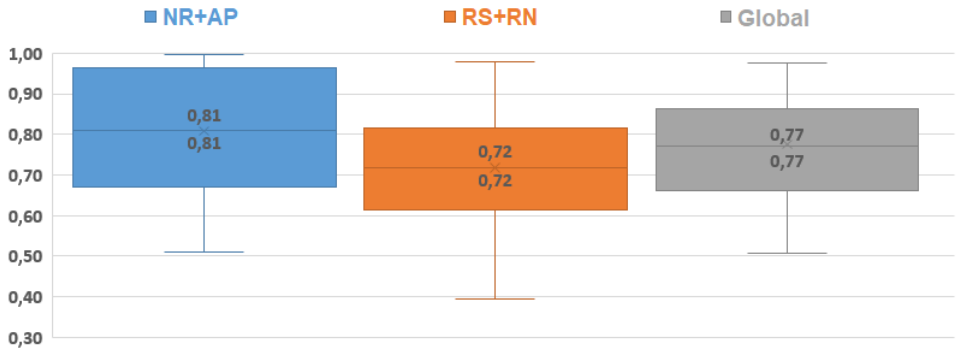

Figure 4.12: Box plot (like box plot of Fig. 4.5) for the evaluation of the results of PDR according to EDR, separated into NR+AP (blue), RS+SN (orange) and global results (gray).

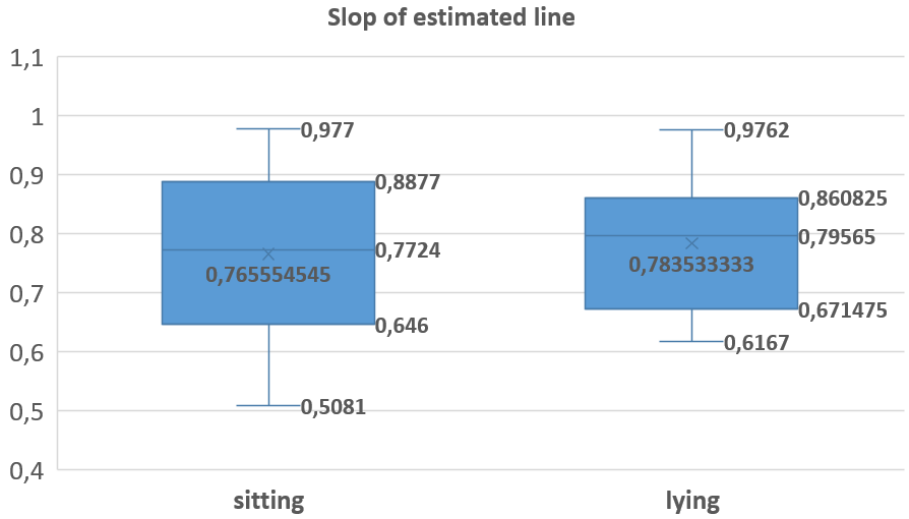

Figure 4.13: Box plot (like box plot of Fig. 4.5) for the evaluation of the results of PDR according to EDR, separated in sitting (left) and lying (right) positions.

Heart Beat-to-Beat Interval

The heart beat-to-beat intervals derived from cardiac sounds were compared to the HRV (R-R interval) calculated from ECG. For each recording, the result was also separated into NR+AP and RS+RN. The ideal relationship should be a straight line y=offset: the initial offset is due only to the delay between R-peak and S sounds. However, the small oscillations are explained by the detection of either S1 or S2. The NR+AP phase showed a good fit but the introduction of noise led to strong S complex mislocations.

Thus, plotting S-S versus R-R intervals showed mainly four groups of points corresponding to R-R vs. S1-S1 (or S2-S2), R-R vs. S1-S2, R-R vs. S2-S1, and outliers when the S1-S2 complex was missed. In the latter case, all the S-S intervals greater than two times the R-R interval were considered outliers and thus removed: a ratio R_{error} was calculated as:

$$R_{error} = 1 - \frac{N_{abnormal}}{N_{total}}$$

where $N_{abnormal}$ is the number of outliers and N_{total} is the total number of points. This ratio was used to weight the final assessment. Once outliers were removed, a first fit line slope (β) was estimated using the solution of: $\underline{SS} = \beta \underline{RR}$. Based on this line, two other shifted lines defined the group separation in considering the averaged S1-S2 interval (0.29 s) and minimum S2-S1 interval (0.5 s). Thus, two boundary lines and one central line are obtained:

$$y1 = \beta x + 0.5$$
$$y2 = \beta x$$
$$y3 = \beta x - 0.29$$

Thus, all points were then separated into three groups (by looking for their nearest line). As in the PDR and EDR assessment, the slope of the linear regression fit line was used to evaluate the S peak detection performance, three different fit lines could be calculated separately for these three groups of points, as in the example shown in Fig. 4.14.

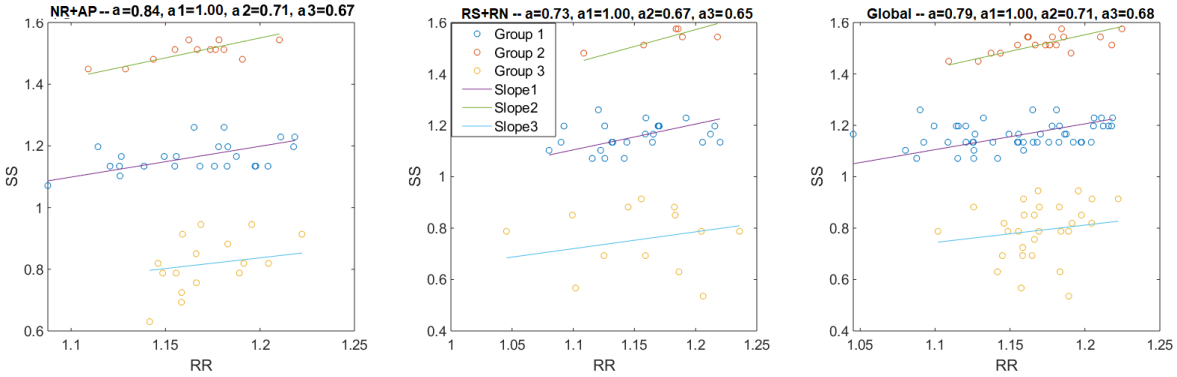

Figure 4.14: The left, middle and right figures show the linear regressions for NR+AP, RS+RN and the whole recording. The blue points are from the group of R-R vs. S1-S1 or S2-S2 (group 1, at the middle group of each figure), the orange points are from the group of R-R vs. S2-S1 (group 2, at the top of each figure), and the yellow points are from the group of R-R vs. S1-S2 (group 3, at the bottom of each figure). The slopes of each fit line are presented the in figure title ($a1$, $a2$ and $a3$ are slopes for the group 1, group 2 and group 3, respectively).

The assessment was based on how close the slope is to 1 (the best theory slope) as follows:

$$a_x = 1 - |a'_x - 1|$$

where a'_x is the slope of the fit line for group x, and a_x is the new slope of group x to evaluate the correlation. Thus an average slope was weighted as:

$$a = R_{error} * \frac{n_1 * a_1 + n_2 * a_2 + n_3 * a_3}{n_1 + n_2 + n_3}.$$

where n_x presents the number of points in group x. For example, in Fig. 4.14, the averaged slopes (a) for NR+AP, RS+RN and the whole recording were 0.84, 0.73 and

0.79, respectively. The results for the 26 recordings are presented in Fig. 4.15. The slope of group 1 in each part was very close to 1, which means a high correlation between the S-S and R-R interval lengths. The medians of the results from RS+RN and NR+AP were significantly different (p=0.00004). The cardiac peaks were more difficult to detect from TS during speech or with environmental noise. Group 2 and group 3 showed even poorer correlations, but despite their relatively small numbers, the global mean still reached 0.89. Thus, the S-S interval obtained from the proposed cardiac peak detection method is a reliable way to estimate heart-rate or as an alternative method to present the heartrate variation (HRV).

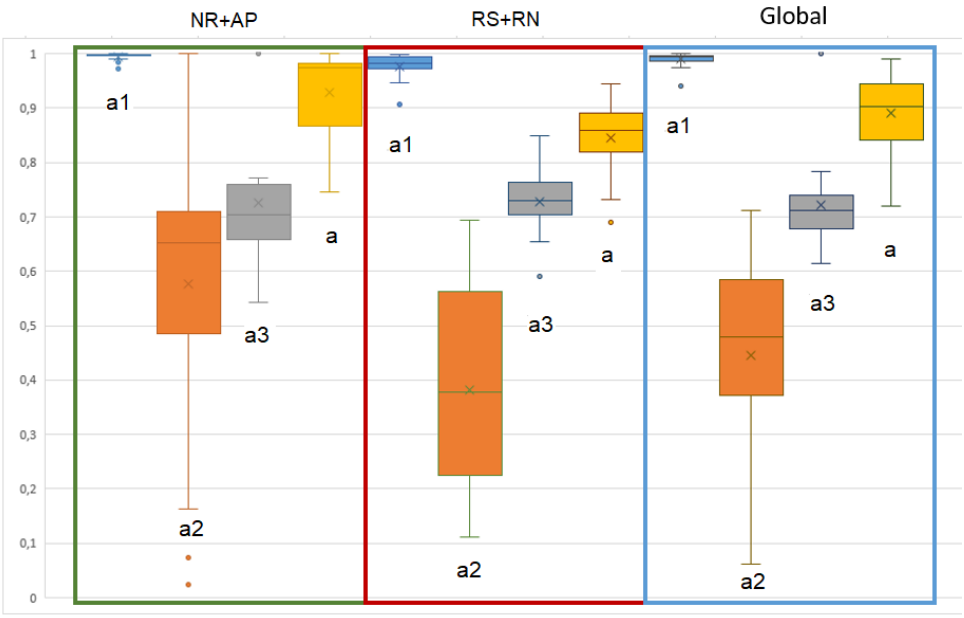

Figure 4.15: Box plot (like the box plot of Fig. 4.5) for the distribution of fit line slopes for each group in each part and the global signal (in different rectangle).

Chapter 5

Discussion and Conclusion

In this thesis, we present an original method for respiratory monitoring based on TS. The first aim was to detect apnea and the second aim was to detect all the phases of the respiration cycle. Previous methods used detection based on either the temporal features of sound or its frequency contents. On the contrary, we combined classifications from the two domains with new signal processing based on cardiac sounds. We thus increased the performances of the classification. In particular, we can underline the following points.

5.1 Performance of algorithm

Fig. 4.8 and the Tab.4.3 show greater sensitivity with PDR than the final combined results. This is because the final decision-making method had in fact missed some events due to delays and different durations in the results of each detection domain (as shown in Fig. 3.6), even though they were well detected in other domains. As a result, false negatives were added and the sensitivity was reduced. On the other hand, some false positives caused by noise could be eliminated in other detection domains (e.g., the temporal envelope could eliminate brief noises and the frequency domain might eliminate long duration noises with different frequency content than respiration). The number of false positives was reduced and therefore the specificity was increased. Even though the sensitivity was ultimately reduced, it was still above the minimum requirement for a detection system ($> 80\%$), so the results remain acceptable. Furthermore, in this study, high specificity was more important than high sensitivity or high accuracy because false positives would mean that apnea had been detected as respiration. In other words, patients would stop breathing but the detection system would not deliver an alarm.

5.2 Method PDR

To our knowledge, the proposed PDR method had never been studied before. In this study, however, we showed the feasibility of evaluating respiratory effort with PDR by comparing the result with EDR. This means that using only a microphone it is possible to continuously monitor cardiac activity, detect the apnea episodes, and eventually discriminate between the type of apnea based on the PDR (apnea with respiratory effort: obstructive apnea; otherwise: central apnea). It should nevertheless be noted that the EDR method is still not widely applied in clinic routine and it is not known to be a good indicator of respiratory effort. More comparisons with a plethysmograph (PSG) are thus needed. Also the proposed algorithm has not yet been tested in individuals with real apnea. Thus, the next step will be to record patients' TS synchronized with PSG to test whether the same algorithm still works correctly. Furthermore, cardiac peak detection may be improved by combining wavelet decomposition [59] (better detection of peak position) and the envelogram by absolute value [56] (better detection of peak amplitude).

5.3 Cardiac peak envelogram

In general, as described in [56], cardiac peaks envelope is better obtained by Shannon energy which attenuates low intensity and emphasizes medium intensity (5.1). But according to our recordings, peaks intensity varies a lot due to respiration in several subjects (§2.2.3). In these cases, peaks during respiratory pauses have small amplitudes like other noises, they are too attenuated to be detected. In another way, the method by absolute value gives the same weight to all the signal which implies that the amplitudes variation can be better represented. Another common used method is wavelet decomposition. The method introduced in [59] had been rejected after testing because it could have an excellent detection of S peak positions, but it also modified S peaks amplitude which is important in order to apply PDR detection. One example of modification of S peak amplitude was demonstrated in Fig. 5.2. Downsampled cardiac signal was presented in blue, the red signal is the obtained envelogram by using wavelet decomposition. An opposite amplitude could be observed between S1 and S2 peak in the sounds and in the envelogram.

The relative amplitude between S1 and S2 is not absolute. Some subjects could have longer S1, others could have longer S2. One subject had these two situations alternatively. But this characteristic doesn't influence the detection result.

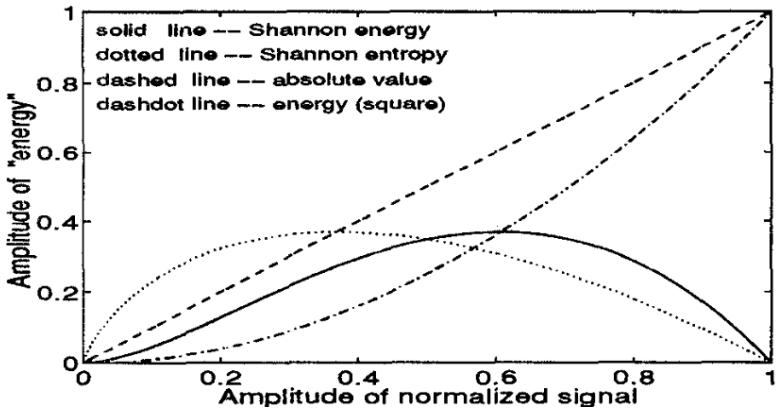

Figure 5.1: The comparison of different envelogram methods [56].

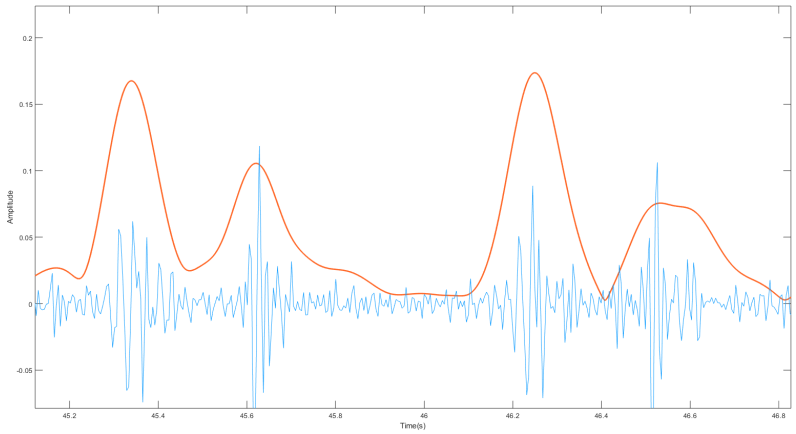

Figure 5.2: Envelogram obtained by wavelet decomposition (in red) modify amplitude of cardiac peaks (heart sounds in blue).

5.4 Noise reduction

This study used two microphones to record TS and environmental noise separately. The ideal would have been to use recorded noise to reduce the environmental noise in the recorded TS by using the Wiener adaptive filter [61]. The principle of filter is illustrated in Fig. 5.3:

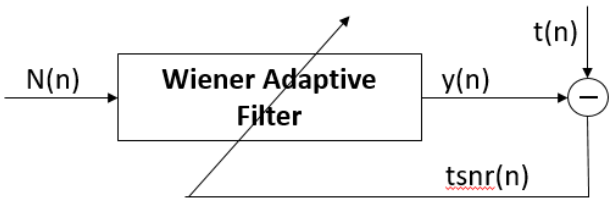

Figure 5.3: The schematic of the Wiener adaptive filter for noise reduction

where the input of this filter is the recorded environment noise N(n), and the coefficients of filter is: ω_0, ω_1, ... the recorded tracheal sounds is the compared signal t(n), then the

output of filter is:

$$y(n) = w_0^* u(n) + w_1^* u(n-1) + ...$$

so the error signal would be the desired signal – tracheal sounds with reduced environment noise :

$$tsnr(n) = t(n) - y(n).$$

The aim of this filter is to minimize the error between its output and the compared signal, to reduce most of environment noise. The error is minimum when the filter is optimal. $\underline{\overset{\Delta}{\omega}}$ (Wiener Hopf equation):

$$\underline{\overset{\Delta}{\omega}} = \left(\underline{\underline{R}}_{NN}\right)^{-1} \underline{R}_{Nt}$$

In present study, the Wiener filter is 10^{th} order. A before and after comparison of noise reduction on last 30 seconds recording (the noisy part) is shown in Fig. 5.4. Reduction of temporal amplitude of noise could be observed, but it didn't help to improve detection result. In the obtained recordings, the noisy environment was simulated by playing specific videos, whose frequency band was higher than the respiratory frequency band (Fig. 2.13d and in Fig. 2.13b) so that it could be easily filtered. A better way would be to record data in a real noisy environment (e.g., on street) to see if the design with noise reduction by two microphones would improve the detection result.

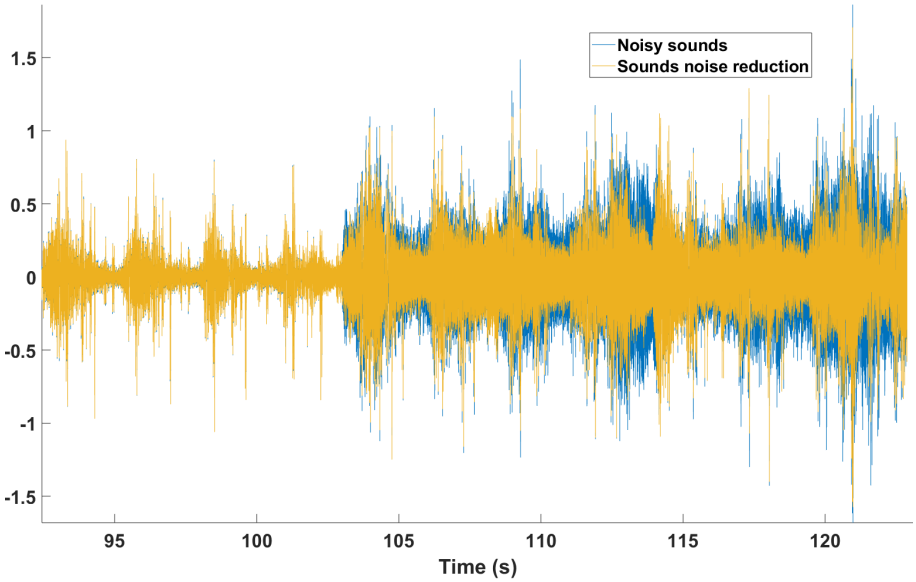

Figure 5.4: Noise reduction by Wiener filter.

5.5 Conclusion

The DP, especially the implanted IT-PNS system appears to be a good choice to restore patient's ventilatory function in the case of respiratory paralysis. But existing systems do

not integrate any respiratory monitoring function to alert users and helpers in case of a respiratory trouble such as apnea. In order to improve systems stimulation efficiency and security, this thesis proposes to add into existing electrical stimulation devices a breathing detection function based on microphone tracheal sounds monitoring. The first aim is to detect if the patient is breathing or not, the second aim is to obtain extra vital information (breathing rate, cardiac rhythm, ...)

Two small microphones were placed at suprasternal notch to record tracheal sounds and environment noises. Recorded sounds were pre-amplified and pre-filtered then processed on PC. Four protocols were designed to record and analyze respiration in different contexts: (1) 15 healthy subjects (30-seconds of respiration with 10 seconds spontaneous apnoea); (2) 1 patient with high tetraplegia under IT-PNS (30 seconds of induced breathing); (3) 13 healthy subjects in sitting and lying positions with reference signals (pneumotachograph, abdominal strap, ...); (4) 30 patients with sleep apnoea PSG and 10 patients with implanted IT-PNS will be included in short future.

Recorded tracheal sounds were processed with Matlab^{TM} (MathWorks, USA) to perform 3 types of detection: temporal envelope detection, frequency (PSD) envelope detection and PDR (cardiac) detection. These 3 detection results were combined to make final decision. The method allowed to obtain good results in protocols 1 to 3 i.e. meeting the minimum requirements for the system. The combination of the 3 detection domains improved the system specificity, i.e. reducing the false positive detections, which was the most important for the final DP system.

According to the results from protocol 3, noises like speech or environments did not influence much the detection result. Different positions could lead to different recorded sounds intensity, but the final detection results were similar. The new proposed respiratory effort evaluation method – PDR showed a good correlation with EDR, which demonstrated the feasibility to use the PDR monitoring the respiration. At the same time, the comparison of R-R intervals and S-S intervals also indicated a good correlation, so that it was also possible to monitor heart activity from tracheal sounds.

To summarize, this thesis showed the feasibility of detecting the apnoea from tracheal sounds, and monitoring cardiac activity using an original algorithm. The extracted signal PDR could be used to identify the type of apnoea (obstructive/central). Furthermore, the recording system with microphone could capture stimulation signals which could indicate a dysfunction of the pacing system and recorded tracheal sounds could give a feedback on the electro-ventilation quality. The synchronization of these two information could indicate if the stimulation settings (intensity, frequency ...) should be adapted.

But this method was not tested yet on patients implanted with electrical stimulation

assistance, so the next step will be to record patient tracheal sounds and oximeter signal to test if the same algorithm could still work well for in this case. This is the object of protocol 4 which has just been validated by ethical committee. The noisy environment in protocol 3 was simulated by playing specific videos, which frequency band might be changed/limited according to the device, a better way would be to record data in real noisy environment (e.g. on street). In this case, the wiener filter reducing noises in tracheal sounds would still be worthy to test. The final decision making method (fusion of the detection results from all the detection domains) increases the number of false negatives, which reduces the sensibility of the system. This decision-making method may be replaced by an artificial neural network (ANN) or adaptive neuro-fuzzy inference system (ANFIS) [62] to give a better result. The cardiac peak detection may be improved by combining wavelet decomposition (better detection of peak position) and the envelogram by absolute value (better detection of peak amplitude). The recording system could also be improved, especially the support for microphone. New design and material may strengthen the tracheal sounds and isolate them from exterior noises.

Monitoring tracheal sounds could be a useful way beyond the very limited niche of patients with DP or have sleep apnoea. Indeed, it would provide a non-invasive way to approximate inspiratory flow that would be useful in all patients requiring respiratory monitoring in acute situations (e.g. as a safety measure during the administration of morphine for acute pain) and in chronic situations (e.g. home mechanical ventilation). And in the construction of smart house, especially for nursing/retirement home, application of tracheal sounds monitoring could provide convenient, robust multi-vital signals monitoring.

Appendix A

Analog card design

Amplifiers

Each microphone is connected to a customized analog card to amplify recorded tracheal sounds before the acquisition, but the noise is much stronger then the respiratory sounds. To avoid the noise attenuate operational amplifiers in the active filters (presented below), a first amplifier is used before the filters and a second one is used after them. The schema of amplifier is in figure A.2, it's a classical non inverse amplifier. The output tension is: $V_{out} = (1 + \frac{R_f}{R_g})V_{in}$. Signals are amplified about 10 times at first, then 23 times. So the resistance values are:

- For 1^{er} amplifier: $R_g = 10k\Omega, R_f = 100k\Omega$;
- For 2^{nd} amplifier: $R_g = 10k\Omega, R_f = 220k\Omega$.

Filters

Compared with the passive filter, the active filter can filter and also amplifier the signal, and his design is easier. Furthermore, with the same filtered effect, the active filter needs less components (space). The active filter structure used is called Sallen & Key. It's a 2^{nd} order active filter, its schema is showed in figure A.1. This structure can compose all types of filter by changing the four passive RC components (Z1 to Z4), and the gain is controlling by only one operational amplifier with two resistances.

A band-pass filter is needed to filter respiratory sounds. But the band-pass filter with one Sallen & Key structure is actually composed by one 1^{er} order high-pass filter and one

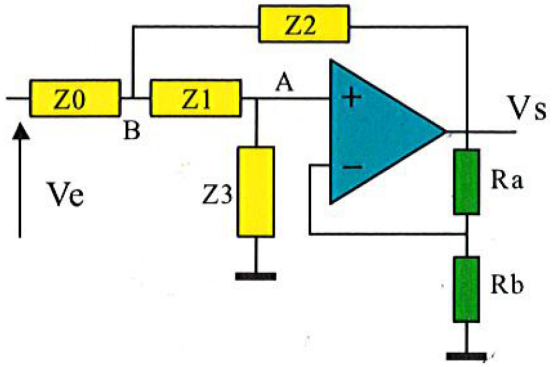

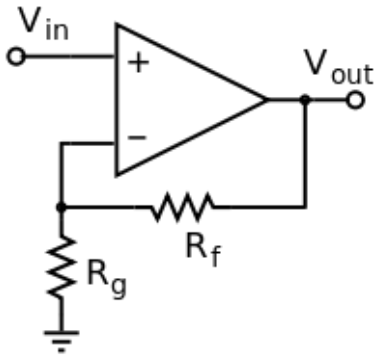

Figure A.1: principle schema Sallen & Key *Figure A.2: amplifier schema*

1^{er} order low-pass filter, it means its stop band roll-off (20dB/decade) is half of the one of a 2^{nd} order filter (40dB/decade). For a better stop band roll-off, two 2^{nd} order Sallen & Key filters are used to compose a band pass filter.

The general transfer function of the structure Sallen & Key is:

$$H = \frac{K \cdot Z_2 \cdot Z_3}{Z_0 \cdot Z_3(1-K) + Z_0(Z_1+Z_2) + Z_2(Z_1-Z_3)}.$$

Based on this function, the transfer function and parameters for high-pass filter and low-pass filter can be determined as the way below:

- If the filter is used as a high pass $Z_0 = Z_1 = 1/Cp\omega; Z_2 = Z_3 = R$. It's transfer function is $H(p) = \frac{K(RCp)^2}{1+RCp(3-K)+(RCp)^2}$. And the canonical transfer function of 2^{nd} order high-pass filter is $H(p) = \frac{H_0\left(\frac{p}{\omega_0}\right)^2}{1+\frac{1}{Q\omega_0}p+\left(\frac{p}{\omega_0}\right)^2}$. The parameters can be determined by combining these two functions:
  - The natural pulsation $\omega_0 = \frac{1}{RC}$.
  - The quality factor $Q = \frac{1}{3-K}$.
  - The gain of the filter $H_0 = K$.
- If the filter is used as a low pass: $Z_0 = Z_1 = R; Z_2 = Z_3 = 1/Cp$. It's transfer function is $H(p) = \frac{K}{1+RCp(3-K)+(RCp)^2}$. And the canonical transfer function of 2^{nd} order low-pass filter is $H(p) = \frac{H_0}{1+\frac{1}{Q\omega_0}p+\left(\frac{p}{\omega_0}\right)^2}$. The parameters are the same with the ones of high-pass filter.
- For both of these two filters, it's the same principle as in A to calculate the gain: $K = (R_a + R_b)/R_b$. Filter Butterworth is applied for having a plat response at pass-band, and the quality factor $Q = \frac{1}{3-K} = 36\sqrt{2}$. It means the quality of the

filter depends on its gain. So $K = (R_a + R_b)/R_b = \frac{1}{\sqrt{2}} \Rightarrow \frac{R_a}{R_b} = 2 - \sqrt{2}$. According to exist value of components, $R_a = 10k\Omega, R_b = 22k\Omega$. The signals are finally amplified $10 \times 23 \times K^2 \approx 480$ times.

- The frequency band of respiratory sounds is about 100Hz up to 1600Hz (vary with height) [33][63][43]. According to the information below, the value of $R \cdot C$ can be determined : $R \cdot C = \frac{1}{2\pi f_0}$. Depending on the available value of the components, the value of resistance and capacitor can be fixed:
  - For high-pass filter, $RC = \frac{1}{2\pi f_0} = 9.9 \times 10^{-5} \Rightarrow R = 15k\Omega, C = 100nF$
  - For low-pass filter, $RC = \frac{1}{2\pi f_0} = 1.33 \times 10^{-4} \Rightarrow R = 68k\Omega, C = 2nF$

Power supply and tension regulator

The output is between -9V and 9V, but the ADC of acquisition card can only take signals between 0V to 3.6V. So the variation of output is kept by a capacitor and a divider bridge is used to straighten the tension. To avoid overload, two diodes are added in the circuit. The microphone works between 2-10V, and the AOP works between (±)5-15V, so the power supply should be (±)5-10V.

Appendix B

Abstract of the protocol description submitted to the ethical committee (Comité de Protection des Personnes CPP)

ENREGISTREMENT DE SONS TRACHEAUX EN VUE DE LA MISE AU POINT D'UN ALGORITHME DE SURVEILLANCE DE LA RESPIRATION

Aspects administratifs

- Numéro d'enregistrement ANSM : 2019-A01813-54
- Demandeur et investigateur principal : Pr Thomas SIMILOWSKI
- Autre(s) investigateur(s) : LU Xinyue (PHD student), Marie-Cécile NIERAT (PhD), Dr Valérie ATTALI, Pr Capucine MORÉLOT-PANZINI, Christine AZEVEDO (PHD).
- Collaborateurs scientifiques : Serge RENAUX, David GUIRAUD (PHD)
- Promoteur : ADOREPS, Association pour le Développement et l'Organisation de la Recherche En Pneumologie et sur le Sommeil (loi 1901)
- Lieu(x) de recherche : Service des Pathologies du Sommeil (population "sommeil") et Service de Pneumologie, Médecine Intensive et Réanimation (population "té-

traplégie"), Département R3S (Respiration, Réanimation, Réhabilitation et Sommeil), Groupe Hospitalier Pitié-Salpêtrière, 47-83 Bd de l'Hôpital, 75651 Paris Cedex 13.

- Assurance : SHAM - 18 Rue Edouard Rochet, 69008 Lyon
- Type d'étude : Recherche interventionnelle avec risques et contraintes minimes (catégorie 2 de la Loi Jardé), en l'absence de toute modification de la prise en charge des patients, d'une part, et en raison de l'utilisation d'un capteur de surface (microphone) dénué de tout risque et n'imposant pas de contrainte supplémentaire.

Justification

Parmi les pathologies ciblées, outre les dysfonctions diaphragmatiques, figurent le syndrome d'Ondine et la tétraplégie haute pour lesquels une solution palliative possible consiste à stimuler le nerf phrénique pour générer la contraction du diaphragme. Mais à ce jour, aucun des dispositifs de stimulation commercialisés n'est équipé d'un système de surveillance de la respiration induite. La phonospirométrie a fait l'objet de diverses études par le passé. Elle n'a cependant pas connu de développement clinique, essentiellement faute des moyens algorithmiques adaptés. L'étude proposée dans la présente demande a pour objectif de valider chez des patients connus pour présenter divers types d'apnées de nouveaux algorithmes, mis au point sur banc d'essai et préalablement testés sur des enregistrements effectués sur des volontaires sains. Le but est de valider la performance des algorithmes pour identifier et décrire les phases inspiratoire et expiratoire du cycle ventilatoire, et à identifier des épisodes apnéiques. Ceci constitue l'objet de la présente étude, dans la perspective, à terme, de proposer un dispositif de surveillance respiratoire non invasif et fiable.

Sujets

Nombre de participants : - 30 patients pour suspicion de SAOS
- 10 patients pour bilan pré-implantation ou de stimulation phrénique implantée

Critères d'inclusion :

- les participants sont adressés à l'hôpital de la Pitié-Salpêtrière, soit pour le dépistage d'un SAOS, soit pour le bilan pré-implantation ou pour le bilan annuel d'une stimulation phrénique déjà implantée ;

- Ils sont majeurs ;
- Ils sont affiliés à un régime de sécurité sociale ;
- Ils ont reçu une information exhaustive sur l'étude délivrée par un investigateur de l'étude et y consentent pleinement.

Critères de non-inclusion :

- Patients mineurs ;
- Femmes enceintes ou en période d'allaitement ;
- Personnes privées de liberté.

Durée de l'étude :

Par sujet : 12h maximum

Pour la totalité de l'étude : Population "sommeil" : 1 à 2 mois ; Population "tétraplégie" : 2 ans.

Objectifs

Valider la capacité de nouveaux algorithmes de phonospirométrie à détecter des évènements apnéiques et cardiaques.

Méthodes :

Le son trachéal est enregistré à l'aide de deux microphones positionnés au niveau du cou (sans contact physique avec le patient). Une carte d'acquisition est connectée avec des microphones et un ordinateur par câbles. Une fois la carte d'acquisition allumée, le système d'enregistrement se déclenche automatiquement. Le signal enregistré est exporté à l'issue de l'enregistrement pour être traité ultérieurement. L'enregistrement des sons trachéaux sera effectué :

- Population "sommeil" : en même temps qu'une nuit de polysomnographie diagnostique. Le pléthysmographie compris dans cette diagnostique sera utilisé comme le signal de référence.

- Population "tétraplégie" : pendant le bilan annuel du système de stimulation du nerf phrénique (examen réalisé en routine dans le suivi médical). Le signal du spiromètre utilisé pour ce bilan sera utilisé comme le signal de référence.

Le signal de référence sera utilisé pour comparer le résultat de détection à partir du son trachéal.

Critères d'évaluation

Critère principal : la spécificité de la détection respiratoire doit être supérieure à 82,86

Critères secondaires :

- Pour chaque événement respiratoire (début, fin, durée), l'erreur temporelle entre les détections obtenues par l'analyse du son trachéal et la méthode de référence doit être inférieure à 10% du cycle respiratoire ;
- La différence des durées inspiratoire et expiratoire estimés à partir des enregistrements du microphone trachéal et de la méthode de référence doit être inférieure à 20% ;
- L'erreur temporelle de détection des événements cardiaques à partir des enregistrements du microphone trachéal et de l'ECG doit être inférieure à 10% du cycle cardiaque.

Balance bénéfices/risques :

Bénéfices : La phonospirométirie (avec un microphone placé sur la trachée) présente des caractéristiques qui semblent parfaitement adaptées à des besoins de détecter en temps réel si le flux respiratoire est correct chez les patients utilisant les systèmes de stimulation électrique. Il apparait aussi possible de dériver une mesure de la fréquence cardiaque à partir d'enregistrements phonospirométriques.

Risques : Cette étude s'inscrit dans le cadre d'une recherche interventionnelle comportant des risques et contraintes minimes. En effet, elle ne comporte que l'addition d'un enregistrement des sons trachéaux, par un dispositif non invasif, à une prise en charge médicale qui n'est en aucune façon modifiée par l'étude. De fait, on peut considérer que l'étude ne comporte aucun risque et une contrainte mineure.

Résultats attendus et perspectives

L'objectif distant du développement d'un dispositif de phonospirométrie est la mise à disposition des patients porteurs de stimulateurs phréniques implantés d'un dispositif de surveillance de l'efficacité ventilatoire de la stimulation fiable, atraumatique et aussi peu contraignant que possible. La démonstration de la capacité d'un tel dispositif à détecter de façon fiable les apnées (l'objectif principal de cette étude) constituera l'élément clef de cette démarche.

My publications

[1] X. LU, D. Guiraud, S. Renaux, T. Similowski, C. Azevedo Coste, and C. Azevedo, "Monitoring phrenic nerve stimulation-induced breathing via tracheal sounds", in *2019 XXIII Annual Conference of the International Functional Electrical Stimulation Society (IFESS)*, May 2019. [Online]. Available: https://hal-lirmm.ccsd.cnrs.fr/lirmm-02304820.

[2] X. LU, D. GUIRAUD, S. RENAUX, T. SIMILOWSKI, and C. AZEVEDO, "Breathing detection from tracheal sounds in both temporal and frequency domains in the context of phrenic nerve stimulation", in *2019 41st Annual International Conference of the IEEE Engineering in Medicine and Biology Society (EMBC)*, IEEE, Jul. 2019, pp. 5473–5476, ISBN: 978-1-5386-1311-5. DOI: 10.1109/EMBC.2019.8856440. [Online]. Available: https://ieeexplore.ieee.org/document/8856440/.

[3] X. LU, C. AZEVEDO, S. RENAUX, T. SIMILOWSKI, and D. GUIRAUD, "**STUDENT TRAINEE AWARDS** – MONITORING PHRENIC NERVE STIMULATION-INDUCED BREATHING VIA TRACHEAL SOUNDS", in *2019 58th International Spinal Cord Society Annual Scientific Meeting (ISCoS)*, The International Spinal Cord Society, 2019, p. 102. [Online]. Available: https://www.iscos.org.uk/uploads/ABSTRACTS/ISCoS_2019_Poster_Abstractsv2.pdf.

[4] X. LU, C. AZEVEDO, M.-C. NIERAT, S. RENAUX, T. SIMILOWSKI, and D. GUIRAUD, "**IN REDACTION** – IMPROVED TRACHEAL SOUND ANALYSIS FOR CONTINUOUS RESPIRATORY MONITORING: TIME-FREQUENCY PROCESSING OF THE PHONOSPIROGRAM COMBINED WITH PHONOCARDIOGRAM-DERIVED DETERMINATION OF RESPIRATORY RHYTHM", 2020.

Bibliography

[5] G. Pocock and C. D. Richards, *Physiologie humaine: les fondements de la médecine*. Masson, 2004, ISBN: 9782294010026. [Online]. Available: https://books.google.fr/books?id=_i7HmdzjqpUC.

[6] C. Ahlström, "Processing of the Phonocardiographic Signal - Methods for the Intelligent Stethoscope", PhD thesis, 2006, pp. 1–68, ISBN: 9185523593. DOI: urn:nbn:se:liu:diva-7538. [Online]. Available: http://liu.diva-portal.org/smash/get/diva2:22548/FULLTEXT01.

[7] R. H. Hyland, M. A. Hutcheon, A. Perl, G. Bowes, N. R. Anthonisen, N. Zamel, and E. A. Phillipson, *Upper airway occlusion induced by diaphragm pacing for primary alveolar hypoventilation: implications for the pathogenesis of obstructive sleep apnea*, 1981. DOI: 10.1164/arrd.1981.124.2.180.

[8] A. Quesnel, B. Veber, F. Proust, E. Agasse, F. Beuret Blanquart, and E. Verin, "What are the perspectives for ventilated tetraplegics? A French retrospective study of 108 patients with cervical spinal cord injury", *Annals of Physical and Rehabilitation Medicine*, vol. 58, no. 2, pp. 74–77, Apr. 2015, ISSN: 18770657. DOI: 10.1016/j.rehab.2014.12.004. [Online]. Available: http://dx.doi.org/10.1016/j.rehab.2014.12.004%20https://linkinghub.elsevier.com/retrieve/pii/S1877065715000032.

[9] W. Randerath, "Central sleep apnoea and Cheyne–Stokes respiration", in *Respiratory Sleep Medicine*, European Respiratory Society, 2012, pp. 39–39. DOI: 10.1183/9781849840248.014211. [Online]. Available: http://erspublications.com/lookup/doi/10.1183/9781849840248.014211.

[10] Genetics Home Reference, *Congenital central hypoventilation syndrome*, 2015. [Online]. Available: https://ghr.nlm.nih.gov/condition/congenital-central-hypoventilation-syndrome.

[11] MEDWIN MEDICAL GROUP, "HAS Avis de la commission - ATROSTIM", Tech. Rep., 2009.

[12] T. Similowski, "La femme qui ne savait pas respirer", *Cerveau & Psycho*, no. 106, pp. 18–22, 2018. [Online]. Available: https://www.cerveauetpsycho.fr/sd/pathologie/syndrome-dondine-la-femme-qui-ne-savait-pas-respirer-15465.php.

[13] T. Similowski and J.-p. Derenne, "Stimulation phrénique implantée", *Médecine thérapeutique*, vol. 7, pp. 457–469, 2001. [Online]. Available: https://www.jle.com/fr/revues/met/e-docs/stimulation_phrenique_implantee_180235/article.phtml.

[14] F. Le Pimpec-Barthes, J. Gonzalez-Bermejo, J. P. Hubsch, A. Duguet, C. Morélot-Panzini, M. Riquet, and T. Similowski, "Intrathoracic phrenic pacing: A 10-year experience in France", *Journal of Thoracic and Cardiovascular Surgery*, vol. 142, no. 2, pp. 378–383, 2011, ISSN: 00225223. DOI: 10.1016/j.jtcvs.2011.04.033.

[15] C. Morélot-Panzini, J. Gonzalez-Bermejo, and T. Similowski, "La stimulation phrénique implantée", *Réanimation*, vol. 20, no. 1, pp. 4–11, Jan. 2011, ISSN: 1624-0693. DOI: 10.1007/s13546-010-0007-3. [Online]. Available: http://link.springer.com/10.1007/s13546-010-0007-3.

[16] A. F. DiMarco, "Diaphragm Pacing", *Clinics in Chest Medicine*, vol. 39, no. 2, pp. 459–471, Jun. 2018, ISSN: 02725231. DOI: 10.1016/j.ccm.2018.01.008. [Online]. Available: https://linkinghub.elsevier.com/retrieve/pii/S027252311830008X.

[17] C. Morélot-Panzini, F. Le Pimpec-Barthes, F. Menegaux, J. Gonzalez-Bermejo, and T. Similowski, "Referred shoulder pain (C4 dermatome) can adversely impact diaphragm pacing with intramuscular electrodes", *European Respiratory Journal*, vol. 45, no. 6, pp. 1751–1754, 2015, ISSN: 13993003. DOI: 10.1183/09031936.00220614.

[18] M. R. Costanzo, R. Augostini, L. R. Goldberg, P. Ponikowski, C. Stellbrink, and S. Javaheri, "Design of the remedē System Pivotal Trial: A Prospective, Randomized Study in the Use of Respiratory Rhythm Management to Treat Central Sleep Apnea", *Journal of Cardiac Failure*, vol. 21, no. 11, pp. 892–902, Nov. 2015, ISSN: 10719164. DOI: 10.1016/j.cardfail.2015.08.344. [Online]. Available: http://dx.doi.org/10.1016/j.cardfail.2015.08.344%20https://linkinghub.elsevier.com/retrieve/pii/S1071916415010416.

[19] M. R. Costanzo, P. Ponikowski, S. Javaheri, R. Augostini, L. Goldberg, R. Holcomb, A. Kao, R. N. Khayat, O. Oldenburg, C. Stellbrink, and W. T. Abraham, "Transvenous neurostimulation for central sleep apnoea: a randomised controlled trial", *The Lancet*, vol. 388, no. 10048, pp. 974–982, 2016, ISSN: 1474547X. DOI: 10.1016/S0140-6736(16)30961-8. [Online]. Available: http://dx.doi.org/10.1016/S0140-6736(16)30961-8.

[20] D. Jagielski, P. Ponikowski, R. Augostini, A. Kolodziej, R. Khayat, and W. T. Abraham, "Transvenous stimulation of the phrenic nerve for the treatment of central sleep apnoea: 12 months' experience with the remedē ® System", *European Journal of Heart Failure*, vol. 18, no. 11, pp. 1386–1393, Nov. 2016, ISSN: 13889842. DOI: 10.1002/ejhf.593. [Online]. Available: http://doi.wiley.com/10.1002/ejhf.593.

[21] S. Joseph and M. R. Costanzo, "A novel therapeutic approach for central sleep apnea: Phrenic nerve stimulation by the remedē® System", *International Journal of Cardiology*, vol. 206, S28–S34, Mar. 2016, ISSN: 01675273. DOI: 10.1016/j.ijcard.2016.02.121. [Online]. Available: https://linkinghub.elsevier.com/retrieve/pii/S0167527316303540.

[22] S. Reynolds, A. Ebner, T. Meffen, V. Thakkar, M. Gani, K. Taylor, L. Clark, G. Sadarangani, R. Meyyappan, R. Sandoval, E. Rohrs, and J. A. Hoffer, "Diaphragm Activation in Ventilated Patients Using a Novel Transvenous Phrenic Nerve Pacing Catheter", *Critical Care Medicine*, vol. 45, no. 7, e691–e694, Jul. 2017, ISSN: 0090-3493. DOI: 10.1097/CCM.0000000000002366. [Online]. Available: http://insights.ovid.com/crossref?an=00003246-201707000-00039.

[23] K. E. Kowalski, J. R. Romaniuk, P. A. Kirkwood, and A. F. DiMarco, "Inspiratory Muscle Activation via Ventral Lower Thoracic High Frequency Spinal Cord Stimulation", *Journal of Applied Physiology*, japplphysiol.01054.2018, Feb. 2019, ISSN: 8750-7587. DOI: 10.1152/japplphysiol.01054.2018. [Online]. Available: https://www.physiology.org/doi/10.1152/japplphysiol.01054.2018.

[24] A. F. DiMarco, R. T. Geertman, K. Tabbaa, and K. E. Kowalski, "Complete Restoration of Respiratory Muscle Function in Three Subjects with Spinal Cord Injury Pilot Interventional Clinical Trial", *American Journal of Physical Medicine & Rehabilitation*, p. 1, Aug. 2018, ISSN: 0894-9115. DOI: 10.1097/PHM.0000000000001018. [Online]. Available: http://insights.ovid.com/crossref?an=00002060-900000000-98442.

[25] J. Verbraecken, "Definitions of sleep disordered breathing", in *Respiratory Sleep Medicine*, European Respiratory Society, 2012, pp. 21–24. DOI: 10.1183/9781849840248.024211. [Online]. Available: http://erspublications.com/lookup/doi/10.1183/9781849840248.024211.

[26] R. L. Riha, "Polysomnography", in *Respiratory Sleep Medicine*, European Respiratory Society, 2012, pp. 120–130. DOI: 10.1183/9781849840248.016211. [Online]. Available: http://erspublications.com/lookup/doi/10.1183/9781849840248.016211.

[27] A. Ghio and B. Teston, "Caractéristiques de la dynamique d ' un pneumotachographe pour l ' étude de la production de la parole : aspects acoustique et aérodynamique", in *Journées d'Etude sur la Parole*, 2002, pp. 24–27. [Online]. Available: https://hal.archives-ouvertes.fr/hal-00142971.

[28] N.Meslier, "Enregistrements respiratoire et cardio-vasculaires au cours du sommeil", *CHU-Angers*, 2006.

[29] A. Boudewyns, M. Willemen, M. Wagemans, W. De Cock, P. Van De Heyning, and W. De Backer, "Assessment of respiratory effort by means of strain gauges and esophageal pressure swings: A comparative study", *Sleep*, vol. 20, no. 2, pp. 168–170, 1997, ISSN: 01618105. DOI: 10.1093/sleep/20.2.168.

[30] M. J. Morrell, P. Palange, P. Levy, and W. De Backer, "Homeostatic regulation during sleep", in *Respiratory Sleep Medicine*, European Respiratory Society, 2012, pp. 13–20. DOI: 10.1183/9781849840248.013811. [Online]. Available: http://erspublications.com/lookup/doi/10.1183/9781849840248.013811.

[31] H. Nakano, M. Hayashi, E. Ohshima, N. Nishikata, and T. Shinohara, "Validation of a new system of tracheal sound analysis for the diagnosis of sleep apnea-hypopnea syndrome", *Sleep*, vol. 27, no. 5, pp. 951–957, 2004, ISSN: 01618105. DOI: 10.1093/sleep/27.5.951.

[32] N. Meslier, I. Simon, A. Kouatchet, H. Ouksel, C. Person, and J. L. Racineux, "Validation of a suprasternal pressure transducer for apnea classification during sleep", *Sleep*, vol. 25, no. 7, pp. 753–757, 2002, ISSN: 01618105. DOI: 10.1093/sleep/25.7.753.

[33] P. Corbishley and E. Rodríguez-Villegas, "Breathing detection: Towards a miniaturized, wearable, battery-operated monitoring system", *IEEE Transactions on Biomedical Engineering*, vol. 55, no. 1, pp. 196–204, 2008, ISSN: 00189294. DOI: 10.1109/TBME.2007.910679.

[34] T. Penzel and A. K. Sabil, "The use of tracheal sounds for the diagnosis of sleep apnoea", *Breathe*, vol. 13, no. 2, e37–e45, 2017, ISSN: 20734735. DOI: 10.1183/20734735.008817.

[35] I. Sanchez and H. Pasterkamp, "Tracheal Sound Spectra Depend on Body Height", *American Review of Respiratory Disease*, vol. 148, no. 4_pt_1, pp. 1083–1087, 1993, ISSN: 0003-0805. DOI: 10.1164/ajrccm/148.4{_}Pt{_}1.1083. [Online]. Available: http://www.atsjournals.org/doi/abs/10.1164/ajrccm/148.4_Pt_1.1083.

[36] J. Sola-Soler, J. A. Fiz, A. Torres, and R. Jane, "Identification of Obstructive Sleep Apnea patients from tracheal breath sound analysis during wakefulness in polysomnographic studies", *2014 36th Annual International Conference of the IEEE Engineering in Medicine and Biology Society, EMBC 2014*, pp. 4232–4235, 2014, ISSN: 1094-687X. DOI: 10.1109/EMBC.2014.6944558.

[37] A. Sabil, J. L. Racineux, T. Penzel, and N. Meslier, "Tracheal sounds in the diagnosis of sleep apnea syndrome", *Medecine du Sommeil*, 2018, ISSN: 17694493. DOI: 10.1016/j.msom.2018.04.003. [Online]. Available: https://doi.org/10.1016/j.msom.2018.04.003.

[38] J. Cummiskey, T. C. Williams, P. E. Krumpe, and C. Guilleminault, "The detection and quantification of sleep apnea by tracheal sound recordings.", *The American review of respiratory disease*, vol. 126, no. 2, pp. 221–4, Aug. 1982, ISSN: 0003-0805. DOI: 10.1164/arrd.1982.126.2.221. [Online]. Available: http://www.ncbi.nlm.nih.gov/pubmed/7103247.

[39] T. Penzel, G. Amend, J. Peter, T. P. .-.-. . . . London, J. Libbey, and U. 1988, "Objective monitoring of therpeutical success in heavy snorers: a new technique", *Chronic Rhonchopathy. London, John Libbey Eurotext*, pp. 273–278, 1988.

[40] N. Meslier and J. L. Racineux, "Use of Tracheal Sound Recordings to Monitor Airflow During Sleep", in *Sleep Related Disorders and Internal Diseases*, Springer Berlin Heidelberg, 1987, pp. 121–124. DOI: 10.1007/978-3-642-72560-9{_}11.

[41] G. Soufflet, G. Charbonneau, M. Polit, P. Attal, A. Denjean, P. Escourrou, and C. Gaultier, "Interaction Between Tracheal Sound and Flow Rate: A Comparison of Some Different Flow Evaluations from Lung Sounds", *IEEE Transactions on Biomedical Engineering*, vol. 37, no. 4, pp. 384–391, 1990, ISSN: 15582531. DOI: 10.1109/10.52345.

[42] J. S. Chuah and Z. Moussavi, "Automated detection of respiratory phases by acoustical means", in *ResearchGate*, IEEE, 2001. [Online]. Available: https://www.semanticscholar.org/paper/AUTOMATED-RESPIRATORY-PHASE-DETECTION-BY-ACOUSTICAL-Chuah-Moussavi/33557244596d8b1aad8e14c8fd18b32f31b4e43b.

[43] P. Hult, T. Fjallbrant, B. Wranne, O. Engdahl, and P. Ask, "An improved bioacoustic method for monitoring of respiration", *Technol Health Care*, vol. 12, no. 4, pp. 323–332, 2004, ISSN: 0928-7329. [Online]. Available: http://www.ncbi.nlm.nih.gov/pubmed/15502283.

[44] P. Hult, T. Fjallbrant, S. Dahle, P. Danielsson, and P. Ask, "A method for respiration monitoring by the use of a bioacoustic signal", in *First International Conference on Advances in Medical Signal and Information Processing*, vol. 2000, Bristol, UK,

IET, 2000, pp. 22–25, ISBN: 0 85296 728 4. DOI: 10.1049/cp:20000312. [Online]. Available: https://ieeexplore.ieee.org/document/889946.

[45] A. Kulkas, E. Huupponen, J. Virkkala, M. Tenhunen, A. Saastamoinen, E. Rauhala, and S. L. Himanen, "New tracheal sound feature for apnoea analysis", *Medical and Biological Engineering and Computing*, vol. 47, no. 4, pp. 405–412, 2009, ISSN: 01400118. DOI: 10.1007/s11517-009-0446-z.

[46] A. Kulkas, E. Huupponen, J. Virkkala, M. Tenhunen, A. Saastamoinen, E. Rauhala, and S.-L. Himanen, "Intelligent methods for identifying respiratory cycle phases from tracheal sound signal during sleep", *Computers in Biology and Medicine*, vol. 39, no. 11, pp. 1000–1005, Nov. 2009, ISSN: 00104825. DOI: 10.1016/j.compbiomed.2009.07.014. [Online]. Available: http://dx.doi.org/10.1016/j.compbiomed.2009.07.014%20http://linkinghub.elsevier.com/retrieve/pii/S0010482509001474.

[47] A. Yadollahi and Z. Moussavi, "Automatic breath and snore sounds classification from tracheal and ambient sounds recordings", *Medical Engineering and Physics*, vol. 32, no. 9, pp. 985–990, 2010, ISSN: 13504533. DOI: 10.1016/j.medengphy.2010.06.013.

[48] A. Yadollahi, E. Giannouli, and Z. Moussavi, "Sleep apnea monitoring and diagnosis based on pulse oximetery and tracheal sound signals", *Medical and Biological Engineering and Computing*, vol. 48, no. 11, pp. 1087–1097, 2010, ISSN: 01400118. DOI: 10.1007/s11517-010-0674-2.

[49] N. Gavriely and D. W. Cugell, "Airflow effects on amplitude and spectral content of normal breath sounds.", *Journal of applied physiology*, vol. 80, no. 1, pp. 5–13, 1996, ISSN: 8750-7587. DOI: doi.org/10.1152/jappl.1996.80.1.5. [Online]. Available: http://www.ncbi.nlm.nih.gov/pubmed/8847331.

[50] M. Mlynczak, E. Migacz, and M. Migacz, "Detecting breathing and snoring episodes using a wireless tracheal sensor – a feasibility study.", Tech. Rep., 2016. DOI: 10.1109/EMBC.2019.8856440. [Online]. Available: https://hal-lirmm.ccsd.cnrs.fr/lirmm-02304820.

[51] C. Kalkbrenner, P. Stark, G. Kouemou, M. E. Algorri, and R. Brucher, "Sleep monitoring using body sounds and motion tracking", *2014 36th Annual International Conference of the IEEE Engineering in Medicine and Biology Society, EMBC 2014*, vol. 6000, pp. 6941–6944, 2014, ISSN: 1557170X. DOI: 10.1109/EMBC.2014.6945224.

[52] Y. Nam, B. A. Reyes, and K. H. Chon, "Estimation of Respiratory Rates Using the Built-in Microphone of a Smartphone or Headset", *IEEE Journal of Biomedical and Health Informatics*, vol. 20, no. 6, pp. 1493–1501, 2016, ISSN: 21682194. DOI: 10.1109/JBHI.2015.2480838.

[53] C. Kalkbrenner, M. Eichenlaub, S. Rüdiger, C. Kropf-Sanchen, W. Rottbauer, and R. Brucher, "Apnea and heart rate detection from tracheal body sounds for the diagnosis of sleep-related breathing disorders", *Medical and Biological Engineering and Computing*, vol. 56, no. 4, pp. 671–681, 2017, ISSN: 17410444. DOI: 10.1007/s11517-017-1706-y.

[54] A. Martin and J. Voix, "In-Ear Audio Wearable: Measurement of Heart and Breathing Rates for Health and Safety Monitoring", *IEEE Transactions on Biomedical Engineering*, vol. 65, no. 6, pp. 1256–1263, Jun. 2018, ISSN: 0018-9294. DOI: 10.1109/TBME.2017.2720463. [Online]. Available: https://ieeexplore.ieee.org/document/7959201/.

[55] M. Schmidt, A. Schumann, J. Müller, K.-J. Bär, and G. Rose, "ECG derived respiration: comparison of time-domain approaches and application to altered breathing patterns of patients with schizophrenia", *Physiological Measurement*, vol. 38, no. 4, pp. 601–615, Apr. 2017, ISSN: 0967-3334. DOI: 10.1088/1361-6579/aa5feb. [Online]. Available: http://stacks.iop.org/0967-3334/38/i=4/a=601?key=crossref.cb48ce16b5b45b07fba6cef64988ed8d.

[56] H. Liang, S. Lukkarinen, and I. Hartimo, "Heart sound segmentation algorithm based on heart sound envelogram", in *Computers in Cardiology 1997*, vol. 24, IEEE, 1997, pp. 105–108, ISBN: 0-7803-4445-6. DOI: 10.1109/CIC.1997.647841. [Online]. Available: http://ieeexplore.ieee.org/document/647841/.

[57] J. Fontecave-jallon, K. Fojtik, and B. Rivet, "Is there an Optimal Localization of Cardio-microphone Sensors for Phonocardiogram Analysis ?", in *EMBC2019*, 2019.

[58] Liang Huiying, L. Sakari, and H. Iiro, "A heart sound segmentation algorithm using wavelet decomposition and reconstruction", vol. 1630, no. C, pp. 1630–1633, 2002. DOI: 10.1109/iembs.1997.757028.

[59] I. Ozkan, S. Member, A. Yilmaz, and G. Celebi, "Improved Segmentation with Dynamic Threshold Adjustment for Phonocardiography Recordings", pp. 6681–6684, 2019.

[60] W. N. Soundscapes, "City Traffic White Noise | 10 Hours | For Sleeping, Studying or to Block Out Noise", Tech. Rep., 2017. [Online]. Available: https://www.youtube.com/watch?v=8s5H76F3SIs&list=WL&index=4&t=26s.

[1] X. LU, D. Guiraud, S. Renaux, T. Similowski, C. Azevedo Coste, and C. Azevedo, "Monitoring phrenic nerve stimulation-induced breathing via tracheal sounds", in *2019 XXIII Annual Conference of the International Functional Electrical Stimulation Society (IFESS)*, May 2019. [Online]. Available: https://hal-lirmm.ccsd.cnrs.fr/lirmm-02304820.

[2] X. LU, D. GUIRAUD, S. RENAUX, T. SIMILOWSKI, and C. AZEVEDO, "Breathing detection from tracheal sounds in both temporal and frequency domains in the context of phrenic nerve stimulation", in *2019 41st Annual International Conference of the IEEE Engineering in Medicine and Biology Society (EMBC)*, IEEE, Jul. 2019, pp. 5473–5476, ISBN: 978-1-5386-1311-5. DOI: 10.1109/EMBC.2019.8856440. [Online]. Available: https://ieeexplore.ieee.org/document/8856440/.

[3] X. LU, C. AZEVEDO, S. RENAUX, T. SIMILOWSKI, and D. GUIRAUD, "**STUDENT TRAINEE AWARDS** – MONITORING PHRENIC NERVE STIMULATION-INDUCED BREATHING VIA TRACHEAL SOUNDS", in *2019 58th International Spinal Cord Society Annual Scientific Meeting (ISCoS)*, The International Spinal Cord Society, 2019, p. 102. [Online]. Available: https://www.iscos.org.uk/uploads/ABSTRACTS/ISCoS_2019_Poster_Abstractsv2.pdf.

[4] X. LU, C. AZEVEDO, M.-C. NIERAT, S. RENAUX, T. SIMILOWSKI, and D. GUIRAUD, "**IN REDACTION** – IMPROVED TRACHEAL SOUND ANALYSIS FOR CONTINUOUS RESPIRATORY MONITORING: TIME-FREQUENCY PROCESSING OF THE PHONOSPIROGRAM COMBINED WITH PHONOCARDIOGRAM-DERIVED DETERMINATION OF RESPIRATORY RHYTHM", 2020.

[61] C. Plapous, C. Marro, and P. Scalart, "Improved signal-to-noise ratio estimation for speech enhancement", *IEEE Transactions on Audio, Speech and Language Processing*, vol. 14, no. 6, pp. 2098–2108, Nov. 2006, ISSN: 15587916. DOI: 10.1109/TASL.2006.872621.

[62] R. Oweis, E. Abdulhay, A. Khayal, and A. Awad, "An alternative respiratory sounds classification system utilizing artificial neural networks", *Biomedical Journal*, vol. 38, no. 2, pp. 153–161, 2015, ISSN: 2319-4170. DOI: 10.4103/2319-4170.137773. [Online]. Available: http://www.biomedj.org/text.asp?2015/38/2/153/137773.

[63] P. Hult, B. Wranne, and P. Ask, "A bioacoustic method for timing of the different phases of the breathing cycle and monitoring of breathing frequency.", *Medical engineering & physics*, vol. 22, no. 6, pp. 425–33, Jul. 2000, ISSN: 1350-4533. [Online]. Available: http://www.ncbi.nlm.nih.gov/pubmed/11086254.

Abstract

Introduction: Patients who have an artificial ventilation dependence are usually treated with mechanical ventilation. If their phrenic nerves and diaphragms are still functional, implanted diaphragm pacing (DP) can provide them a more natural respiration. But existing DP systems cannot monitor patient's induced respiration and stimulate with a current of constant intensity and frequency. Adding adaptive abilities to existing systems would improve the efficiency of the delivered stimulation and could also deliver an alarm in case of an apnea detection. A respiratory monitoring method based on recordings from tracheal sounds by microphone is introduced. This method aims at being ambulatory and non-invasive for all-day long real-time use.

Methods: Tracheal sounds were recorded by a microphone inserted into a 3D printed bell-shape support, which was stuck over patient's neck. Recorded signals were filtered and pre-amplified then saved and processed in a computer. Four protocols were designed to record and analyze respiration in different contexts: (1) 15 healthy subjects; (2) 1 patient with high tetraplegia under IT-PNS; (3) 13 healthy subjects in sitting and lying positions with reference signals; (4) 30 patients with sleep apnoea and 10 patients with implanted IT-PNS will be included in short future. One real-time processing algorithm detected all inspiration/expiration phases by combining results from temporal envelope detection, frequency detection, and also PDR detection (PCG-derived respiration: variation of cardiac peak amplitude corresponds to respiration). Combining the detection results in these 3 domains allowed for a better specificity of system (less false positives).

Results: The application of the algorithms to protocols 1 to 3 data lead to good detection results that met the minimum requirements for the system. These result also showed that noises like speech or environments and different body position do not influence much the detection results. The new proposed respiratory effort evaluation method – PDR showed a good correlation with EDR, this demonstrates the feasibility to use the PDR to monitor respiration. At a good correlation between R-R intervals and S-S intervals also showed that it would also be possible to monitor heart activity from tracheal sounds.

Conclusions: This thesis shows the feasibility of detecting the apnoea and of monitoring

cardiac activity from tracheal sounds. The extracted signal PDR could be used to identify the type of apnoea (obstructive/central). Furthermore, the microphone-based recording system could capture stimulation signals which can indicate a dysfunction of the pacing system and recorded tracheal sounds could give a feedback of the electro-ventilation quality. The next step is to record patient's tracheal sounds signals and test if the same algorithm could still work well in this context (the protocol 4). Monitoring tracheal sounds could provide a non-invasive way to approximate inspiratory flow that would be useful in all patients requiring respiratory monitoring in acute situations (e.g. as a safety measure during the administration of morphine for acute pain) and in chronic situations (e.g. home mechanical ventilation). And in the construction of smart house, especially for nursing/retirement home, application of tracheal sounds monitoring could provide convenient, robust multi-vital signals monitoring.

Résumé

Introduction : Les patients dépendant d'une ventilation artificielle sont principalement placés sous ventilation mécanique. Si leur nerf phrénique et leur diaphragme demeurent fonctionnels, un implant de stimulation du diaphragme (DP) peut permettre une respiration plus naturelle. Mais les systèmes DP existants ne peuvent monitorer la respiration induite du patient et ne permettent que de stimuler à intensité et à fréquence constantes. Ajouter une capacité d'adaptation à ces systèmes pourrait améliorer l'efficacité de la stimulation. Une méthode de monitoring respiratoire basée sur l'enregistrements de sons trachéaux via un microphone a été introduite dans cette thèse. Cette méthode a été conçue pour être portable et non-invasive, et capable de fonctionner une journée complète et en temps réel.

Méthodes : Les sons trachéaux ont été enregistrés à l'aide d'un microphone placé dans un support en forme de cloche réalisé par impression 3D, et placé sur le cou du patient. Les signaux récupérés ont été filtrés et pré-amplifiés puis enregistrés et traités sur ordinateur. Quatre protocoles ont été conçus pour enregistrer des sons trachéaux dans divers contextes : (1) 15 sujets sains ; (2) 1 patient ayant une tétraplégie haute sous IT-PNS ; (3) 13 sujets sains assis puis couchés, avec des signaux de référence ; (4) 30 patients souffrant d'apnée du sommeil et 10 patients avec un système IT-PNS implanté seront includes prochainement. Un algorithme de traitement du signal en temps réel a permis de détecter toutes les phases d'inspiration et d'expiration par détection d'enveloppe dans les domaines temporel, fréquentiel, et également une détection à partir du PDR (PCG-derived respiration : la variation d'amplitude des pics cardiaques correspond à la respiration). La combinaison de ces trois détections permet une meilleure spécificité du système (moins de faux-positifs).

Résultats : 'application de l'algorithme aux données des protocoles 1 et 3 a conduit à de bons résultats de détection qui satisfont le minimum requis pour système. Ces résultats ont aussi montré que les bruits tels que la parole ou l'environnement extérieur, et les différentes position du corps n'influencent pas le résultat de la détection. La nouvelle méthode d'évaluation de l'effort respiratoire proposé – PDR montre une bonne corrélation avec EDR, ce qui démontre la faisabilité de l'utilisation de PDR pour le monitoring de la respiration. Une bonne correlation entre des intervalles R-R et S-S montre également qu'il serait donc également possible de monitorer l'activité du coeur à partir des sons trachéaux.

Conclusions : Cette thèse a démontré la faisabilité de détecter des épisodes d'apnée à partir de sons trachéaux et de monitorer l'activité cardiaque. Le signal extrait PDR peut permettre d'identifier le type d'apnée (obstructive / centrale). De plus, le système d'enregistrement par microphone peut permettre d'observer les signaux de stimulation électrique chez les patients implantés et indiquer un dysfonctionnement éventuel du système implanté. Les sons trachéaux peuvent aussi fournir un retour sur la qualité de l'électroventilation. La prochaine étape sera donc d'obtenir les enregistrements de patients et de tester si ce même algorithme fonctionne dans ce cas (protocole 4). Le monitoring des sons trachéaux peut fournir une méthode non-invasive pour estimer le flux inspiratoire dans le cas de patients nécessitant un monitoring respiratoire dans les situations extrêmes (e.g. comme une mesure de sécurité pour l'administration de morphine pour les douleurs aiguës) et dans les situations chroniques (e.g. la ventilation mécanique à domicile). Et dans le cas de maisons connectées, en particulier pour les maisons de retraite, les applications de monitoring des sons trachéaux peut permettre un monitoring robuste et efficace des signes multi-vitaux.